THE RADIATION EFFICIENCY OF A DIPOLE ANTENNA ABOVE AN IMPERFECTLY CONDUCTING GROUND

by

Peder Meyer Hansen

A dissertation submitted in partial fulfillment
of the requirements for the degree of
Doctor of Philosophy in
The University of Michigan
1970

Doctoral Committee

Professor Chen-To Tai, Chairman
Professor Charles L. Dolph
Professor Dale M. Grimes
Professor John A. M. Lyon
Professor Newbern Smith

ABSTRACT

THE RADIATION EFFICIENCY OF A DIPOLE ANTENNA ABOVE AN IMPERFECTLY CONDUCTING GROUND

by

Peder Meyer Hansen

Chairman: Chen-To Tai

Theoretical expressions for the radiation efficiency of three types of antennas are derived. It is assumed that the antennas are located above an infinite plane earth having a finite conductivity. The dyadic Green's function for this geometry is developed as an Ohm-Rayleigh type expansion in terms of the Hansen vector wave functions. The dyadic Green's function is used to find the fields due to three assumed current distributions. These assumed currents correspond to the case of the vertical Hertzian dipole, the horizontal Hertzian dipole and the vertical half-wave thin dipole. Expressions for the radiated power are found by integration of the Poynting's vector over two plane surfaces; one above the antenna, and one below the antenna. The integral over the upper plane represents radiated power while the integral over the lower surface represents power lost. These expressions are reduced to integrals that lend themselves to numerical evaluation by digital computer.

Extensive numerical results are presented in graphical form as plots of antenna efficiency versus feed point height. The calculations have been done for various values of ground parameters that are representative of conditions expected in practice. Also, radiation resistance plots and antenna patterns are included.

It is shown that location of the antenna very near the ground results in very inefficient operation. Short vertical dipoles have a pronounced peak of efficiency at a height of .15 wavelengths, while the vertical half-wave

dipole has a peak of efficiency when its center height is .25 wavelengths. The location of the efficiency peak for the horizontal Hertzian dipole depends upon the ground parameters and it is not so pronounced as the peak for the vertical dipole case.

PREFACE

Special acknowledgment is given to Professor Chen-To Tai who suggested the area of research and continuously provided guidance and encouragement.

I also wish to express my deep appreciation to all the members of my doctoral committee for their comments and criticism.

Special thanks are due to both Dr. M. P. Ristenbatt, of the Cooley Electronics Laboratory and Professor R. E. Hiatt, Head of the Radiation Laboratory for their generous help. Thanks are also due to Mrs. Ann Fulmer and Mrs. Claire White for their help in preparing the manuscript.

Finally, I wish to express my appreciation to the many other individuals who have assisted me in the completion of this dissertation.

TABLE OF CONTENTS

LIST OF ILLUSTRATIONS

LIST OF APPENDICES

CHAPTER I

INTRODUCTION

The purpose of this thesis is to theoretically study the radiation efficiency of an antenna system including a lossy ground plane.

The calculation of the radiation efficiency of a transmitting antenna near a lossy object involves two major steps. First the expressions for the electromagnetic fields need to be derived in order to obtain the Poynting's vector. Secondly, Poynting's vector must be integrated over appropriate surfaces in order to obtain the power relationships necessary to calculate the efficiency, namely the power radiated and power dissipated.

The geometry of the problem considered here is illustrated in Fig. 1-1. The dipole is located at a height z_o above the ground. The integral of the z directed Poynting's vector over the surface above the antenna (surface 1) is called S_+, while the integral of the -z directed Poynting's vector over the surface between the antenna and the ground (surface 2) is called S_-. Since S_+ and S_- are independent of z_1 and z_2, as long as the upper surface is above the antenna and the lower surface is between the antenna and the ground, the term $S_+ + S_-$ represents the total output power of the antenna and is proportional to the radiation resistance while S_- represents the dissipated power. Accordingly the radiation efficiency η of the dipole, as defined in Ref. 1, can be expressed as

$$\eta = \frac{S_+}{S_+ + S_-} \quad . \tag{1.1}$$

Historically, the problem of finding the electromagnetic radiation from an elementary Hertzian dipole in the presence of a flat earth bounded by a smooth plane interface has been considered by several authors. Sommerfeld (Ref. 2) was the first to consider the problem. He found the fields due to a vertical electric dipole located on the interface by expanding the Hertzian potential in terms of cylindrical wave functions. The horizontal Hertzian dipole was treated by Horschelman (Ref. 3) shortly afterwards .

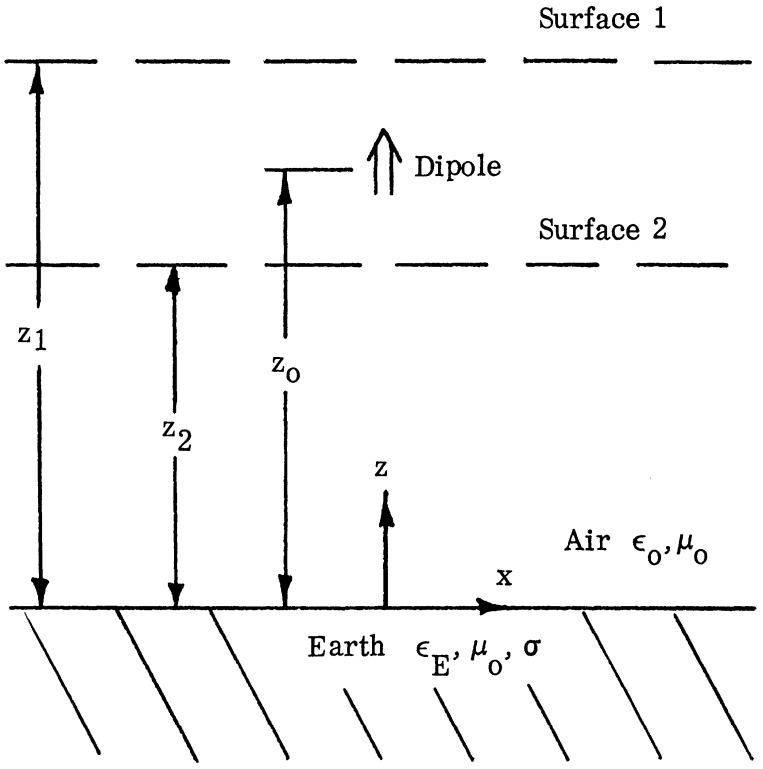

FIG. 1-1: Geometric Configuration.

The general vertical dipole was probably first treated by Elias (Ref. 4). The Hertzian potential may also be expanded in terms of inhomogeneous plane waves. This method was used by Weyl (Ref. 5) and Kruger (Ref. 6). Solutions for all four cases of vertical and horizontal electric and magnetic dipoles were published by Sommerfeld (Ref. 7) in 1926. Recently, Banõs (Ref. 8) has collected most of the work in this area and presented it in a concise manner along with some of his own results. He gives general integral representations of the fields due to all four configurations of Hertzian dipoles as well as closed form approximations.

In this dissertation the method used to calculate the fields is that of

dyadic Green's function. The dyadic Green's function for this geometry with a perfectly conducting boundary was first presented by Levine and Schwinger (Ref. 9 and 10), while the dyadic Green's function for mixed boundary conditions was found by Tai (Ref. 11).

In order to calculate the radiation resistance and the efficiency of an antenna near a lossy object the power relationships must be studied. Sommerfeld and Renner (Ref. 12) published a paper in which they derive the exact expressions for the radiation resistance of two types of antennas. The antennas they studied were the vertical Hertzian dipole and the horizontal Hertzian dipole . The radiation resistance expressions do not occur in closed form. Consequently Sommerfeld and Renner turned to approximation techniques in order to evaluate the expressions. Their approximation involved the assumption that the complex index of refraction is strictly imaginary. As far as numerical results are concerned, they have only dealt with the case of sea water at 40 meters wavelength. The radiation resistance curves for this case as well as a summary of the paper are contained in Reference 13.

W. W. Hansen and J.G. Beckerley (Ref. 14) have derived a method for calculating total power radiated from an arbitrary current distribution above a plane lossy earth as proportional to the sum of the squares of expansion coefficients of the current. J.R. Wait (Ref. 15) presents an integral expression for the radiation resistance of a vertical magnetic dipole, while Bhattacharyya (Ref. 16) uses Wait's expression and Sommerfeld's expression to calculate radiation resistance curves for the vertical magnetic and horizontal electric dipole for the special case when $\frac{\sigma}{\omega} \gg \epsilon$.

In Chapter II a derivation of the dyadic Green's function for mixed boundary conditions is presented. The derivation follows the scattering superposition scheme suggested by Tai (Ref. 17). This Green's function is used in Chapter III in order to derive the fields due to a vertical and horizontal Hertzian dipole. These results are then verified against the

original results of Sommerfeld, and then used to derive expressions for the radiation resistance and the efficiency of the above two antennas.

In Chapter IV the Green's function is used to derive the fields due to a vertical antenna with an arbitrary length and a sinusoidal current distribution. From these expressions the radiation resistance and radiation efficiency formulae for a half-wave dipole are derived.

Chapter V contains the results of various computer-aided numerical calculations. The most important of these are the plots of radiation resistance versus height for the three types of dipoles. The ground parameters were chosen to be representative of those actually encountered in practice, and the frequency was varied over a broad range. Other numerical results included are radiation resistance curves and far field power patterns.

In Chapter VI we discuss the physical interpretation of the numerical results as well as suggest areas where we feel future efforts would be productive.

CHAPTER II

DYADIC GREEN'S FUNCTIONS

2.1 Definition of Dyadic Green's Functions and Some Properties

We are seeking solutions to the inhomogeneous vector wave equations (2.1) and (2.2), subject to certain boundary conditions.

$$\nabla x \nabla x \bar{E} - k^2 \bar{E} = i\omega\mu \bar{J} \tag{2.1}$$

$$\nabla x \nabla x \bar{H} - k^2 \bar{H} = \nabla x \bar{J} \quad . \tag{2.2}$$

The time dependence is assumed to be of the form $e^{-i\omega t}$ and the propagation constant is defined by

$$k^2 = \omega^2 \mu \epsilon \left(1 + i \frac{\sigma}{\omega}\right) \quad .$$

The dyadic Green's function for the vector wave equation is defined by

$$\nabla x \nabla x \bar{\bar{G}} - k^2 \bar{\bar{G}} = \bar{\bar{I}}\, \delta(\bar{R}-\bar{R}') \tag{2.3}$$

where $\bar{\bar{G}}$ is the dyadic Green's function which, as we will show, may be used to integrate (2.1). The unit dyadic, $\bar{\bar{I}}$, sometimes called the idem-factor, is defined such that

$$\bar{\bar{I}} \cdot \bar{a} = \bar{a} \cdot \bar{\bar{I}} = \bar{a}$$

where $\bar{a}$ is any arbitrary vector. The delta function is defined by

$$\iiint_V \delta(\bar{R}-\bar{R}')dV = 1 \qquad \bar{R}' \in V \tag{2.4}$$

$$\delta(\bar{R}-\bar{R}') = 0 \qquad \bar{R} \neq \bar{R}' \quad . \tag{2.5}$$

A dyadic may be presented as the conjunction of two vectors

$$\bar{\bar{G}} = \bar{A}\,\bar{B} = \sum_{i=1}^{3} \sum_{j=1}^{3} G_{ij}\, \hat{x}_i \hat{x}_j$$

where $\bar{A}$ and $\bar{B}$ represent two vector functions and the $\hat{x}_i$ are unit vectors. Thus, it is apparent that $\bar{\bar{G}}$ may be represented by a matrix with elements G_{ij}. The transpose of $\bar{\bar{G}}$ is written $\tilde{\bar{\bar{G}}}$ and is defined as follows

$$\tilde{\tilde{G}} = \sum_{i=1}^{3} \sum_{j=1}^{3} G_{ji} \hat{x}_i \hat{x}_j = \bar{B}\,\bar{A} \quad .$$

The above definition of $\tilde{\tilde{G}}$ may be used to demonstrate that

$$\bar{a} \cdot \tilde{\tilde{G}} = \tilde{\tilde{G}} \cdot \bar{a} \tag{2.6}$$

or

$$\tilde{\tilde{G}} \cdot \bar{a} = \bar{a} \cdot \tilde{\tilde{G}} \tag{2.7}$$

where $\bar{a}$ is any arbitrary vector.

The solutions to (2.3) depend upon the particular boundary conditions arising from a particular problem. In general the boundary conditions applied to $\tilde{\tilde{G}}$ are very similar to those imposed upon $\bar{E}$.

The radiation condition, due to Sommerfeld*, is used as a boundary condition for infinite domain problems. The corresponding condition applied to the dyadic Green's function is given by

$$\lim_{R \to \infty} R \left[\nabla \times \tilde{\tilde{G}} - ik \hat{R} \times \tilde{\tilde{G}} \right] = 0 \quad . \tag{2.8}$$

At a boundary between a dielectric and a perfectly conducting material the tangential $\bar{E}$ field vanishes. The corresponding condition on the dyadic Green's function is given by

$$\hat{n} \times \tilde{\tilde{G}} = 0 \quad . \tag{2.9}$$

An important property of the dyadic Green's function is the so-called symmetry relationship given by

$$\tilde{\tilde{G}}(\bar{R}|\bar{R}') = \tilde{\tilde{G}}(\bar{R}'|\bar{R}) \quad . \tag{2.10}$$

The proof of this identity follows from the vector Green's theorem** (2.11) and the differential equation for $\tilde{\tilde{G}}$:

---

* See Ref. 18, pages 485-486

** See Ref. 18, pages 464-468

$$\iiint_V \left[\bar{\bar{A}} \cdot \nabla \times (\nabla \times \bar{\bar{B}}) - \bar{\bar{B}} \cdot \nabla \times (\nabla \times \bar{\bar{A}})\right] dV$$

$$= \oiint_S \left[\bar{\bar{B}} \times (\nabla \times \bar{\bar{A}}) - \bar{\bar{A}} \times (\nabla \times \bar{\bar{B}})\right] \cdot \hat{n}\, dS \ , \qquad (2.11)$$

where $\hat{n}$ is the outward directed unit vector normal to the surface. The surface integral of (2.11) may be written in a more convenient form by use of the scalar triple product identity giving

$$\iiint_V \left[\bar{\bar{A}} \cdot \nabla \times (\nabla \times \bar{\bar{B}}) - \bar{\bar{B}} \cdot \nabla \times (\nabla \times \bar{\bar{A}})\right]$$

$$= \oiint_S \left[(\nabla \times \bar{\bar{A}}) \cdot (n \times \bar{\bar{B}}) - (\nabla \times \bar{\bar{B}}) \cdot (n \times \bar{\bar{A}})\right] dS \ . \qquad (2.12)$$

If we substitute for $\bar{\bar{A}}$ and $\bar{\bar{B}}$ in (2.12) the vector functions

$$\bar{\bar{G}}(\bar{R}|\bar{R}') \cdot \bar{a}' \quad \text{and} \quad \bar{\bar{G}}(\bar{R}|\bar{R}'') \cdot \bar{a}''$$

and integrate over the volume by use of (2.3) we obtain

$$\left[\bar{a}' \cdot \bar{\bar{G}}(\bar{R}'|\bar{R}'') - \bar{\bar{G}}(\bar{R}''|\bar{R}') \cdot \bar{a}'\right] =$$

$$\oiint_S \left[(\nabla \times \bar{\bar{G}}(\bar{R}|\bar{R}') \cdot \bar{a}') \cdot (\hat{n} \times \bar{\bar{G}}(\bar{R}|\bar{R}'') \cdot \bar{a}'')\right.$$

$$\left. - (\nabla \times \bar{\bar{G}}(\bar{R}|\bar{R}'') \cdot \bar{a}'') \cdot (\hat{n} \times \bar{\bar{G}}(\bar{R}\,\bar{R}') \cdot \bar{a}')\right] dS \qquad (2.13)$$

where the surface of integration will include any perfectly conducting objects and the surface at infinity. The surface integral is seen to vanish on the perfectly conducting objects by (2.9). The integral over the surface at infinity may be shown to vanish by the radiation condition of (2.8). Thus the entire surface integral is zero and Eq. (2.13) is seen to imply (2.10)

For a two medium problem such as illustrated in Fig. 2-1, we define the dyadic Green's function as follows:

$$\bar{\bar{G}}(\bar{R}|\bar{R}') = \begin{cases} \bar{\bar{G}}^{11}(\bar{R}|\bar{R}') & \bar{R} \text{ in medium 1} \\ \bar{\bar{G}}^{21}(\bar{R}|\bar{R}') & \bar{R} \text{ in medium 2} \end{cases} .$$

Here we have assumed all sources ($\bar{R}'$) are in medium 1. The differential equations that $\bar{\bar{G}}^{11}$ and $\bar{\bar{G}}^{21}$ satisfy are

$$\begin{aligned} &\nabla x \nabla x \bar{\bar{G}}^{(11)}(\bar{R}|\bar{R}') - k_1^2 \bar{\bar{G}}^{(11)}(\bar{R}|\bar{R}') = \bar{\bar{I}}\,\delta(\bar{R}-\bar{R}') \\ &\nabla x \nabla x \bar{\bar{G}}^{(21)}(\bar{R}|\bar{R}') - k_2^2 \bar{\bar{G}}^{(21)}(\bar{R}|\bar{R}') = 0 \quad . \end{aligned} \tag{2.14}$$

At the boundary between the two media the fields must satisfy the so-called mixed boundary conditions. These insure that tangential $\bar{E}$ and $\bar{H}$ are continuous as long as σ_1 and σ_2 remain finite. The corresponding conditions for the dyadic Green's function are

$$\hat{n} \times \bar{\bar{G}}^{(11)}(\bar{R}|\bar{R}') = \hat{n} \times \bar{\bar{G}}^{(21)}(\bar{R}|\bar{R}') \qquad \bar{R} \text{ on interface}$$

$$\frac{\hat{n}}{\mu_1} \times \nabla \times \bar{\bar{G}}^{(11)}(\bar{R}|\bar{R}') = \frac{\hat{n}}{\mu_2} \times \nabla x \bar{\bar{G}}^{(21)}(\bar{R}|\bar{R}') \qquad \bar{R} \text{ on interface} .$$

For sources in medium 2 we may define a $\bar{\bar{G}}^{(22)}$ and $\bar{\bar{G}}^{(12)}$ similar to (2.14) but interchanging the roles of k_1 and k_2. The symmetry relationships for the two media case are:

$$\bar{\bar{G}}^{(11)}(\bar{R}|\bar{R}') = \tilde{\bar{\bar{G}}}^{(11)}(\bar{R}'|\bar{R})$$

$$\frac{1}{\mu_2} \bar{\bar{G}}^{(21)}(\bar{R}|\bar{R}') = \frac{1}{\mu_1} \tilde{\bar{\bar{G}}}^{(12)}(\bar{R}'|\bar{R})$$

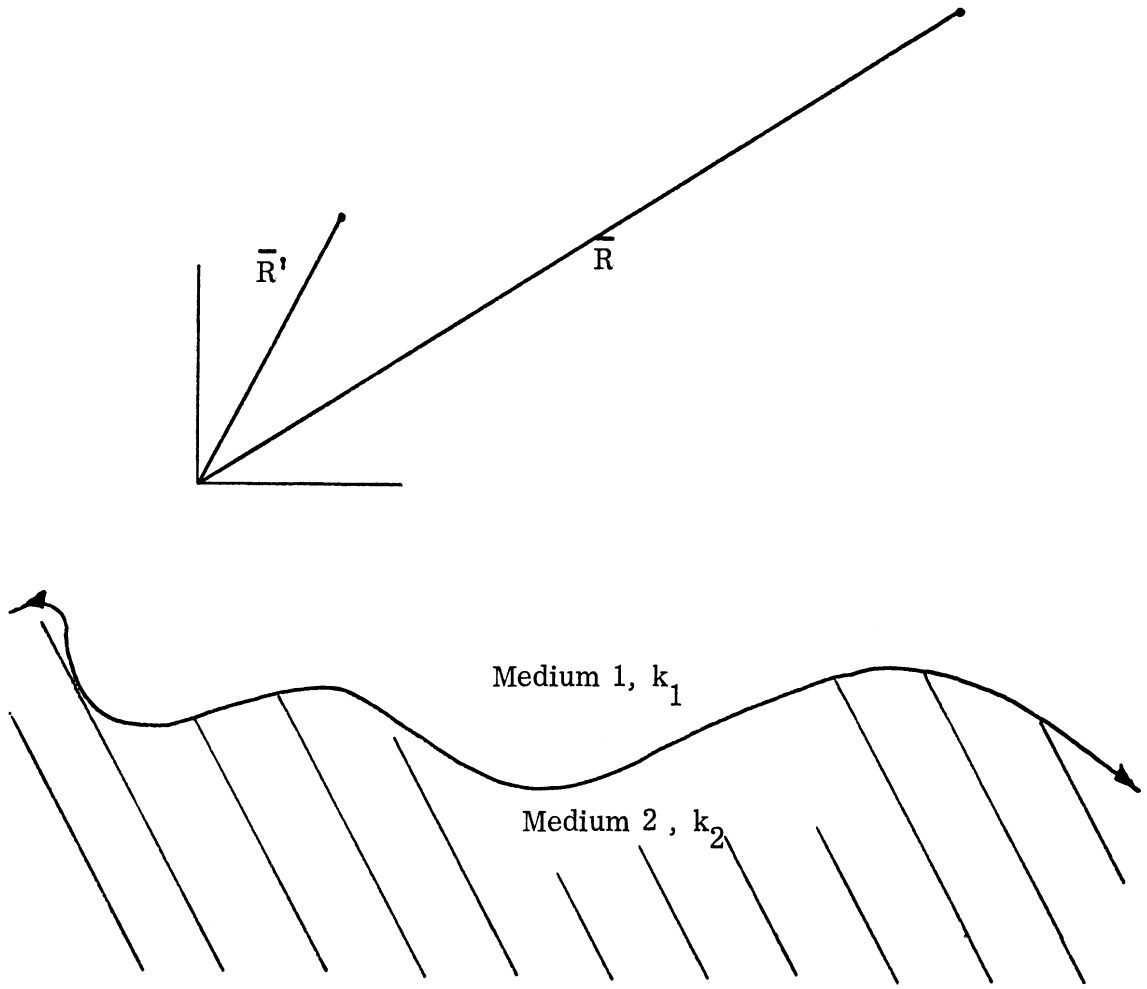

FIG. 2-1: General Two Media Problem Geometry.

2.2 Integration of the Vector Wave Equation

The integral expression for the field due to a known current source $\bar{J}$ can be derived by substituting the vector functions $\bar{E}$ and $\bar{\bar{G}} \cdot \bar{a}$ respectively for $\bar{A}$ and $\bar{B}$ in Eq. (2.12). We then apply (2.1) and (2.3) in order to integrate over the volume. Interchanging $\bar{R}$ with $\bar{R}'$ we obtain

$$\left\{ \bar{E}(\bar{R}) - i\omega\mu \iiint_{V'} \bar{J}(\bar{R}') \cdot \bar{\bar{G}}(\bar{R}'|\bar{R})\, dV' = \right.$$

$$\left. \oiint_{S} \left[(\nabla \times \bar{E}) \cdot (\hat{n} \times \bar{\bar{G}}) - (\hat{n} \times \bar{E}) \cdot (\nabla \times \bar{\bar{G}}) \right] dS \right\} \cdot \bar{a}$$

where the vector $\bar{a}$ may be factored out as it is arbitrary. If the domain is infinite including only perfectly conducting surfaces, the surface integral vanishes. By use of the symmetry property the final result for the field is

$$\bar{E}(\bar{R}) = \iiint_{V'} \bar{\bar{G}}(\bar{R}|\bar{R}') \cdot \bar{J}(\bar{R}')\, dV' \quad . \tag{2.15}$$

For the two media problem the result is similar. Substitute for $\bar{A}$ and $\bar{B}$ of (2.12) the vector functions $\bar{E}(\bar{R})$ and $\bar{\bar{G}}(\bar{R}|\bar{R}') \cdot \bar{a}$. Integration over medium 1 yields

$$\left\{ \bar{E}_1(\bar{R}) - i\omega\mu_1 \iiint_{V_1'} \bar{J}(\bar{R}') \cdot \bar{\bar{G}}^{(11)}(\bar{R}|\bar{R}')\, dV' \right.$$

$$\left. = \oiint_{S} \left[(\nabla \times \bar{E}_1) \cdot (\hat{n} \times \bar{\bar{G}}^{(11)}) - (\hat{n} \times \bar{E}_1) \cdot (\nabla \times \bar{\bar{G}}^{(11)}) \right] dS \right\} \cdot \bar{a} \tag{2.16}$$

Integration over medium 2 where there are no source currents yields

$$\left\{ \iint_S \left[(\nabla \times \bar{E}_2) \cdot (\hat{n} \times \bar{\bar{G}}^{(21)}) - (\hat{n} \times \bar{E}_2) \cdot (\nabla \times \bar{\bar{G}}^{(21)}) \right] dS = 0 \right\} \cdot \bar{a} \quad . \tag{2.17}$$

The surface integrals of (2.16) and (2.17) are reduced to integration over the interface between the two media by the radiation condition. Applying the boundary conditions on $\bar{E}$ and $\bar{\bar{G}}$ we obtain

$$\left\{ \iint_{\text{Boundary}} \left[(\nabla \times \bar{E}_2) \cdot (\hat{n} \times \bar{\bar{G}}^{(11)}) - (\hat{n} \times \bar{E}_1) \cdot (\nabla \times \bar{\bar{G}}^{(21)}) \right] dS = 0 \right\} \cdot \bar{a} \quad .$$

Using the scalar triple product identity we obtain

$$\left\{ \iint_{\text{Boundary}} \left[\hat{n} \times (\nabla \times \bar{E}_2) \cdot (\bar{\bar{G}}^{(11)}) - \bar{E}_1 \cdot (\hat{n} \times (\nabla \times \bar{\bar{G}}^{(21)})) \right] dS = 0 \right\} \cdot \bar{a} \quad .$$

Again applying the boundary conditions on $\nabla \times \bar{E}$ and $\nabla \times \bar{\bar{G}}$ we obtain

$$\left\{ \iint_{\text{Boundary}} \left[\hat{n} \times (\nabla \times \bar{E}_1) \cdot (\bar{\bar{G}}^{(11)}) - \bar{E}_1 \cdot (\hat{n} \times (\nabla \times \bar{\bar{G}}^{(11)})) \right] dS = 0 \right\} \cdot \bar{a} \quad ,$$

and again applying the scalar triple product we obtain the identity

$$\left\{ \iint_{\text{Boundary}} \left[(\nabla \times \bar{E}_1) \cdot (\hat{n} \times \bar{\bar{G}}^{(11)}) - (\hat{n} \times \bar{E}_1) \cdot (\nabla \times \bar{\bar{G}}^{(11)}) \right] dS = 0 \right\} \cdot \bar{a} \quad .$$

This identity implies that the surface integral of (2.16) vanishes, implying:

$$\bar{E}_1(\bar{R}) = i\omega\mu_1 \iiint_{V_1'} \bar{\bar{G}}^{(11)}(\bar{R}|\bar{R}') \cdot \bar{J}(\bar{R}') \, dV' \quad . \tag{2.18}$$

Similarly it can be shown that

$$\bar{E}_2(\bar{R}) = i\omega\mu_1 \iiint_{V_1'} \bar{\bar{G}}^{(21)}(\bar{R}|\bar{R}') \cdot \bar{J}(\bar{R}')\, dV' \quad . \tag{2.19}$$

Equations (2.18) and (2.19) are equivalent to

$$\bar{E}(\bar{R}) = i\omega\mu \iiint \bar{\bar{G}}(\bar{R}|\bar{R}') \cdot \bar{J}(\bar{R}')\, dV \quad .$$

Thus, once the dyadic Green's function for a particular gometry has been found, the fields due to a known current source $\bar{J}$ may be directly expressed in integral form.

2.3 The Vector Wave Functions

W. W. Hansen (Ref. 14) first introduced a method for generating solutions to the vector wave equation making use of three so-called vector wave functions. These functions are defined in terms of a scalar potential ψ which satisfies the scalar wave equation as follows

$$\bar{L} = \nabla\psi$$
$$\bar{M} = \nabla \times \bar{a}\,\psi$$
$$\bar{N} = \frac{1}{K} \nabla \times \bar{M}$$

where ψ is a solution of

$$\nabla^2 \psi + K^2 \psi = 0 \quad . \tag{2.20}$$

Note that K is an arbitrary constant.

In order that $\bar{M}$ and $\bar{N}$ be solutions or eigenfunctions of the equation

$$\nabla \times \nabla \times \bar{F} - K^2 \bar{F} = 0 \quad .$$

Senior (Ref. 19) and Spence and Wells (Ref. 20) have shown that $\bar{a}$ must be a

linear combination of the radial vector $\bar{R}$ with any arbitrary constant vector. These functions are presumed to be complete and therefore may be used to expand any arbitrary wave function*. If the wave function is solenoidal then the expansion need only contain terms of $\bar{M}$ and $\bar{N}$.

For the cylindrical coordinate system the solutions of (2.20) may be written in the form

$$\psi_{\substack{e\\o}n\lambda}(h) = Z_n(\lambda r) \begin{matrix}\cos\\ \sin\end{matrix} n\phi \, e^{\pm ihz}$$

where Z_n is an appropriate solution to the Bessel's equation and $\lambda^2 + h^2 = K^2$. Z_n is usually chosen to be the cylindrical Bessel function J_n. If the Hankel function of the first or second kind is chosen then the vector wave functions are written with the appropriate superscript; i.e., $\bar{M}^{(1)}$ represents the vector wave function where Z_n has been chosen as the Hankel function of the first kind. The sign of ih is chosen to give an outward traveling wave in the $+z$ direction in order to satisfy the radiation condition.

The vector wave functions are sometimes classified according to what vector $\bar{a}$ is actually used for their definition. For example, if the unit vector x were used then the vector wave functions would be written $\bar{M}^{(x)}$ and $\bar{N}^{(x)}$. The same is true for $\bar{a}$ equal to y, z or $\bar{R}$. The various types of vector wave functions are not independent. For example, $\bar{M}^{(x)}$ can be represented in terms of the $\bar{M}^{(z)}$ and $\bar{N}^{(z)}$ functions**. For the following we will be dealing mostly with the $M^{(z)}$ and $N^{(z)}$ functions and thus the z superscript is implied unless otherwise specified.

---

*See Ref. 21, page 393 .

**See Ref. 23 .

The specific vector wave functions that we will be using are expressed below.

$$\bar{M}_{\substack{e\\o}n\lambda}(h) = \left[\mp \frac{n}{r} J_n(\lambda r) \begin{matrix}\sin\\\cos\end{matrix} n\phi\, \hat{r} - \frac{\partial J_n}{\partial r}(\lambda r) \begin{matrix}\cos\\\sin\end{matrix} n\phi\, \hat{\phi}\right] e^{ihz} \tag{2.21}$$

$$\bar{N}_{\substack{e\\o}n\lambda}(h) = \frac{1}{\sqrt{\lambda^2+h^2}} \left[ih \frac{\partial J_n}{\partial r}(\lambda r) \begin{matrix}\cos\\\sin\end{matrix} n\phi\, \hat{r} \mp \frac{ihn}{r} J_n(\lambda r) \begin{matrix}\sin\\\cos\end{matrix} n\phi\, \hat{\phi} + \lambda^2 J_n(\lambda r) \begin{matrix}\cos\\\sin\end{matrix} n\phi\, \hat{z}\right] e^{ihz} \quad . \tag{2.22}$$

These two functions satisfy

$$\nabla x\, \nabla x \begin{Bmatrix}\bar{M}\\\bar{N}\end{Bmatrix} - k^2 \begin{Bmatrix}\bar{M}\\\bar{N}\end{Bmatrix} = 0 \tag{2.23}$$

when

$$k^2 = h^2 + \lambda^2 \quad . \tag{2.24}$$

Note that Eq. (2.23) and the definition of the $\bar{M}$ and $\bar{N}$ functions implies that the following relationships hold.

$$\nabla x\, \bar{M} = k\, \bar{N}$$
$$\nabla x\, \bar{N} = k\, \bar{M} \, .$$

Because of the orthogonal properties of the scalar wave functions ψ the vector wave functions also exhibit orthogonal properties. These orthogonality relationships facilitate the expansion of certain functions in terms of the vector wave functions. Some orthogonal properties of the cylindrical vector wave functions have been discussed by Stratton (Ref. 21) and more completely by Tai (Ref. 17). The relationships that we will use are given below.

$$\iiint \bar{M}_{e_o n\lambda}(h) \cdot \bar{N}_{e_o n'\lambda'}(-h')dV = 0$$

$$\iiint \bar{M}_{e_o n\lambda}(h) \cdot \bar{M}_{e_o n'\lambda'}(-h')\, dV = \iiint \bar{N}_{e_o n\lambda}(h) \cdot \bar{N}_{e_o n'\lambda'}(-h')\, dV$$

$$= 2\delta_{nn'}(1+\delta_o)\pi^2\lambda\,\delta(\lambda-\lambda')\,\delta(h-h') \qquad (2.25)$$

where δ_o is defined by

$$\delta_o = \begin{cases} 1 & n = 0 \\ 0 & n \neq 0 \end{cases}$$

and $\delta_{nn'}$ is defined by

$$\delta_{nn'} = \begin{cases} 1 & n=n' \\ 0 & n \neq n' \end{cases} .$$

2.4 Delta Function Expansion and Free Space Green's Function

We wish to find an expansion to the unit dyadic delta function of Eq. (2.3). The method of expansion used is the Ohm-Rayleigh or eigenfunction expansion method. First we write the delta function as an expansion over all possible eigenvalues (n, λ, h) of the eigenfunctions $\bar{M}$ and $\bar{N}$.

$$\bar{\bar{I}}\,\delta(\bar{R}-\bar{R}') = \int_0^\infty d\lambda \int_{-\infty}^{\infty} dh \sum_{n=o}^{\infty} \bar{M}_{e_o n\lambda}(h)\bar{A}_{e_o n\lambda}(h) + \bar{N}_{e_o n\lambda}(h)\bar{B}_{e_o n\lambda}(h) , \qquad (2.26)$$

with $\bar{A}$ and $\bar{B}$ being unknown vector functions to be determined. The λ integration is only semi-infinite because $J_1(\lambda r)$ is not independent of $J_1(-\lambda r)$. In order to find $\bar{A}$ and $\bar{B}$ we multiply (2.26) by $\bar{M}_{e_o n'\lambda'}(-h')$ and integrate over all space. As a result of (2.25) we obtain

$$\bar{A}_{e_o n\lambda}(h) = \frac{2-\delta_o}{4\pi^2\lambda}\,\bar{M}'_{e_o n\lambda}(-h)$$

where the $\bar{M}'$ indicates the vector wave function is defined with respect to the primed coordinate system (r', ϕ', z'). Similarly, multiplication by $\bar{N}_{e_o n'\lambda'}(-h')$ yields

$$\bar{B}_{e_o n\lambda}(h) = \frac{2-\delta_o}{4\pi^2\lambda}\,\bar{N}'_{e_o n\lambda}(-h) \quad .$$

Thus the final form of the expansion may be written

$$\bar{\bar{I}}\,\delta(\bar{R}-\bar{R}') = \frac{1}{4\pi^2}\int_{-\infty}^{\infty} dh \int_0^{\infty} \frac{d\lambda}{\lambda} \sum_{n=o}^{\infty} (2-\delta_o)$$

$$\left\{\bar{M}_{e_o n\lambda}(h)\bar{M}'_{e_o n\lambda}(-h) + \bar{N}_{e_o n\lambda}(h)\bar{N}'_{e_o n\lambda}(-h)\right\} \quad .$$

The free space dyadic Green's function $\bar{\bar{G}}_o$ satisfies (2.3) as well as the radiation condition. Expansion of $\bar{\bar{G}}_o$ in the form of (2.26) and substitution into (2.3) yields

$$\bar{\bar{G}}_o = \frac{1}{4\pi^2}\int_{-\infty}^{\infty} dh \int_0^{\infty} \frac{d\lambda}{\lambda} \sum_{n=o}^{\infty} \frac{(2-\delta_o)}{h^2+\lambda^2-k^2}$$

$$\left\{\bar{M}_{e_o n\lambda}(h)\bar{M}'_{e_o n\lambda}(-h) + \bar{N}_{e_o n\lambda}(h)\bar{N}'_{e_o n\lambda}(-h)\right\} \quad . \qquad (2.27)$$

The integration over h may be accomplished by treating h as a complex variable and making use of Cauchy's theorem. The result is

$$\bar{\bar{G}}_o(\bar{R}|\bar{R}') = \frac{i}{4\pi}\int_0^{\infty} \frac{d\lambda}{\lambda} \sum_{n=o}^{\infty} \frac{2-\delta_o}{h}$$

$$\begin{cases} \bar{M}_{e_o n\lambda}(h)\bar{M}'_{e_o n\lambda}(-h) + \bar{N}_{e_o n\lambda}(h)\bar{N}'_{e_o n\lambda}(-h) & z > z' \\ \bar{M}_{e_o n\lambda}(-h)\bar{M}'_{e_o n\lambda}(h) + \bar{N}_{e_o n\lambda}(-h)\bar{N}'_{e_o n\lambda}(h) & z < z' \end{cases}$$

where

$$h = \pm\sqrt{k^2-\lambda^2}\,.$$

The sign of $\sqrt{k^2-\lambda^2}$ is always chosen in such a way that the imaginary part of h is positive, therefore, insuring that the radiation condition is satisfied as $z \to \pm\infty$. ▲

2.5 Flat Earth Dyadic Green's Function

Assume that space is partitioned into two halves as illustrated in Fig. 1-1. The upper medium is assumed to be air while the lower half space is assumed to be a homogeneous lossy dielectric with a permeability equal to that of free space. The boundary between the two media is assumed to be a flat plane of infinite extent located at $z = 0$. This type of configuration corresponds to that of a flat earth. We assume that the constitutive constants of air are the same as free space ($\mu_o, \epsilon_o, \sigma = 0$) while the earth is characterized by the constants $(\mu_o, \epsilon_E, \sigma)$, $\sigma \neq \infty$. The propagation constants in the two media are thus

$$k^2 = k_o^2 = \omega^2 \mu_o \epsilon_o$$

$$k_E^2 = k_o^2 \left(\frac{\epsilon_E}{\epsilon_o} + i \frac{\sigma}{\omega \epsilon_o} \right)$$

where the subscript E stands for in the earth. The complex index of refraction may also be used to describe such a boundary. It is defined as

$$n^2 = \frac{\epsilon_E}{\epsilon_o} \left(1 + i \frac{\sigma}{\omega \epsilon_o}\right) \quad . \tag{2.28}$$

The electric field must satisfy

$$\nabla \times \nabla \times \bar{E} - k^2 \bar{E} = i\omega\mu_o \bar{J} \qquad z \geq 0$$

$$\nabla \times \nabla \times \bar{E} - k_E^2 \bar{E} = 0 \qquad z \leq 0$$

where we have assumed that there are no current sources in the earth. The field satisfies the following conditions on the boundary:

$$\hat{z} \times (\bar{E}-\bar{E}_E) = 0$$

$$\hat{z} \cdot (\bar{E}-n^2 \bar{E}_E) = 0 \quad .$$

The Green's function for this geometry is constructed by the scattering superposition method. We assume the Green's function has the following form:

$$\bar{\bar{G}}^{(11)}(\bar{R}|\bar{R}') = \bar{\bar{G}}_o(\bar{R}|\bar{R}') + \bar{\bar{G}}_s^{(11)}(\bar{R}|\bar{R}') \qquad z \geq 0$$

$$\bar{\bar{G}}^{(21)}(\bar{R}|\bar{R}') = \bar{\bar{G}}_s^{(21)}(\bar{R}|\bar{R}') \qquad z \leq 0 \quad .$$

The two scattering terms will be assumed to have the following forms:

$$\bar{\bar{G}}_s^{(11)} = \frac{i}{4\pi} \int_0^\infty \frac{d\lambda}{\lambda} \sum_{n=o}^{\infty} \frac{2-\delta_o}{h} \left\{ a \bar{M}_{o e n\lambda}(h) \bar{M}'_{o e n\lambda}(h) + b \bar{N}_{o e n\lambda}(h) \bar{N}'_{o e n\lambda}(h) \right\}$$

$$\bar{\bar{G}}_s^{(21)} = \frac{i}{4\pi} \int_0^\infty \frac{d\lambda}{\lambda} \sum_{n=o}^{\infty} \frac{2-\delta_o}{h} \left\{ c \bar{M}_{o e n\lambda}(-h_E) \bar{M}'_{o e n\lambda}(h) + d \bar{N}_{o e n\lambda}(-h_E) \bar{N}'_{o e n\lambda}(h) \right\} ,$$

where

$$h_E = \sqrt{k_E^2 - \lambda^2} \quad .$$

The imaginary part of h_E must be greater than zero. This in turn implies the sign of the square root function and eliminates any ambiguity.

We have chosen $\bar{M}(h)$ and $\bar{N}(h)$ as the anterior elements of $\bar{\bar{G}}_s^{(11)}$ because they will have to satisfy the radiation condition at $z \to \infty$. Similarly, we have chosen $\bar{M}(-h_E)$ and $\bar{N}(-h_E)$ because they are solutions to the vector wave equation in the earth and satisfy the radiation condition at $z \to -\infty$. The posterior elements are taken to be the same as those of $\bar{\bar{G}}_o$ when $z < z'$ in order to satisfy the boundary conditions at $z = 0$. The functions a, b, c and d

are to be determined such that $\overline{\overline{G}}$ will satisfy

$$\hat{z} \times \overline{\overline{G}}^{(11)} = \hat{z} \times \overline{\overline{G}}^{(21)}$$

$$\hat{z} \times \nabla \times \overline{\overline{G}}^{(11)} = \hat{z} \times \nabla \times \overline{\overline{G}}^{(21)}$$

on the boundary $z=0$. The necessary functions are

$$a = \frac{h-h_E}{h+h_E} \tag{2.29}$$

$$b = \frac{n^2 h-h_E}{n^2 h+h_E} \tag{2.30}$$

$$c = \frac{2h}{h+h_E} \tag{2.31}$$

$$d = \frac{2nh}{n^2 h+h_E} \quad . \tag{2.32}$$

The complete expressions for $\overline{\overline{G}}^{(11)}$ and $\overline{\overline{G}}^{(21)}$ are given below:

$$\overline{\overline{G}}^{(11)} = \frac{i}{4\pi} \int_0^\infty \frac{d\lambda}{\lambda} \sum_{n=0}^{\infty} \frac{2-\delta_o}{h} \cdot$$

$$\left\{ \begin{array}{l} \overline{M}_{e_{o}n\lambda}(h)\left[\overline{M}'_{e_{o}n\lambda}(-h)+a\,\overline{M}'_{e_{o}n\lambda}(h)\right]+\overline{N}_{e_{o}n\lambda}(h)\left[\overline{N}'_{e_{o}n\lambda}(-h)+b\,\overline{N}'_{e_{o}n\lambda}(h)\right] \quad z \geq z' \\ \left[\overline{M}_{e_{o}n\lambda}(-h)+a\overline{M}_{e_{o}n\lambda}(h)\right]\overline{M}'_{e_{o}n\lambda}(h)+\left[\overline{N}_{e_{o}n\lambda}(-h)+b\overline{N}_{e_{o}n\lambda}(h)\right]\overline{N}'_{e_{o}n\lambda}(h) \quad 0 \leq z \leq z' \end{array} \right. \tag{2.33}$$

$$\overline{\overline{G}}^{(21)} = \frac{i}{4\pi} \int_0^\infty \frac{d\lambda}{\lambda} \sum_{n=o}^{\infty} \frac{2-\delta_o}{h} \cdot$$

$$\cdot \left\{ c\bar{M}_{o_{e_{n\lambda}}}(-h_E)\bar{M}'_{o_{e_{n\lambda}}}(h) + d\bar{N}_{o_{e_{n\lambda}}}(-h_E)\bar{N}'_{o_{e_{n\lambda}}}(h) \right\} \quad z \leq 0 , \tag{2.34}$$

where a, b, c and d are given by Eqs. (2.29) through (2.32) and h and h_E are defined below.

$$h = \sqrt{k^2 - \lambda^2} \qquad \text{Im } h > 0$$

$$h_E = \sqrt{k_E^2 - \lambda^2} \qquad \text{Im } h_E > 0 .$$

Thus knowing $\overline{\overline{G}}$ the integral form of the fields due to a known current source, as given in Section 2.4 may be written

$$\bar{E}(\bar{R}) = i\omega\mu_o \iiint \overline{\overline{G}}^{(11)}(\bar{R}|\bar{R}') \cdot \bar{J}(\bar{R}')\, dV' \qquad z \geq 0$$

$$\bar{E}(\bar{R}) = i\omega\mu_o \iiint \overline{\overline{G}}^{(21)}(\bar{R}|\bar{R}') \cdot \bar{J}(\bar{R}')\, dV' \qquad z \leq 0$$

where it has been assumed that the current source is in the air. This dyadic Green's function will be used in Chapters III and IV to derive the field expressions for various types of antennas.

CHAPTER III

HERTZIAN DIPOLES

3.1 General Remarks

From this point on we will be dealing with various sources located above an imperfectly conducting ground. The geometry and assumptions are detailed in Section 2.5 where the dyadic Green's function for this case is derived. The Green's function will be used to find integral expressions for the fields in the region above the earth due to an x-directed and a z-directed Hertzian dipole. The fields below the earth are not needed for our calculations.

The fields will be shown to be equivalent to Sommerfeld's original results and then used to find the z component of Poynting's vector. Finally the integral expressions for S_+ and S_- are obtained by integration of Poynting's vector over surfaces above and below the antenna as outlined in Chapter I.

3.2 The Fields Due to a Hertzian Dipole above a Flat Earth

3.2.1 z-Directed Dipole. From Chapter II we know that the $\bar{E}$ field may be found from a knowledge of the currents and the dyadic Green's function. The specific relationship is repeated here.

$$\bar{E} = i\omega\mu_o \iiint \bar{\bar{G}}(\bar{R}|\bar{R}') \cdot \bar{J}(\bar{R}')\, dV' \qquad (2.15)$$

For a z-directed infinitesimal dipole located at a height z_o above the ground, the current distribution can be expressed as

$$\bar{J}(\bar{R}') = \hat{z}\, \delta(x'-0)\delta(y'-0)\delta(z'-z_o)\, I\ell \quad . \qquad (3.1)$$

The antenna current distribution is assumed to be uniform, with time dependence $e^{i-\omega t}$, and having a magnitude of I. If the length of the antenna is ℓ then in the limit as ℓ goes to zero the dipole moment $I\ell$ is assumed to have a finite value.

Since the Green's function for this case (2.33) and (2.34), contain posterior terms of the $\bar{M}'_{\substack{e\\o}n\lambda}(\pm h)$ and $\bar{N}'_{\substack{e\\o}n\lambda}(\pm h)$ type, the following two relationships, which arise from the explicit expressions for the $\bar{M}$ and $\bar{N}$ functions given in (2.21) and (2.22), will enable us to write the expression for the fields due to this source.

$$\iiint \bar{M}'_{\substack{e\\o}n\lambda}(\pm h)\cdot\bar{J}(\bar{R}')dV = 0 \tag{3.2}$$

$$\iiint \bar{N}'_{\substack{e\\o}n\lambda}(\pm h)\cdot\bar{J}(\bar{R}')dV = I\ell\,\frac{\delta_o\lambda^2}{k}\,e^{\pm ihz_o} \quad . \tag{3.3}$$

Equations (3.2) and (3.3) imply that the final expression for $\bar{E}$ will contain only terms of the $\bar{N}_{e0\lambda}$ type. Since the $\bar{M}$ functions have no z component, (3.2) would hold for any z-directed current source and implies that the field for these type currents would be represented in terms of the $\bar{N}$ type functions only.

The $\bar{E}$ field above the earth is found by substituting Eqs. (3.2) and (3.3) into (2.15), where $\bar{\bar{G}}$ is now the part of the Green's function Eq. (2.33) that applies for $z > 0$, and is expressed below.

$$\bar{E} = -\frac{\omega\mu_o I\ell}{4\pi k}\int_0^\infty d\lambda\,\frac{\lambda}{h}\begin{cases}\bar{N}_{e0\lambda}(h)\left[e^{-ihz_o}+be^{ihz_o}\right] & z > z_o\\ \left[\bar{N}_{e0\lambda}(-h)+b\bar{N}_{e0\lambda}(h)\right]e^{ihz_o} & 0 \le z < z_o\end{cases} \quad . \tag{3.4}$$

The magnetic field in the same region is found by use of one of Maxwell's equations:

$$\bar{H} = \frac{1}{i\omega\mu_o} \nabla \times \bar{E} \ .$$

This equation plus the relationships between $\bar{M}$ and $\bar{N}$ (given in Sect. 2.3), enable us to write directly:

$$\bar{H} = + \frac{i I \ell}{4\pi} \int_0^\infty d\lambda \frac{\lambda}{h} \begin{cases} \bar{M}_{e0\lambda}(h) \left[e^{-ihz_o} + b e^{ihz_o} \right] & z > z_o \\ \left[\bar{M}_{e0\lambda}(-h) + b \bar{M}_{e0\lambda}(h) \right] e^{ihz_o} & 0 \leq z < z_o \end{cases} \quad (3.5)$$

Sommerfeld originally derived the field from the Hertzian potential. For the z-directed dipole he found that a z-directed potential would work. This potential is expressed below.

$$\bar{\Pi} = \Pi_z \hat{z} = i \int_0^\infty \frac{\lambda}{h} d\lambda J_0(\lambda \ell) \left[e^{ih|z-z_o|} + b e^{ih|z+z_o|} \right] \hat{z} \quad z > 0 \ .$$

The electric field is derived from the Hertz potential as follows:

$$\bar{E} = \nabla \times \nabla \times \bar{\Pi} \ .$$

Note that

$$\bar{N}_{e0\lambda}(\pm h) = \frac{1}{k} \nabla \times \nabla \times (J_0(\lambda r) e^{\pm ihz} \hat{z}) \ .$$

Then Sommerfeld's expression for $\bar{E}$ may be written directly in terms of $\bar{N}$ functions as

$$\bar{E} = ik \int_0^\infty d\lambda \frac{\lambda}{h} \begin{cases} \bar{N}_{e0\lambda}(h) \left[e^{-ihz_o} + b e^{ihz_o} \right] & z > z_o \\ \left[\bar{N}_{e0\lambda}(-h) + b \bar{N}_{e0\lambda}(h) \right] e^{ihz_o} & 0 \leq z < z_o \end{cases} \ .$$

This equation agrees with (3.4) with the exception of Sommerfeld's normalization factor which is $\left(\frac{4\pi k^2}{i\omega\mu_o I \ell} \right)$.

3.2.2 x-Directed Dipole. For an x-directed infinitesimal dipole at height z_o with unit current moment, the current distribution may be written as

$$\bar{J}(\bar{R}') = \hat{x}\,\delta(x'-0)\delta(y'-0)\delta(z'-z_o)I\ell \quad .$$

The following equations arise from the definition of the $\bar{M}$ and $\bar{N}$ functions in Eqs. (2.21) and (2.22).

$$\iiint \bar{M}'_{\substack{e\\o}n\lambda}(\pm h)\cdot\bar{J}(\bar{R}')dV' = I\ell\,\delta_{n1}\frac{\lambda}{2}e^{\pm ihz_o} \quad \text{odd parts only} \tag{3.6}$$

$$\iiint \bar{N}'_{\substack{e\\o}n\lambda}(\pm h)\cdot\bar{J}(\bar{R}')dV' = I\ell\,\delta_{n1}\frac{\pm ih}{k}\frac{\lambda}{2}e^{\pm ihz_o} \quad \text{even parts only} \quad . \tag{3.7}$$

Equations (3.6) and (3.7) imply that only terms involving vector wave functions of the type $\bar{M}_{e1\lambda}(\pm h)$ and $\bar{N}_{e1\lambda}(\pm h)$ are needed to represent the field in this case. The $\bar{E}$ field is derived from Eqs. (2.15), (2.33), (3.6) and (3.7) and is

$$\bar{E} = -\frac{\omega\mu_o I\ell}{4\pi k}\int_0^\infty d\lambda \left[\frac{k}{h}\begin{Bmatrix}\bar{M}_{o1\lambda}(h)\left[e^{-ihz_o}+ae^{ihz_o}\right]\\ \left[\bar{M}_{o1\lambda}(-h)+a\bar{M}_{o1\lambda}(h)\right]e^{ihz_o}\end{Bmatrix}\right.$$
$$\left. +\,i\begin{Bmatrix}\bar{N}_{e1\lambda}(h)\left[-e^{-hz_o}+be^{ihz_o}\right] & z>z_o\\ \left[\bar{N}_{e1\lambda}(-h)+b\bar{N}_{e1\lambda}(h)\right]e^{ihz_o} & 0\le z<z_o\end{Bmatrix}\right] \tag{3.8}$$

The magnetic field is found using the method of Section 3.2.1 and is

$$\bar{H}=+\frac{iI\ell}{4\pi}\int_0^{\infty} d\lambda \left[\frac{k}{h} \left\{ \begin{matrix} \bar{N}_{o1\lambda}(h)\left[e^{-ihz_o}+ae^{ihz_o}\right] \\ \left[\bar{\bar{N}}_{o1\lambda}(-h)+a\bar{N}_{o1\lambda}(h)\right]e^{ihz_o} \end{matrix} \right\} \right.$$

$$\left. +i \left\{ \begin{matrix} \bar{M}_{e1\lambda}(h)\left[-e^{-ihz_o}+be^{ihz_o}\right] \\ \left[\bar{\bar{M}}_{e1\lambda}(-h)+b\bar{M}_{e1\lambda}(h)\right]e^{ihz_o} \end{matrix} \right\} \right] \begin{matrix} z > z_o \\ 0 \le z < z_o \end{matrix} \quad . (3.9)$$

For the x-directed dipole Sommerfeld found a Hertz potential with both $\hat{x}$ and $\hat{z}$ components , which can be written as

$$\bar{\Pi} = i\int_0^{\infty} d\lambda \frac{\lambda}{h} \left\{ J_0(\lambda r)\left[e^{ih|z-z_o|}+ae^{ih|z+z_o|}\right]\hat{x} \right.$$

$$\left. +i\frac{h}{\lambda}J_1(\lambda r)\cos\phi\,(a+b)\,e^{ih(z+z_o)} \right\}\hat{z} \quad .$$

The following two identities will be used to find $\bar{E}$:

$$\bar{N}^{(x)}_{e0\lambda}(\pm h)=\frac{1}{k}\nabla x\,\nabla x\left[J_o(\lambda r)e^{\pm ihz}\hat{x}\right]$$

$$\bar{N}_{e1\lambda}(\pm h)=\frac{1}{k}\nabla x\,\nabla x\left[J_1(\lambda r)\cos\phi\, e^{\pm ihz}\hat{z}\right]$$

where the $\bar{N}^{(x)}$ are cylindrical vector wave functions of the x type. The field is found from the Hertz potential as follows:

$$\bar{E}=\nabla x\,\nabla x\,\bar{\Pi} = ik\int_0^{\infty} d\lambda \frac{\lambda}{h} \left[\left\{ \begin{matrix} \bar{N}^{(x)}_{e0\lambda}(h)\left[e^{-ihz_o}+ae^{ihz_o}\right] \\ \left[\bar{N}^{(x)}_{e0\lambda}(-h)+\bar{N}^{(x)}_{e0\lambda}(h)\right]e^{ihz_o} \end{matrix} \right\} \right.$$

$$\left. +\frac{ih}{\lambda}\left\{(a+b)\,\bar{N}_{e1\lambda}(h)\,e^{ihz_o}\right\}, \right] \qquad (3.10)$$

where the upper line of $\bar{N}^{(x)}$ terms applies for $z > z_o$ and the lower line applies for $0 \leq z < z_o$. The $\bar{N}_{e1\lambda}(h)$ terms apply for $z \geq 0$.

The x type vector wave functions are related to the z type functions in general (see Ref. 23). Specifically it can be shown that

$$\bar{N}^{(x)}_{e0\lambda}(h) = -\frac{ih}{\lambda}\bar{N}_{e1\lambda}(h) + \frac{k}{\lambda}\bar{M}_{o1\lambda}(h) \quad .$$

If this identity for $\bar{N}^{(x)}_{eo\lambda}$ is substituted into (3.10) the result is

$$\bar{E} = ik\int_0^\infty d\lambda \frac{k}{h}\left[\begin{array}{l}\left\{\begin{array}{l}\bar{M}_{o1\lambda}(h)\left[e^{-ihz_o} + ae^{ihz_o}\right] \\ \left[\bar{M}_{o1\lambda}(-h) + a\bar{M}_{o1\lambda}(h)\right]e^{ihz_o}\end{array}\right\} \\ + \frac{ih}{k}\left\{\begin{array}{l}\bar{N}_{e1\lambda}(h)\left[-e^{-ihz_o} + be^{ihz_o}\right] \\ \left[\bar{N}_{e1\lambda}(-h) + b\bar{N}_{e1\lambda}(h)\right]e^{-ihz_o}\end{array}\right\}\end{array}\right] \begin{array}{l} z > z_o \\ 0 \leq z < z_o \end{array} ,$$

which agrees with Eq. (3.8) except for the normalization constant $\left(\frac{4\pi k^2}{i\omega\mu_o I\ell}\right)$. Thus the Sommerfeld result and the Green's function result are the same, as it should be.

3.2.3 Far-Zone Fields. The asymptotic form of Eqs. (3.4) and (3.8) as kR becomes very large are determined by the saddle point method of integration. This method and its limitations are discussed in detail in Appendix B. The asymptotic expression for the z directed dipole is

$$\bar{E} = \frac{i\omega\mu_o I\ell}{2\pi}\sin\theta\,\frac{e^{ikR}}{R}\left[e^{-ikz_o\cos\theta} + b(\theta)e^{ikz_o\cos\theta}\right]\hat{\theta}$$

and the asymptotic expression for the x directed dipole is

$$\bar{E} = -\frac{i\omega\mu_o I\ell}{2\pi}\,\frac{e^{ikR}}{R}\cdot\left\{ i\left[e^{-ikz_o\cos\theta} + a(\theta)e^{+ikz_o\cos\theta}\right]\sin\phi\,\hat{\phi} + \left[-e^{-ikz_o\cos\theta} + b(\theta)e^{+ikz_o\cos\theta}\right]\cos\theta\cos\phi\,\hat{\theta}\right\}$$

where $a(\theta)$ is the plane wave reflection coefficient for horizontally polarized waves while $b(\theta)$ is the corresponding coefficient for vertically polarized waves.

$$a(\theta) = \frac{\cos\theta - \sqrt{n^2 - \sin^2\theta}}{\cos\theta + \sqrt{n^2 - \sin^2\theta}} \quad , \quad b(\theta) = \frac{n^2\cos\theta - \sqrt{n^2 - \sin^2\theta}}{n^2\cos\theta + \sqrt{n^2 - \sin^2\theta}} \quad .$$

The power patterns given in Chapter V are normalized plots of $R^2\left|\bar{E}\right|^2$ where the $\bar{E}$ was calculated by using the asymptotic expressions given above.

3.3 Radiation Resistance and Efficiency

3.3.1 Poynting's Theorem. The time averaged z-directed Poynting's vector may be written

$$P_z = \frac{1}{2}\,\mathrm{Re}\left[\bar{E} \times \bar{H}^*\right]\cdot\hat{z} = \frac{1}{4}\left[E_r H_\phi^* + E_r^* H_\phi\right] . \qquad (3.11)$$

The integral of P_z over an infinite plane surface parallel to the ground will be called S_+ or S_- depending on whether the surface is above the antenna or below it. Poynting's theorem states that the surface integral of the time average Poynting's vector over a closed surface corresponds to the time average energy flow through the surface or the average power dissipated within the volume. The total power dissipated by the antenna is equal to $S_+ + S_-$ plus the integral of the r-directed Poynting's vector taken over a cylinder of infinite radius placed between the surfaces of integration used for S_+ and S_-. This integral is zero, because as we shall show, the integrals S_+ and S_- are independent of the location of their respective surface of integration as long as $z > z_o$ for S_+ and $0 \leq z < z_o$ for S_-. Thus the

radiation resistance R defined as

$$R = \frac{\oint\!\!\oint \bar{P} \cdot d\bar{s}}{I_o^2} = \frac{S_+ + S_-}{I_o^2} \qquad (3.12)$$

will be proportional to $S_+ + S_-$ (where I_o is the RMS value of the antenna input terminal current).

If we enclose the earth with an infinite surface, part of which is a surface directly on the earth air interface, then the integral of the normal Poynting's vector over this surface will be the power dissipated in the earth and is equal to S_- since the value of S_- is independent of the location of the surface of integration for $0 \leq z < z_o$.

Since the total antenna output power is $S_+ + S_-$ and the power dissipated in the earth is S_-, the radiated power must be equal to S_+. Reference 1 defines radiation efficiency as the ratio of radiated power to antenna input power. In this case radiation efficiency η will be

$$\eta = \frac{S_+}{S_+ + S_-} \,. \qquad (1.1)$$

Thus we see that both radiation resistance and radiation efficiency may be calculated from a knowledge of S_+ and S_-. Therefore in the following sections only expressions for S_+ and S_- will be derived. These expressions will be independent of the height of the surfaces of integration but dependent upon the source height z_o, and when evaluated may be used to find R and η as a function of z_o.

3.3.2 z-Directed Dipole. The fields that make up the z-directed Poynting's vector are E_r, H_ϕ, E_ϕ and H_r. For the z-directed Hertzian dipole these are found (using Eqs. (3.4), (3.5) and the definitions of the $\bar{M}$ and $\bar{N}$ functions) to be

$$E_r = \frac{i\omega\mu_o I\ell}{4\pi k^2}\int_0^\infty d\lambda\,\lambda^2 J_1(\lambda r)\left[\mp e^{ih|z-z_o|} + be^{ih|z+z_o|}\right]$$

$$= \frac{i\omega\mu_o I\ell}{4\pi k^2}\int_0^\infty d\lambda\,\lambda^2 J_1(\lambda r) f_1(h,z) \quad ,$$

$$H_\phi = +\frac{iI\ell}{4\pi}\int_0^\infty d\lambda\,\lambda^2\, J_1(\lambda r)\left[-\frac{e^{ih|z-z_o|} + be^{ih|z+z_o|}}{h}\right]$$

$$= +\frac{iI\ell}{4\pi}\int_0^\infty d\lambda\,\lambda^2 J_1(\lambda r) f_2(h,z) \quad ,$$

$$E_\phi = 0 \ ,$$

$$H_r = 0$$

where the upper sign corresponds to the region $z > z_o$ and the lower sign corresponds to the region $0 \leq z < z_o$. Thus the integral of the z-directed Poynting's vector over a plane surface can be written in this case as

$$S_{\mp} = \mp\frac{1}{2}\,\mathrm{Re}\int_0^\infty r\,dr\int_0^{2\pi} d\phi\left[\bar{E}\times\bar{H}^*\cdot\hat{z}\right] = \mp\pi\,\mathrm{Re}\int_0^\infty r\,dr\;E_r H_\phi^* \quad .$$

Substituting for E_r and H_ϕ we find

$$S_{\mp} = \mp\frac{\omega\mu_o I^2\ell^2}{16\pi k^2}\,\mathrm{Re}\int_0^\infty d\lambda\lambda^2\int_0^\infty d\ell\,\ell^2\int_0^\infty r\,dr\left[J_1(\lambda r)J_1(\ell r)\right]$$

$$\left[f_1(h, z_{\mp})f_2^*(h_\ell, z_{\mp})\right] \ ,$$

where ℓ is used for one variable of integration instead of λ , and h_ℓ is defined by

$$h_\ell^2 = k^2 - \ell^2 \quad .$$

Since the plane of integration is at a fixed height, say $z_+ > z_o$ for S_+ and $0 \leq z_- < z_o$ for S_-, $f_1(h,z)$ and $f_2(h,z)$ are evaluated at z_+ or z_- depending upon whether or not S_+ or S_- is being calculated. The notation $z_{\pm}$ implies the use of z_+ for S_+ and z_- for S_-. Applying the general orthogonality relationship for Bessel's functions*

$$\int_0^\infty J_n(\lambda r)J_n(\ell r)r\,dr = \frac{\delta(\lambda-\ell)}{\sqrt{\lambda\ell}} \tag{3.13}$$

we obtain the following

$$S_{\pm} = \pm \frac{\omega\mu_o I^2 \ell^2}{16\pi k^2} \operatorname{Re} \int_0^\infty d\lambda\, \lambda^3 \left[f_1(h, z_{\pm}) f_2(h, z_{\pm})\right] . \tag{3.14}$$

This equation may be shown to agree with Sommerfeld and Renner's result again excepting the normalization constant** .

From Chapter II it is recalled that the spectral variable h is defined as

$$h = \sqrt{k^2-\lambda^2} \qquad \begin{matrix} \operatorname{Im} h \leq 0 \\ \operatorname{Re} h \leq 0 \end{matrix} .$$

In our case k is real and thus h will be real for $\lambda \leq k$ and imaginary for $\lambda > k$. Therefore,

$$h-h^* = \begin{cases} 0 & \lambda \leq k \\ 2h & \lambda > k \end{cases} . \tag{3.15}$$

---

*See, for example, Ref. 13, page 111.

**Sommerfeld defines the spectral variable $\mu^2 = \lambda^2 - R^2$. Thus, the verification procedure involves the substitution of $\mu = -ih$ in Sommerfeld's equations. See Ref. 13, page 272.

These equations will be used to simplify the expression for $S_{\pm}$ of Eq. (3.14). Expand the function $\left[f_1 f_2^*\right]$:

$$\left[f_1(h, z_{\pm}) \cdot f_2^*(h, z_{\pm})\right] =$$

$$\left(\pm e^{\pm ih\,|z_{\pm}-z_o|} + be^{ih(z_{\pm}+z_o)}\right)\left(\frac{e^{-ih^*|z_{\pm}-z_o|} + b^* e^{-ih^*(z_{\pm}+z_o)}}{h^*}\right)$$

$$= \pm\frac{1}{h^*} e^{i(h-h^*)\,|z_{\pm}+z_o|} \pm \frac{b^*}{h^*} e^{ih\,|z_{\pm}-z_o| - ih^*(z_{\pm}+z_o)}$$

$$+ \frac{b}{h^*} e^{ih(z_{\pm}+z_o) - ih\,|z_{\pm}-z_o|} + \frac{bb^*}{h^*} e^{i(h-h^*)(z_{\pm}+z_o)} \quad . \tag{3.16}$$

The real part of the first term of (3.16) may be reduced using (3.15).

$$\mathrm{Re}\left\{\pm\frac{1}{h^*} e^{i(h-h^*)\,z_{\pm}-z_o}\right\} = \begin{cases} \pm\dfrac{1}{h} & \lambda \leq k \\ 0 & \lambda > k \end{cases} \quad .$$

Note the independence of $z_{\pm}$. Similarly, the real part of term four of Eq. (3.16) may be written

$$\mathrm{Re}\left\{\frac{bb^*}{h^*} e^{i(h-h^*)(z+z_o)}\right\} = \begin{cases} \dfrac{bb^*}{h} & \lambda \leq k \\ 0 & \lambda > k \end{cases} \quad .$$

Again there is no dependence on $z_{\pm}$. In order to reduce terms two and three they are combined, but separate consideration must be given to the $z > z_o$ and $0 \leq z < z_o$ cases. First, we consider the real part of terms two and three for $z > z_o$.

$$\mathrm{Re}\left\{\frac{b^*}{h^*}e^{ih(z_+-z_o)-ih^*(z_++z_o)}+\frac{b}{h^*}e^{ih(z_++z_o)-ih^*(z_+-z_o)}\right\}$$

$$=\mathrm{Re}\left\{\frac{b^*}{h^*}e^{i(h-h^*)z_+-i(h+h^*)z_o}+\frac{b}{h^*}e^{i(h-h^*)z_++i(h+h^*)z_o}\right\}$$

$$=\mathrm{Re}\left\{\frac{1}{h^*}\left(be^{i(h+h^*)z_o}+b^*e^{-i(h+h^*)z_o}\right)e^{i(h-h^*)z_+}\right\}.$$

The term in brackets is real because it is the sum of complex conjugates and in light of (3.15) this term may be written

$$\frac{1}{h}\left(be^{2ihz_o}+b^*e^{-2ihz_o}\right)\quad \lambda\leq k$$

$$0\quad \lambda>k\quad .$$

This expression is again independent of z_+. Now consider terms two and three of (3.16) for $0\leq z<z_o$.

$$\mathrm{Re}\left\{-\frac{b^*}{h^*}e^{ih(z_o-z_-)-ih^*(z_o+z)}+\frac{b}{h^*}e^{ih(z_o+z_-)-ih^*(z_o-z_-)}\right\}$$

$$=\mathrm{Re}\left\{-\frac{b^*}{h^*}e^{-i(h+h^*)z_-+i(h-h^*)z_o}+\frac{b}{h^*}e^{i(h+h^*)z_-+i(h-h^*)z_o}\right\}$$

$$=\mathrm{Re}\left\{\frac{1}{h^*}\left(be^{i(h+h^*)z_-}-b^*e^{-i(h-h^*)z_-}\right)e^{i(h-h^*)z_o}\right\}. \qquad (3.17)$$

In this case the term in brackets is imaginary since it is the difference of complex conjugates and in view of Eqs. (3.15), Eq. (3.17) becomes

$$\frac{1}{h^*}\left[b-b^*\right]e^{2ih^*z_o}\quad \lambda\geq k$$

$$0\quad \lambda<k\quad .$$

Define S_r as

$$S_r = \lim_{r \to \infty} \int_0^{2\pi} \int_{z_-}^{z_+} r \, d\phi \, dz \, P_r \, .$$

Then from Poynting's theorem the total output power of the antenna is

$$\text{Power output} = S_+ + S_- + S_r = \text{constant.}$$

Since S_+ and S_- are independent of z_+ and z_-, then S_r is also independent of z_+ and z_-. Its value is seen to be zero if both z_+ and z_- are allowed to approach z_o. If z_+ is allowed to approach infinity before r is increased the result for S_r may be different. However the sum of S_r and S_+ remains unchanged.

The S_+ terms are all 0 for $\lambda > k$ and therefore the λ integration of (3.14) will have limits of 0 and k for S_+. While for S_- there will be two integrals, one with limits of 0 and k, and the other with limits of k and ∞. The resulting expressions for S_+ and S_- are

$$S_+ = \frac{\omega \mu_o I^2}{16\pi k^2 \ell^2} \int_0^k d\lambda \frac{\lambda^3}{h} \left\{ 1 + bb^* + be^{2ihz_o} + b^* e^{-2ih^* z_o} \right\} \qquad (3.18)$$

$$S_- = -\frac{\omega \mu_o I_o^2}{16\pi k^2 \ell^2} \left\{ \int_0^k d\lambda \frac{\lambda^3}{h} (1 + bb^*) + \int_k^\infty d\lambda \frac{\lambda^3}{h^*} \left[be^{2ihz_o} - b^* e^{-2ih^* z_o} \right] \right\}. \qquad (3.19)$$

The integrations in (3.18) and (3.19) are with respect to λ while the function b and the exponential terms are given in terms of h. Therefore, it is convenient to transform the integrations to the h variable. Thus in (3.18) let

$$\lambda^2 = k^2 - h^2$$

then

$$\lambda^3 d\lambda = -(k^2 - h^2) \, h \, dh$$

and the respective limits will go from k to 0 . Reversing sign and limits we have

$$S_+ = \frac{\omega \mu_o I^2}{16\pi k^2 \ell^2} \int_0^i dh(k^2-h^2)\left\{1+bb^*+be^{2ihz_o}+b^*e^{-2ihz_o}\right\} . \qquad (3.20)$$

For the S_- expression of (3.19) we use the same substitution for λ . The first integral transformation is the same as the one for S_+ however the second integral has different limits and will be handled as follows

$$\int_k^\infty \frac{\lambda^3 d\lambda}{h^*} = +\int_0^{i\infty} (k^2-h^2)dh \quad .$$

Thus the equation for S_- becomes

$$S_- = -\frac{\omega \mu_o I^2}{16\pi k^2 \ell^2}\left\{\int_0^k dh(k^2-h^2)\,(1-bb^*) + \int_0^{i\infty} dh(k^2-h^2)\left(be^{2ihz_o}-b^*e^{-2ih^*z_o}\right)\right\} . \qquad (3.21)$$

In order to identify the free space and perfectly conducting parts of the expressions for $S_\pm$ the function b will be written in two parts, a constant plus a term with a limit of zero as perfect conductivity is approached.

$$b = \frac{n^2h-h_E}{n^2h+h_E} = 1 - \frac{2h_E}{n^2h+h_E} = 1 - B . \qquad (3.22)$$

Note that B approaches zero in the limit of perfect conductivity (i.e., $n^2 = i\infty$).

Substituting (3.22) for b in (3.20) and (3.21) and using the following changes of variables

$$h = ku \text{ for } \int_0^k$$

and

$$h = ikv \quad \text{for} \int_0^{i\infty}$$

we obtain

$$S_+ = \frac{\omega\mu_o k I^2 \ell^2}{16\pi} \int_0^1 du(1-u^2)\left\{2+2\cos \xi u + |B|^2 - (B+B^*) - 2RE\,(Be^{i\xi u})\right\},$$

$$S_- = -\frac{\omega\mu_o k I^2 \ell^2}{16\pi}\left\{\int_0^1 du(1-u^2)\left[(B+B^*) - |B|^2\right] + 2\,\mathrm{Im}\int_0^\infty dv(1+v^2)Be^{-\xi V}\right\}$$

where $\xi = 2kz_o$ and it is understood that B has been transformed from a function of h to a function of u or v depending upon the variable of integration. In the perfectly conducting case the only two non-zero terms are the first two terms of S_+. These terms may be integrated in closed form to give

$$\lim_{n^2 \to \infty} S_+ = \frac{\omega\mu_o k I^2 \ell^2}{12\pi}\left\{1+3\,\frac{\sin\xi - \xi\cos\xi}{\xi^3}\right\}.$$

For the perfectly conducting case S_- is zero and the radiation resistance will be S_+ divided by the RMS value of input current squared ($I^2/2$) or

$$R = \frac{\omega\mu_o k\ell^2}{16\pi}\left\{1+3\,\frac{\sin\xi-\xi\cos\xi}{\xi^3}\right\} \doteq 798\,(\frac{\ell}{\lambda})^2\left\{1+3\,\frac{\sin\xi-\xi\cos\xi}{\xi^3}\right\}.$$

This expression agrees with the result obtained by integration of the far field Poynting vector due to a dipole above a perfectly conducting ground. Note that the variable part approaches zero as z_o goes to infinity and the constant, or free space term agrees with Kraus' result (Ref. 24, pg. 137).

The final results for S_+ and S_- are normalized by this free space radiation resistance times $I^2/2$ and are given below

$$S_+ = 1+3\frac{\sin\xi-\xi\cos\xi}{\xi^3}+\frac{3}{4}\int_0^1 du\,(1-u^2)\left(|B|^2-(B+B^*)\right)$$

$$-\frac{3}{2}\,\mathrm{Re}\int_0^1 Be^{i\xi u}(1-u^2)du \qquad (3.23)$$

$$S_- = -\frac{3}{4}\int_0^1 du(1-u^2)\left(|B|^2-(B+B^*)\right)-\frac{3}{2}\,\mathrm{Im}\int_0^\infty dv(1+v^2)Be^{-\xi v} \qquad (3.24)$$

These results are used in Chapter V to obtain numerical results for radiation resistance and efficiency.

3.3.3 x-Directed Dipole. The fields necessary to find the z component of Poynting's vector are E_r, H_ϕ, E_ϕ and H_r. For the x-directed Hertzian dipole they are found from (3.8) and (3.9) to be

$$E_r = -\frac{\omega\mu_o I\ell}{4\pi k}\int_0^\infty d\lambda\left\{\frac{k}{h}\frac{J_1(\lambda r)}{r}\left[e^{ih|z-z_o|}+ae^{ih(z+z_o)}\right]\right.$$

$$\left.+\frac{h}{k}\frac{dJ_1(\lambda r)}{dr}\left[e^{ih|z-z_o|}-be^{ih(z+z_o)}\right]\right\}\cos\phi$$

$$=-\frac{\omega\mu_o I\ell}{4\pi k}\int_0^\infty d\lambda\left\{\frac{J_1(\lambda r)}{r}f_1(h,z)+\frac{\partial J_1(\lambda r)}{\partial r}f_2(h,z)\right\}\cos\phi$$

$$H_\phi = -\frac{I\ell}{4\pi}\int_0^\infty d\lambda\left\{\frac{J_1(kr)}{r}\left[\pm e^{ih|z-z_o|}+ae^{ih(z+z_o)}\right]+\right.$$

$$\left.\frac{\partial J_1(\lambda r)}{\partial r}\left[\pm e^{ih|z-z_o|}-be^{ih(z+z_o)}\right]\right\}\cos\phi$$

$$=-\frac{I\ell}{4\pi}\int_0^\infty d\lambda\left\{\frac{J_1(\lambda r)}{r}f_3(h,z)+\frac{\partial J_1(\lambda r)}{\partial r}f_4(h,z)\right\}\cos\phi$$

$$E_\phi = + \frac{\omega \mu_o I \ell}{4\pi k} \int_0^\infty d\lambda \left\{ \frac{k}{h} \cdot \frac{\partial J_1(\lambda r)}{\partial r} \left[e^{ih|z-z_o|} + ae^{ih(z+z_o)} \right] \right.$$

$$\left. + \frac{h}{k} \frac{J_1(\lambda r)}{r} \left[e^{ih|z-z_o|} - be^{ih(z+z_o)} \right] \right\} \sin \phi$$

$$= + \frac{\omega \mu_o I \ell}{4\pi k^2} \int_0^\infty d\lambda \left\{ \frac{dJ_1(\lambda r)}{\partial r} f_1(h, z) + \frac{J_1(\lambda r)}{r} f_2(h, z) \right\} \sin \phi$$

$$H_r = - \frac{I \ell}{4\pi} \int_0^\infty d\lambda \left\{ \frac{\partial J_1(\lambda r)}{\partial r} \left[\pm e^{ih|z-z_o|} + ae^{ih(z+z_o)} \right] \right.$$

$$\left. + \frac{J_1(\lambda r)}{r} \left[\pm e^{ih|z-z_o|} - be^{ih(z+z_o)} \right] \right\} \sin \phi$$

$$= - \frac{I \ell}{4\pi} \int_0^\infty d\lambda \left\{ \frac{\partial J_1(\lambda r)}{\partial r} f_3(h, z) + \frac{J_1(\lambda r)}{r} f_4(h, z) \right\} \sin \phi \, .$$

For this case E_ϕ and H_r are not zero and therefore the integral of the z-directed Poynting's vector over a plane surface will be

$$S_\pm = \pm \frac{1}{2} \mathrm{Re} \int_0^\infty \int_0^{2\pi} (E_r H_\phi^* - E_\phi H_r^*) \, r \, dr \, d\phi \quad .$$

The ϕ integration is easily done since

$$\int_0^{2\pi} \begin{matrix} \cos^2 \phi \\ \sin^2 \phi \end{matrix} d\phi = \pi$$

leaving

$$S_{\pm} = \frac{\omega\mu_o I^2 \ell^2}{32\pi k} \mathrm{Re} \int_0^\infty r\,dr \int_0^\infty d\lambda \int_0^\infty d\ell \Bigg[f_1(h, z_{\pm}) f_3^*(h_\ell, z_{\pm}) \left\{ \frac{J_1(\lambda r)}{r} \frac{J_1(\ell r)}{r} + \frac{\partial J_1(\lambda r)}{\partial r} \frac{\partial J_1(\ell r)}{\partial r} \right\}$$

$$+ f_1(h, z_{\pm}) f_4^*(h_\ell, z_{\pm}) \left\{ \frac{J_1(\lambda r)}{r} \frac{\partial J_1(\ell r)}{\partial r} + \frac{\partial J_1(\lambda r)}{\partial r} \frac{\partial J_1(\ell r)}{\partial r} \right\}$$

$$+ f_2(h, z_{\pm}) f_3^*(h_\ell, z_{\pm}) \left\{ \frac{\partial J_1(\lambda r)}{\partial r} \frac{J_1(\ell r)}{r} + \frac{J_1(\lambda r)}{r} \frac{\partial J_1(\ell r)}{\partial r} \right\}$$

$$+ f_2(h, z_{\pm}) f_4^*(h_\ell, z_{\pm}) \left\{ \frac{\partial J_1(\lambda r)}{\partial r} \frac{\partial J_1(\ell r)}{\partial r} + \frac{J_1(\lambda r)}{r} \frac{J_1(\ell r)}{r} \right\} \Bigg], \quad (3.25)$$

where we have used ℓ instead of λ for one variable of integration and define h_ℓ as follows

$$h_\ell^2 = k^2 - \ell^2 \ .$$

In order to proceed with the r integration of (3.25), we need to know the result of the following two integrals:

$$\int_0^\infty r\,dr \left\{ \frac{\partial J_1(\lambda r)}{\partial r} \frac{J_1(\ell r)}{r} + \frac{J_1(\lambda r)}{r} \frac{\partial J_1(\ell r)}{\partial r} \right\} = 0$$

$$\int_0^\infty r\,dr \left\{ \frac{J_1(\lambda r)}{r} \frac{J_1(\ell r)}{r} + \frac{\partial J_1(\lambda r)}{\partial r} \frac{\partial J_1(\ell r)}{\partial r} \right\} = \sqrt{\lambda\ell}\ \delta(\lambda - \ell) \ .$$

The first integral may be evaluated from the fact that

$$\frac{1}{r} \frac{d}{dr} \left\{ J_1(\lambda r) J_1(\ell r) \right\} = \left\{ \frac{\partial J_1(\lambda r)}{\partial r} \frac{J_1(\ell r)}{r} + \frac{J_1(\lambda r)}{r} \frac{\partial J_1(\ell r)}{\partial r} \right\} \ .$$

Therefore the integral will be

$$\int_0^\infty \frac{d}{dr}\left\{J_1(\lambda r)J_1(\ell r)\right\}dr = J_1(\lambda r)J_1(\ell r)\Big|_0^\infty = 0 \ .$$

The second integral may be evaluated by using the following identity:

$$\left\{\frac{J_1(\lambda r)}{4r}\,\frac{J_1(\ell r)}{r} + J\,\frac{\partial J_1(\lambda r)}{\partial r}\,\frac{\partial J_1(\ell r)}{\partial r}\right\} = \lambda\ell\left\{J_0(\lambda r)J_0(\ell r) - \frac{1}{r}\,\frac{d}{dr}\,J_1(\lambda r)J_1(\ell r)\right\} \ .$$

Therefore the integral becomes

$$\lambda\ell\int_0^\infty dr\ r\ J_0(\lambda r)J_0(\ell r) - \lambda\ell\int_0^\infty \frac{\partial}{\partial r}\left\{J_1(\lambda r)J_1(\ell r)\right\}dr$$

$$= \frac{\lambda\ell}{\sqrt{\lambda\ell}}\,\delta(\ell-\lambda) - \lambda\ell\ J_1(\lambda r)J_1(\ell r)\Big|_0^\infty = \sqrt{\lambda\ell}\ \delta(\ell-\lambda) \ .$$

Thus the integration of (3.25) yields

$$S_{\pm} = \frac{\omega\mu_o I^2\ell^2}{32\pi k}\,\mathrm{Re}\int_0^\infty d\lambda\ \lambda\left[f_1(h,z_{\pm})\ f_3^*(h,z_{\pm}) + f_2(h,z_{\pm})f_4^*(h,z_{\pm})\right] \ . \tag{3.26}$$

The contents of the brackets can be expanded as follows

$$\left[f_1 f_3^* + f_2 f_4^*\right] = \pm\left\{\frac{k}{h}+\frac{h}{k}\right\} e^{i(h-h^*)|z-z_o|} + \left\{\frac{k}{h}a^* - \frac{h}{k}b^*\right\} e^{ih|z-z_o| - ih^*(z+z_o)}$$

$$\pm\left\{\frac{k}{h}a - \frac{h}{k}b\right\} e^{ih(z+z_o) - ih^*|z-z_o|} + \left\{\frac{k}{h}aa^* + \frac{h}{k}bb^*\right\} e^{i(h-h^*)(z+z_o)} .$$

The real part of each term is examined using the fact that h is real for $\lambda \leq k$ and imaginary for $\lambda > k$. First consider the real part of term one.

$$\pm \mathrm{Re}\left\{\frac{k}{h}+\frac{h}{k}\right\} e^{i(h-h^*)|z_\pm - z_o|} = \pm \begin{cases} \left(\frac{k}{h}+\frac{h}{k}\right) & \lambda \leq k \\ 0 & \lambda > k \end{cases} .$$

An examination of term four yields

$$\mathrm{Re}\left(\frac{k}{h}|a|^2 + \frac{h}{k}|b|^2\right) e^{i(h-h^*)(z_\pm + z_o)} = \begin{cases} \frac{k}{h}|a|^2 + \frac{h}{k}|b|^2 & \lambda \leq k \\ 0 & \lambda > k \end{cases} .$$

Terms two and three are considered together and yield a different result for z_+ and z_-. First, consider the z_+ case

$$\left\{\frac{k}{h}a^* - \frac{h}{k}b^*\right\} e^{i(h-h^*)z_+ - i(h+h^*)z_o} + \left\{\frac{k}{h}a - \frac{h}{k}b\right\} e^{i(h-h^*)z_+ + i(h+h^*)z_o}$$

$$= \left\{\frac{k}{h}\left(ae^{i(h+h^*)z_o} + a^* e^{-i(h+h^*)z_o}\right) - \frac{h}{k}\left(be^{i(h+h^*)z_-} + b^* e^{-i(h+h^*)z_-}\right)\right\} e^{i(h-h^*)z_o} .$$

Since both terms in brackets are always real, the real part of terms two and three reduces to

$$\begin{cases} 2\,\mathrm{Re}\left\{\frac{k}{h}\,a e^{2ihz_o} - \frac{h}{k}\,b e^{2ihz_o}\right\} & \lambda \leq k \\ 0 & \lambda > k \end{cases} .$$

Now we examine terms two and three for $0 \leq z_- < z_o$.

$$\left\{\frac{k}{h}a^* - \frac{h}{k}\,b^*\right\} e^{-i(h+h^*)z_- + i(h-h^*)z_o} - \left\{\frac{k}{h}a - \frac{h}{k}\,b\right\} e^{i(h+h^*)z_- + i(h-h^*)z_o}$$

$$= \left\{\frac{k}{h}\left(-a e^{i(h+h^*)z_-} + a^* e^{-i(h+h^*)z_-}\right) + \frac{h}{k}\left(b e^{i(h+h^*)z_-} - b^* e^{-i(h+h^*)z_-}\right)\right\} e^{i(h-h^*)z_o} .$$

In this case both terms in brackets are imaginary and the entire term will be real only when h is imaginary or for $\lambda \geq k$. Thus the real part of terms two and three for z_- becomes

$$\begin{cases} 2\ \mathrm{Im}\left\{-\frac{k}{h}\,a + \frac{h}{k}\,b\right\} e^{2ihz_o} & \lambda \geq k \\ 0 & 0 \leq \lambda < k \end{cases} .$$

As in the vertical dipole case all of these expressions are independent of $z_\pm$. This fact implies that the surface integral of the r-directed Poynting's vector over an infinite circular cylinder will be zero. The above terms are now substituted in (3.26) to give

$$S_+ = -\frac{\omega\mu_o I^2 \ell^2}{32\pi k}\,\mathrm{Re}\int_0^k d\lambda\,\lambda \left\{ + \left(\frac{k}{h} + \frac{h}{k}\right) + \frac{k}{h}\,|a|^2 + \frac{h}{k}\,|b|^2 + 2\,\mathrm{Re}\left(\frac{k}{h}\,a - \frac{h}{k}\,b\right) e^{2ihz_o} \right\} \qquad (3.27)$$

$$S_- = -\frac{\omega\mu_o I^2 \ell^2}{32\pi k}\,\mathrm{Re}\left\{\int_0^k d\lambda\,\lambda\left[-\left(\frac{k}{h}+\frac{h}{k}\right)+\frac{k}{h}|a|^2+\frac{h}{k}|b|^2\right]\right.$$

$$\left. +2\ \mathrm{Im}\int_k^\infty d\lambda\,\lambda\left[-\frac{k}{h}a+\frac{h}{k}b\right]e^{2ihz_o}\right\}. \qquad (3.28)$$

The function a may be expanded into a perfectly conducting part plus a perturbation similar to (3.22) for b.

$$a = \frac{h-h_E}{h+h_E} = 1 + \frac{2h}{h+h_E} = -1 + A \qquad (3.29)$$

$$b = 1 - B\,, \qquad (3.30)$$

where $h_E^2 = k_E^2 - \lambda^2 = n^2k^2 - \lambda^2$. It is seen that A approaches zero as n^2 approaches i ∞. If (3.29) and (3.30) are substituted in the equations for $S_\pm$ and the variable of integration is changed from λ to h we obtain

$$S_+ = \frac{\omega\mu_o I^2 \ell^2}{32\pi k}\,\mathrm{Re}\int_0^k dh\,h\left\{2\left(\frac{k}{h}+\frac{h}{k}\right)-2\,\mathrm{Re}\left[\left(\frac{k}{h}+\frac{h}{k}\right)e^{2ihz_o}\right]\right.$$

$$\left. +\frac{k}{h}\left(|A|^2-(A+A^*)\right)+\frac{h}{k}\left(|B|^2-(B+B^*)\right)+2\mathrm{Re}\left[\left(\frac{k}{h}A+\frac{h}{k}B\right)e^{2ihz_o}\right]\right\}$$

$$S_- = -\frac{\omega\mu_o I^2 \ell^2}{32\pi k}\,\mathrm{Re}\left\{\int_0^k dh\,h\left[\frac{k}{h}\left(|A|^2-(A+A^*)\right)+\frac{h}{k}\left(|B|^2-(B+B^*)\right)\right]\right.$$

$$\left. +2\ \mathrm{Im}\int_0^{i\infty} dh\,h\left[\left(-\frac{k}{h}A-\frac{h}{k}B\right)e^{2ihz_o}\right]\right\}.$$

Note that the first two terms of S_+ are integrable in closed form as

$$\int_0^k dh\,h\left(\frac{k}{h}+\frac{h}{k}\right) = \frac{4}{3}k^2\,,$$

$$\mathrm{Re}\int_0^k \left\{\left(\frac{k}{h}+\frac{h}{k}\right)e^{2ihz_o}\right\} h\,dh = 2k^2\,\frac{(\xi^2-1)\sin\xi+\xi\cos\xi}{\xi^3}$$

where

$$\xi = 2kz_o \quad .$$

Using these two equations plus the following changes of variables

$$\text{for}\int_0^k h\,dh \qquad \text{use } h = ku$$

$$\text{for}\int_0^{i\infty} h\,dh \qquad \text{use } h = ikv$$

gives

$$S_+ = \left\{1 - \frac{3}{2}\,\frac{(\xi^2-1)\sin\xi+\xi\cos\xi}{\xi^3} + \frac{3}{8}\int_0^1 du\left[\left(|A|^2-(A+A^*)\right)+u^2\left(|B|^2-(B+B^*)\right)+2\,\mathrm{Re}\left\{(A+u^2B)e^{i\xi u}\right\}\right]\right\} \tag{3.31}$$

$$S_- = -\left\{\frac{3}{8}\int_0^1 du\left[\left(|A|^2-(A+A^*)\right)+u^2\left(|B|^2-(B+B^*)\right)\right] - \frac{3}{4}\,\mathrm{Im}\int_0^\infty dv\,(A-v^2B)e^{-\xi v}\right\}, \tag{3.32}$$

where both equations have been normalized to the free space radiation resistance times $(I^2/2)$ or

$$798\left(\frac{\ell}{\lambda}\right)^2\frac{I^2}{2} \quad .$$

This means that the radiation resistance of this antenna is

$$R = 798 \left(\frac{\ell}{\lambda}\right)^2 (S_+ + S_-) \text{ ohms} . \tag{3.33}$$

The portion of (3.33) that corresponds to the radiation resistance of a dipole in free space is in agreement with the result quoted by Kraus, while the term that corresponds to the perturbation due to a perfectly conducting ground checks with Sommerfeld's result.

These expressions have been used to obtain numerical results for the radiation efficiency and radiation resistance of a horizontal Hertzian dipole. The curves are given in Chapter IV.

CHAPTER IV

LONG VERTICAL DIPOLES WITH SINUSOIDAL CURRENT DISTRIBUTIONS

4.1 The Fields Due to a Vertical Dipole of Arbitrary Length

4.1.1 General Field Expressions . The geometry for the case of a long center fed vertical dipole is illustrated in Fig. 4-1.

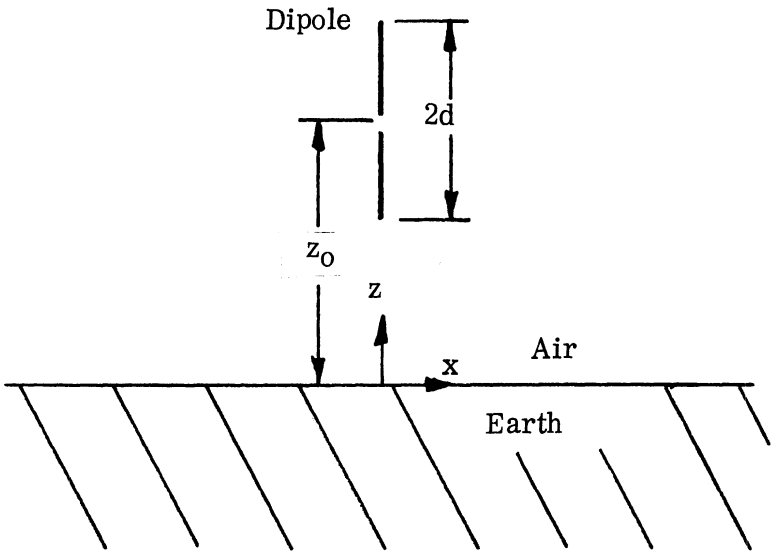

FIG. 4-1: Geometry for the Long Vertical Dipole

The center, or feed point, of the dipole is assumed to be at the point $(0, 0, z_0)$ while the total length of the antenna is assumed to be $2d$. The center height of the antenna is always greater than or equal to the half length of the antenna so that the antenna never enters the earth. Also it is assumed that the antenna is infinitesimally thin, hence the current distribution is sinusoidal. The assumed current density will have the following form:

$$\bar{J} = \begin{cases} \hat{z}\, I\, \delta(x'-0)\delta(y'-0)\sin k(d-|z'-z_o|) & \text{for } |z-z_o| \leq d \\ 0 & \text{for } |z-z_o| > d \end{cases} \quad . \tag{4.1}$$

In order to find the fields for this case by the Green's function method it will be necessary to find the volume integral of the dot product of $\bar{M}'$ and $\bar{N}'$ functions and the current distribution of Eq. (4.1). These integrals follow from the definitions of the $\bar{M}'$ and $\bar{N}'$ functions in Chapter II and are

$$\iiint \bar{M}'_{e_{o}n\lambda}(\pm h) \cdot \bar{J}(\bar{R}')\, dv' = 0 \tag{4.2}$$

$$\iiint \bar{N}_{e_{o}n\lambda}(\pm h) \cdot \bar{J}(\bar{R}')dv' = \delta_o\, 2\, I\, P(h,d)\, e^{\pm ihz_o} \tag{4.3}$$

where we have defined the function P(h, d) as

$$P(h,d) = \cos h\, d - \cos k\, d \quad . \tag{4.3a}$$

As previously mentioned in Chapter III, the $\bar{M}$ functions do not contain a z-component and therefore the fields due to an arbitrary z-directed current will only contain $\bar{N}$ type functions.

It is appropriate at this point to consider the function P(h, d) for two special cases. The first case to be considered is where the antenna is assumed to be a half wave dipole. For this case $d = \lambda_o/4$, where λ_o is the free space wavelength. Since the half wave dipole is the special case to be considered in this chapter, this expression for $P(h, \frac{\lambda_o}{4})$ will be used in the final expressions for S_+ and S_- in this chapter. From Eq. (4.3a)

$$P(h, \frac{\lambda_o}{4}) = \cos(\frac{\lambda_o}{4} h) \quad . \tag{4.4}$$

The other case to be considered is the limiting case when d becomes

very small. The resulting expressions for P(h, d) will be used to compare the fields due to a very small dipole with a sinusoidal current distribution. The method used to obtain this limiting expression is to expand cos (hd) and cos (kd) in a Maclaurin series and disregard fourth and higher order terms. The resulting expression for P(h, d) is

$$\lim_{d \to 0} P(h,d) = \frac{d^2}{2}(k^2-h^2) = \frac{d^2}{2}\lambda^2 \quad . \tag{4.5}$$

It should be pointed out that the λ of (4.5) is the spectral variable λ and not the constant λ_o which represents the free space wavelength .

In order to better compare the fields due to a Hertzian dipole and a very small dipole with a sinusoidal current distribution, the concept of current moment will be used. Current moment is defined as

$$M = \int_{\ell} \bar{I} \cdot \overline{d\ell} \quad .$$

The current moment of the current density of Eq. (4.1), in the limit as d approaches zero, is obtained through the use of Maclaurin's series and is given by

$$M_s = I k d^2 \tag{4.6}$$

where the subscript s indicates a small dipole with sinusoidal current distribution. The Hertzian dipole is often thought of as a dipole of length ℓ , with a uniform current distribution I, in the limit as ℓ approaches zero and I approaches infinity where the limit is taken such that the product $I\ell$ remains constant. The current moment of such an antenna is

$$M_H = I\ell \quad , \tag{4.7}$$

where the subscript H indicates a Hertzian dipole. In order to compare the values of M_s and M_H one must recall that the short dipole has an input current magnitude of Ikd where d is the half length of the antenna, while

the Hertzian dipole has an input current magnitude of I and a half length of $\ell/2$. If the input current to both antennas is assumed to be equal it may be seen that

$$M_s = \frac{1}{2} M_H \quad .$$

Equations (4.6) and (4.7) will be used to compare the fields of a short dipole to those of a Hertzian dipole.

The fields above the ground plane due to the current density of (4.1) are found by substituting (4.2) and (4.3) into (2.33). The electric field for this case is given by

$$\bar{E} = i\omega\mu_o \iiint \bar{\bar{G}}(\bar{R}'|\bar{R}) \cdot \bar{J}(\bar{R}')\, dV'$$

$$= -\frac{\omega\mu_o I}{2\pi} \int_0^\infty \frac{d\lambda}{\lambda h} P(h,d) \begin{cases} \bar{N}_{e0\lambda}(h)\left[e^{-ihz_o} + be^{ihz_o}\right] & z \geq z_o + d \\ \left[\bar{N}_{e0\lambda}(-h) + b\bar{N}_{e0\lambda}(h)\right] e^{ihz_o} & 0 \leq z \leq z_o - d \end{cases} . \tag{4.8}$$

The field within the earth may be easily derived by the same method but is not needed to find S_+ and S_-, and therefore it is not included here. The magnetic field may be found from the electric field by Maxwell's equations and the relationship between $\bar{M}$ and $\bar{N}$ functions, and is given by the following:

$$\bar{H} = \frac{1}{i\omega\mu_o} \nabla \times \bar{E}$$

$$= \frac{ik\, I}{2\pi} \int_0^\infty \frac{d\lambda}{\lambda h} P(h,d) \begin{cases} \bar{M}_{e0\lambda}(h)\left[e^{-ihz_o} + be^{ihz_o}\right] & z \geq z_o + d \\ \left[\bar{M}_{e0\lambda}(-h) + b\bar{M}_{e0\lambda}(h)\right] e^{ihz_o} & 0 \leq z \leq z_o - d \end{cases} . \tag{4.9}$$

As a check, we substitute for P(h,d) the short dipole limit given in (4.5) and then use the definition of the current moment given by (4.6). The electric

field expression reduces to

$$\bar{E} = -\frac{\omega \mu_o M_s}{4\pi k} \int_0^\infty d\lambda \frac{\lambda}{h} \begin{cases} \bar{N}_{e0\lambda}(h)\left[e^{-ihz_o} + be^{ihz_o}\right] & z \geq z_o + d \\ \left[\bar{N}_{e0\lambda}(-h) + b\bar{N}_{e0\lambda}(h)\right] e^{ihz_o} & 0 \leq z \leq z_o - d \end{cases} .$$

This expression is exactly the same as Eq. (3.4) except for the different current moment.

4.1.2 Far Zone Fields. The asymptotic form for (4. 8) as kR becomes very large is determined by the saddle point method. The method is exactly the same as for the short dipole cases and is discussed further in Appendix B. The result for a half wave dipole is

$$\bar{E} = \frac{i\omega\mu_o I}{\pi k} \frac{e^{ikR}}{R} \frac{\cos\left(\frac{\pi}{2}\cos\theta\right)}{\sin\theta} \left[e^{-ikz_o\cos\theta} + b(\theta)e^{ikz_o\cos\theta}\right] \hat{\theta} \qquad (4.10)$$

where $b(\theta)$ is the plane wave reflection coefficient for vertically polarized waves.

$$b(\theta) = \frac{n^2\cos\theta - \sqrt{n^2 - \sin^2\theta}}{n^2\cos\theta + \sqrt{n^2 - \sin^2\theta}} .$$

Equation (4. 10) normalized was used to obtain the plots of $|\bar{E}(\theta)|^2$ given in Chapter V. The limitation of these patterns are further discussed in Appendix B.

4.2 Radiation Resistance and Efficiency Expressions for a Vertical Half Wave Dipole

The field expressions for a long vertical dipole, as given by Eqs. (4.3) and (4.4), are very similar to the field expressions due to a vertical Hertzian dipole. Therefore, the following derivation of the equations for S_+ and S_- due to the vertical half wave dipole follow very closely the derivation given in Section 3.3.2

The fields that comprise the z-directed Poynting's vector are E_r, H_ϕ, E_ϕ, and H_r. They are found from Eqs. (4.8) and (4.9) and the definitions of the $\overline{M}$ and $\overline{N}$ functions to be

$$E_r = \frac{i\omega\mu_o I}{2\pi k}\int_0^\infty d\lambda\, P(h,d)\left\{\pm e^{ih|z-z_o|} + be^{ih(z+z_o)}\right\}J_1(\lambda r)$$

$$= \frac{i\omega\mu_o I}{2\pi k}\int_0^\infty d\lambda\, P(h,d) f_1(h,z) J_1(\lambda r) \quad , \tag{4.10}$$

$$H_\phi = \frac{i\,I\,k}{2\pi}\int_0^\infty d\lambda\, P(h,d)\left\{\frac{e^{ih|z-z_o|} + be^{ih(z+z_o)}}{h}\right\}J_1(\lambda r)$$

$$= \frac{iIk}{2\pi}\int_0^\infty d\lambda\, P(h,d)\, f_2(h,z)\, J_1(\lambda r) \quad , \tag{4.11}$$

$$E_\phi = 0 \ ,$$

$$H_r = 0 \ .$$

Since the general function $P(h,d)$ is still present, these equations represent the fields due to an antenna of arbitrary length. The upper sign in (4.10) and (4.11) corresponds to the region where $z \geq z_o + d$, while the lower sign corresponds to the region where $0 \leq z \leq z_o - d$. These field expressions are not valid for values of z such that

$$|z - z_o| < d \ ,$$

or for the region within the earth itself where $z < 0$. In the definition of S_+ and S_- we must include the fact that the respective planes of integration are located either clearly above or clearly below the antenna. Let S_+ be the integral of the z-directed Poynting's vector over a plane parallel to the earth's

surface located at a height z_+ such that

$$z_+ \geq z_o + d \quad .$$

Similarly, define S_- as the integral of the negative z-directed Poynting's vector taken over a plane surface parallel to the earth's surface but now located at a height z_- such that

$$0 \leq z_- \leq z_o - d \, .$$

It will be shown that both S_+ and S_-, as defined above, are independent of the height of their respective planes of integration. It will also be shown that the expression for $S_+ + S_-$ as z_o becomes infinite is identical to the result obtained by integration of the R-directed Poynting's vector over a closed surface surrounding the antenna. These two facts imply that the integral of the r-directed Poynting's vector over a cylinder of infinite radius and finite height is zero. Hence, it is seen that the radiation resistance of the antenna is proportional to $S_+ + S_-$ while power dissipated in the earth is equal to S_-. In the case when E_ϕ and H_r are equal to zero the expressions for $S_\pm$ are

$$S_\pm = \pm \frac{1}{2} \mathrm{Re} \int_0^{2\pi} \int_0^{\infty} r \, dr \, d\phi \, (E_r H_\phi^*) \quad .$$

We are considering the case of a vertical antenna, consequently there is no ϕ-dependence and the expressions for $S_\pm$ become

$$S_\pm = \pm \pi \, \mathrm{Re} \int_0^{\infty} r \, dr \, (E_r H_\phi^*) \quad .$$

Substitution of (4.10) and (4.11) for E_r and H_ϕ gives the following result:

$$S_\pm = \pm \frac{\omega \mu_o I^2}{4\pi} \mathrm{Re} \int_0^{\infty} r \, dr \int_0^{\infty} d\lambda \int_0^{\infty} d\delta J_1(\lambda r) J_1(\delta r) P(h, d) P^*(h_\delta, d) \cdot \left[f_1(h, z_\pm) \cdot f_2^*(h_\delta, z_\pm) \right] \quad .$$

In order to avoid confusion, the variable of integration in the expression for H_ϕ has been changed from λ to δ and h_δ is accordingly defined as

$$h_\delta^2 = k^2 - \delta^2 \quad .$$

If we apply the general orthogonality relationship for Bessel's functions as given in (3.13) and integrate first over r, and then over δ, the following result is obtained:

$$S_\pm = \pm \frac{\omega \mu_o I^2}{4\pi} \mathrm{Re} \int_0^\infty \frac{d\lambda}{\lambda} |P(h,d)|^2 \left[f_1(h, z_\pm) \cdot f_2^*(h, z_\pm) \right] , \qquad (4.12)$$

where the functions f_1 and f_2, defined by (4.10) and (4.11), are exactly the same as the bracketed functions of (3.14).

If the limiting expressions for P(h, d) as d becomes very small, is used in (4.12), then the radiation resistance expression implied by (4.12) will be that of a small dipole with a sinusoidal current distribution. Comparison of this equation with (3.14) shows that the Hertzian dipole has a radiation resistance equal to four times that of a small dipole with sinusoidal current distribution.

We have previously stated that the bracketed terms of (3.14) and (4.12) are exactly the same. Consequently, the same treatment applied to this term in Section 3.3.2 may be applied here. The resulting expressions for S_+ and S_- are

$$S_+ = \frac{\omega \mu_o I^2}{4\pi} \mathrm{Re} \int_0^k \frac{d\lambda}{\lambda h} |P(h,d)|^2 \left\{ 1 + |b|^2 + 2be^{2ihz_o} \right\}$$

$$S_- = -\frac{\omega \mu_o I^2}{4\pi} \left\{ \int_0^\infty \frac{d\lambda}{\lambda h} |P(h,d)|^2 \left[-1 + |b|^2 \right] + 2 \, \mathrm{Im} \int_0^\infty \frac{d\lambda}{\lambda h^*} |P(h,d)|^2 be^{2ihz_o} \right\} .$$

From Sec. 3.3.2 we find that the dependence on z_+ and z_- conveniently cancels out and the expressions for S_+ and S_- are independent of the height of the plane of integration, with the stipulation that the plane for S_+ is above the antenna and the plane for S_- is below the antenna.

These expressions will now be reduced to a form that is more convenient to handle numerically and lends itself to the physical interpretation of the various terms. First, we change the variable of integration from λ to h giving

$$S_+ = \frac{\omega\mu_o I^2}{4\pi} \mathrm{Re} \int_0^k dh \frac{|P(h,d)|^2}{(k^2-h^2)} \left\{ 1-|b|^2 + 2be^{2ihz_o} \right\}, \tag{4.13}$$

$$S_- = -\frac{\omega\mu_o I^2}{4\pi} \left\{ \int_0^k dh \frac{|P(h,d)|^2}{(k^2-h^2)} \left[-1+|b|^2 \right] \right.$$

$$\left. -2\mathrm{Re} \int_0^{i\infty} dh \frac{|P(h,d)|^2}{(k^2-h^2)} \, i \, \mathrm{Im}[b] \, e^{2ihz_o} \right\} . \tag{4.14}$$

Consider the case of a half wave dipole where $d = \lambda_o/4$. The appropriate expression for $|P(h, \frac{\lambda_o}{4})|^2$ can be obtained from (4.4) and, by using the fact that h is real or imaginary but never complex, the result is

$$|P(h, \frac{\lambda_o}{4})|^2 = \cos^2 (\frac{\lambda_o}{4} h) \quad . \tag{4.15}$$

In order to examine the physical meaning of the terms of S_+ and S_-, the function b will be divided into a constant part plus a variable part which vanishes in the perfectly conducting case. The division of b is explained in Section 3.3.2 and the result is

$$b = 1 - B \, . \tag{3.22}$$

Substitution of Eqs. (3.22) and (4.15) into (4.13) and (4.14) and application of the following changes of variables

$$h = ku \qquad \text{for} \int_0^k dh \tag{4.16}$$

$$h = ikv \qquad \text{for} \int_0^{i\infty} dh \tag{4.17}$$

gives the following result

$$S_+ = \frac{\omega\mu_o I^2}{4\pi k} \operatorname{Re} \int_0^1 du \, \frac{\cos^2(\frac{\pi}{2}u)}{1-u^2} \left\{ 2+2e^{i\xi u} - 2Be^{i\xi u} + |B|^2 - (B+B^*) \right\} \tag{4.18}$$

$$S_- = -\frac{\sqrt{\omega\mu_o} I^2}{4\pi k} \left\{ \int_0^1 du \, \frac{\cos^2(\frac{\pi}{2}u)}{1-u^2} \left[|B|^2 - (B+B^*) \right] - i \int_0^\infty dv \, \frac{\cosh^2(\frac{\pi}{2}v)}{1+v^2} \left[B^* - B \right] e^{-\xi v} \right\}, \tag{4.19}$$

where the function B is assumed to have undergone the appropriate change of variables, as defined by (4.16) and (4.17), depending upon whether the variable of integration is u or v.

The expression for S_+ may be further reduced by making use of the following identity*

$$\lim_{\epsilon \to 0} \int_0^{1-\epsilon} \frac{\cos\beta u}{1-u^2} du = \lim_{\epsilon \to 0} \frac{\cos\beta}{2} \left\{ \operatorname{Ln}(\tfrac{2}{\epsilon}) - \operatorname{Cin}(2\beta) + \frac{\sin\beta}{2} \operatorname{Si}(2\beta) \right\}. \tag{4.20}$$

---

* The Si and Cin functions are defined in Kraus (Ref. 24, p. 535). For a derivation of the result of this integral with $\beta = \pi/2$, see Kraus, p. 144.

If $\beta = n\frac{\pi}{2}$ (where n is odd) the function $\cos\beta u/1-u^2$ has a limit of $n\pi/4$ as u approaches one and therefore the integral of (4.20) will be finite and equal to

$$\lim_{\epsilon\to 0}\int_0^{1-\epsilon} \frac{\cos\beta u}{1-u^2}\,du = \frac{1}{2}\,\mathrm{Si}(2\beta) \quad .$$

The first term of (4.18) may thus be reduced as follows

$$\lim_{\epsilon\to 0}\int_0^{1-\epsilon} \frac{\cos^2(\frac{\pi}{2}u)}{1-u^2} = \lim_{\epsilon\to 0}\int_0^{1-\epsilon} \frac{(1+\cos\pi u)}{1-u^2}\,du$$

$$= \lim_{\epsilon\to 0}\frac{1}{2}\left\{\frac{1}{2}\,\mathrm{Ln}\left(\frac{1+x}{1-x}\right) - \frac{1}{2}\,\mathrm{Ln}\left(\frac{2}{\epsilon}\right) + \frac{1}{2}\,\mathrm{Cin}(2\pi)\right\} = \frac{1}{4}\,\mathrm{Cin}(2\pi) = \frac{2.44}{4} \quad .$$

Thus the entire first term of (4.18) reduces to

$$\frac{\omega\mu_o I^2}{8\pi k}\,\mathrm{Cin}(2\pi) = 73.2\frac{I^2}{2}\ \text{ohms} \quad . \tag{4.21}$$

For harmonic time dependence the rms input current to a half wave dipole is $I/\sqrt{2}$. Division of Eq. (4.21) by rms input current squared implies that the constant term of the radiation resistance is 73.2 ohms which is the well known value of the radiation resistance for a half wave dipole in free space*.

If Eqs. (4.18) and (4.19) are normalized by the factor $(73.2I^2/2)$ of (4.21) the final result is

---

*See Tai (Ref. 26, p. 3-2) .

$$S_+ = 1 + \frac{1}{Cin(2\pi)} \int_0^1 \frac{\cos^2(\frac{\pi}{2}u)}{1-u^2} \cos\xi u \, du + \frac{2}{Cin(2\pi)} \int_0^1 \frac{\cos^2(\frac{\pi}{2}u)}{1-u^2}$$

$$(|B|^2 - B - B^*) du - \frac{4}{Cin(2\pi)} \operatorname{Re} \int_0^1 B e^{i\xi u} \frac{\cos^2(\frac{\pi}{2}u)}{1-u^2} \, du \qquad (4.22)$$

$$S_- = \frac{2}{Cin(2\pi)} \int_0^1 (|B|^2 - B - B^*) \frac{\cos^2(\frac{\pi}{2}u)}{1-u^2} \, du$$

$$- \operatorname{Re} \frac{2i}{Cin(2\pi)} \int_0^\infty \frac{(B-B^*)}{1+v^2} e^{-\xi v} \cosh^2(\frac{\pi}{2}) \, dv \quad . \qquad (4.23)$$

When an antenna is placed above a perfectly conducting ground plane the input impedance and the radiating characteristics of such an antenna may be calculated by the assumption of an image antenna located at an equal distance below the plane of the ground but now in free space. Several authors have attacked the problem of finding the mutual impedance between two such colinear dipoles*. Since the radiation resistance is proportional to $S_+ + S_-$ and recalling that the function B vanishes when the ground is perfectly conducting the real part of the mutual impedance of two colinear dipoles R_M is represented by the second term of Eq. (4.18). This term may be treated as follows:

---

*See Refs. 24, 25 and 26 .

$$\lim_{\epsilon \to 0} \mathrm{Re} \int_0^{1-\epsilon} \frac{\cos^2(\frac{\pi}{2}u)}{1-u^2} e^{i\xi u} du = \lim_{\epsilon \to 0} \int_0^{1-\epsilon} \frac{\cos^2(\frac{\pi}{2}u)}{1-u^2} \cos \xi u \, du$$

$$= \lim_{\epsilon \to 0} \frac{1}{2} \int_0^{1-\epsilon} \frac{du}{1-u^2} (\cos \xi u + \cos \pi u \cos \xi u)$$

$$= \lim_{\epsilon \to 0} \frac{1}{4} \int_0^{1-\epsilon} \frac{du}{1-u^2} \left\{ 2\cos \xi u + \cos(\xi+\pi) u + \cos(\xi-\pi) u \right\} .$$

Application of (4.20), cancellation of terms, and division by the square of the rms input current gives the following result.

$$R_M = 15 \cos(\xi) \left\{ -2\mathrm{Cin}(2\xi) + \mathrm{Cin}(2\xi+2\pi) + \mathrm{Cin}(2\xi-2\pi) \right\}$$
$$+15 \sin(\xi) \left\{ 2\mathrm{Si}(2\xi) - \mathrm{Si}(2\xi+2\pi) - \mathrm{Si}(2\xi-2\pi) \right\} .$$

This result is identical to the result obtained by Carter (Ref. 25) using the induced emf method. This same result may also be obtained by integration of the R-directed Poynting's vector over a hemisphere of infinite radius and dividing by the square of the rms input current.

Equations (4.22) and (4.23) have been numerically evaluated for various ground constants and the resulting curves of radiation resistance and radiation efficiency versus center height of the antenna may be found in Chapter V.

4.3 The Physical Significance of Terms of S_+ and S_-

This section attempts to attach physical significance to the terms of (4.22) and (4.23). The physical interpretation of the terms of S_+ and S_- for the Hertzian dipoles follow quite easily from the discussion in this section.

The right hand side of Eq. (4.22) contains four terms. They will be referred to in order of their proximity to the equals sign (i.e. term 1 = 1). The two terms of (4.23) will be called term five and term six respectively. Note that terms three and five are equivalent except for a minus sign.

For the perfectly conducting case A and B vanish leaving S_{-} equal to zero. The first term corresponds to the free space radiation resistance while the second term corresponds to the change caused by a perfectly conducting ground plane. All other terms are zero.

At infinite height the only non-vanishing terms are one, three and five. Since three and five cancel out when calculating radiation resistance, term one must correspond to the free space radiation resistance. Since term five is not zero, it corresponds to the power absorbed by the ground when the antenna is very far away. This term is the one that limits the efficiency as the antenna is moved far away from the earth.

Terms four and six may be interpreted as the changes introduced by the fact that the ground has a finite conductivity and the antenna height is finite.

5.2 Ground Constants

The nature of the ground can be characterized by its complex index of refraction n, where

$$n^2 = \epsilon_E / \epsilon_o \left\{ 1+i \frac{\sigma_E}{\omega \epsilon_E} \right\} .$$

The ground constants chosen for the calculations are representative of sea water, fresh water, good earth and poor earth. The values of these constants were taken from Ref. 28, 29 and 30 and are given in Table 5.1:

TABLE 5.1

Type of Ground	ϵ_E / ϵ_o	σ_E (Mhos/meter)
Sea Water	80	5
Fresh Water	80	2×10^{-4}
Good Earth	10	10^{-2}
Poor Earth	4	10^{-4}

Each of the graphs in Sections 5.3 and 5.4 contains a family of curves parametric in values of n^2. Each family represents one particular type of ground because the real part of n^2 is the same for each curve. The frequency implied by a given value of n^2 is calculated by the following formula which arises from the definition of n^2.

$$f_{MHz} = \frac{18 \times 10^3 \cdot \sigma_E}{\mathrm{Im}\{n^2\}}$$

where

f_{MHz} = frequency in MHz,

σ_E = earth conductivity in Mhos/meter.

CHAPTER V

NUMERICAL CALCULATIONS

5.1 General

In this chapter we present four different types of curves. These are radiation efficiency, radiation resistance, reflection coefficient modulus and radiation patterns. Of these the most important ones are the radiation efficiency curves, since the primary purpose of this thesis is to investigate the radiation efficiency of certain antennas in the presence of a lossy earth. These curves have been calculated for a range of frequencies and ground constants that should be representative of grounds actually encountered in practice.

The efficiency curves in conjunction with the radation patterns will enable the antenna designer to choose an optimum height for the three types of antennas treated here. In addition a knowledge of these curves will give the antenna designer an indication of the values of efficiency to be expected from other types of radiating systems. Also these curves will help to provide some insight into the effects of changing ground parameters, frequency, and height on more general types of antennas.

Since the calculation of the radiation resistance is an integral part of the efficiency calculation we have included the radiation resistance curves for completeness. Several other authors have presented radiation resistance curves for dipoles above a ground plane (Ref. 12, 13, 15, 16, 31). Except for the work of Vogler and Nobel (Ref. 31), most of these calculations are based upon the assumption of low frequency or high conductivity so that n^2 may be approximated by its imaginary part. Since our calculations are numerical evaluations of the exact expressions for S_+ and S_- we do not need to restrict the values of n^2.

The curves of radiation resistance and radiation efficiency were calculated by substituting the values of S_+ and S_- into the two equations given below :

$$R = S_+ + S_- \quad , \qquad \eta = \frac{S_+}{S_+ + S_-}$$

where the expressions used for S_+ and S_- are given in Chapters III and IV. Unfortunately, these expressions consist of integrals that cannot be expressed in terms of known functions. Thus, use of a computer was necessary in order to evaluate these expressions.

It may be of some interest to point out the effort involved in the programming of this program. All the programming was done in the FORTRAN IV language and the program was run on The University of Michigan IBM 360/67 system. In order to avoid roundoff error as a result of the tremendous number of operations involved with numerical integration, the entire program used the double precision mode.

The integration of each term of S_+ and S_- was handled separately . A separate subroutine was written to calculate each function to be integrated. The separation of the program in this manner facilitates the verification of program accuracy. To this end each subroutine was hand checked at several points.

A major part of the programming effort was directed towards the selection of a suitable integration scheme. Since the accuracy of a particular method of numerical integration depends upon the function to be integrated, great care must be exercised in the selection of the quadrature method to be used. Several different schemes were examined, including some of our own design. The radiation efficiency and radiation resistance calculations have an accuracy of better than three significant figures using the quadrature methods finally chosen. Appendix A contains a detailed description of the quadrature methods used as well as a complete program listing.

The frequencies corresponding to the various grounds and the values of n^2 that were used in the calculations are given in Table 5.2 . The value of ϵ_E for sea water is the same as that of fresh water, however, their conductivities are quite different. Thus, the same family of curves applies to both cases but the value of n^2 implies quite different frequencies for each case (see Table 5.2).

TABLE 5.2

n^2/ϵ_r	Sea Water ϵ_r=80 σ=5 Mhos	Fresh Water ϵ_r=80 σ= 2x10^{-4}	Good Earth ϵ_r= 10 σ=10^{-2}	Poor Earth ϵ_r = 4 σ=10^{-4}
1+i.01	112.5 GHz	4.5 MHz	.18 GHz	45 GHz
1+i1	1.125 GHz	45 KHz	18 MHz	450 MHz
1+i3	374 MHz	15 KHz	6 MHz	150 MHz
1+i10	112.5 MHz	4.5 KHz	1.8 MHz	45 MHz
1+i30	37.4 MHz	1.5 KHz	600 KHz	15 MHz
1+i100	11.25 MHz	450 Hz	180 KHz	4.5 MHz
1+i300	3.74 MHz	150 Hz	60 KHz	1.5 MHz
1+i1000	1.125 MHz	45 Hz	18 KHz	450 KHz

5.3 Radiation Efficiency Curves

The following curves (Figs. 5-1 through 5-9) are the result of computer calculations of the radiation efficiency.

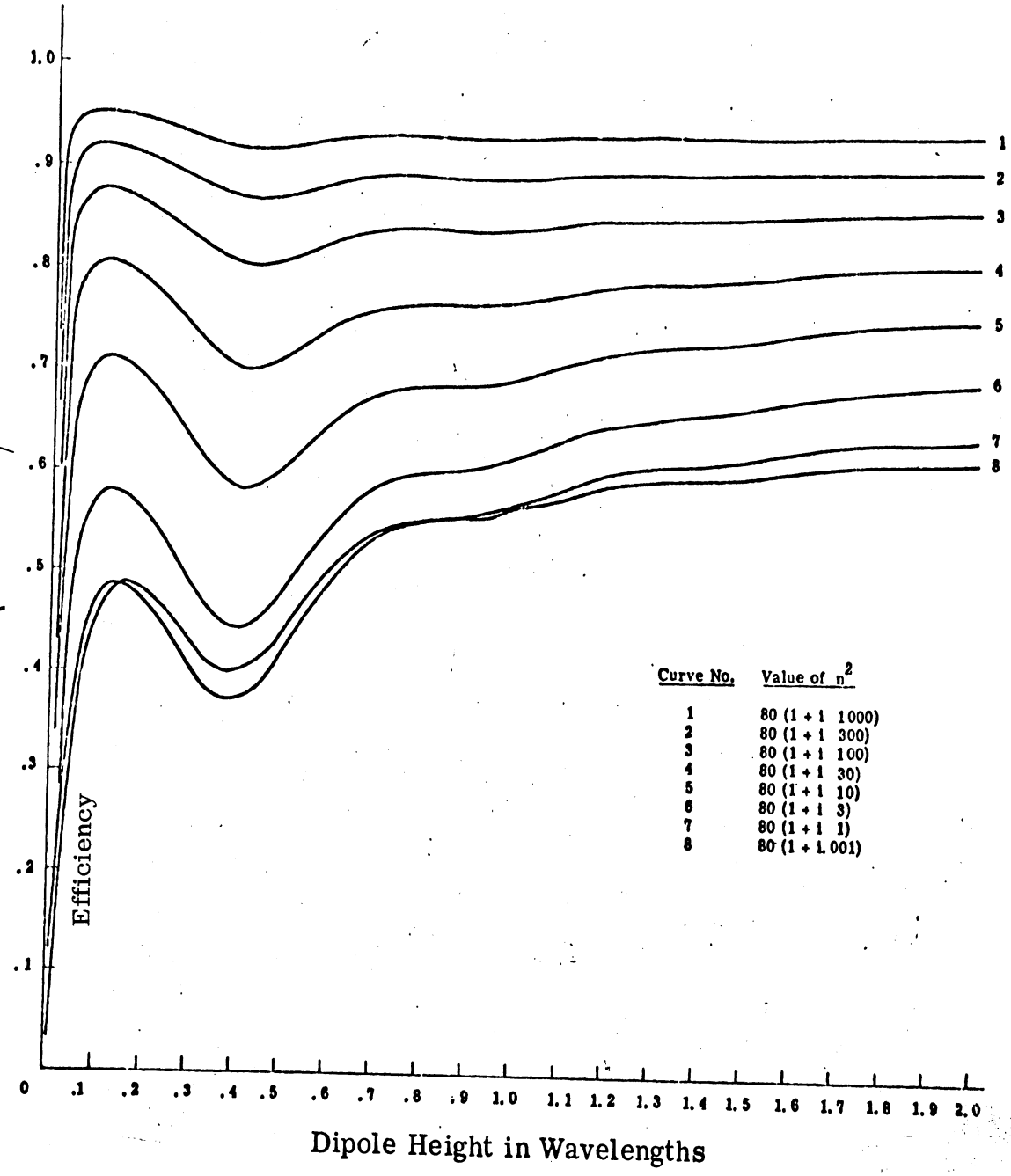

FIG. 5-1: Radiation Efficiency of the Vertical Hertzian Dipole.

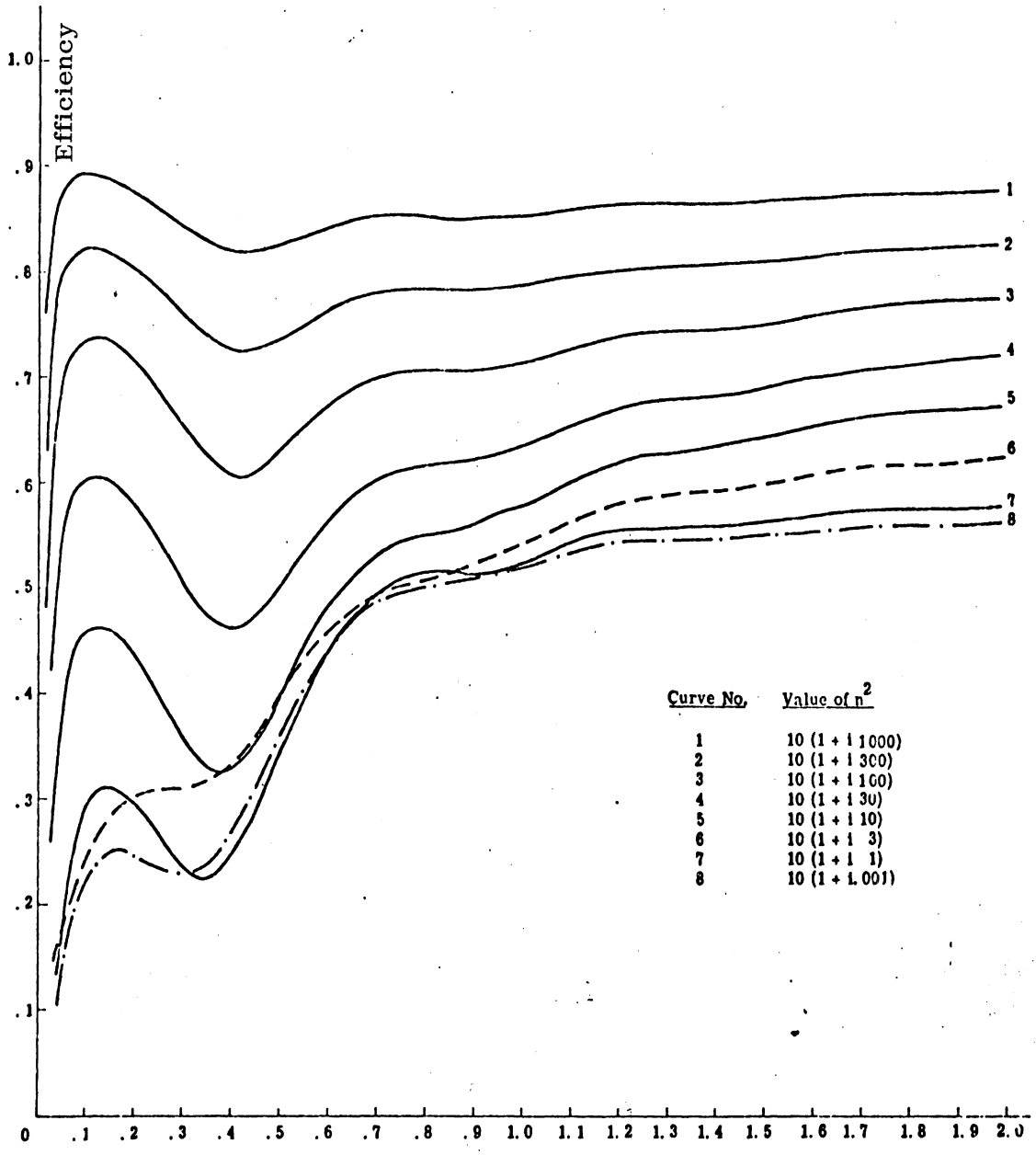

FIG. 5-2: Radiation Efficiency of the Vertical Hertzian Dipole.

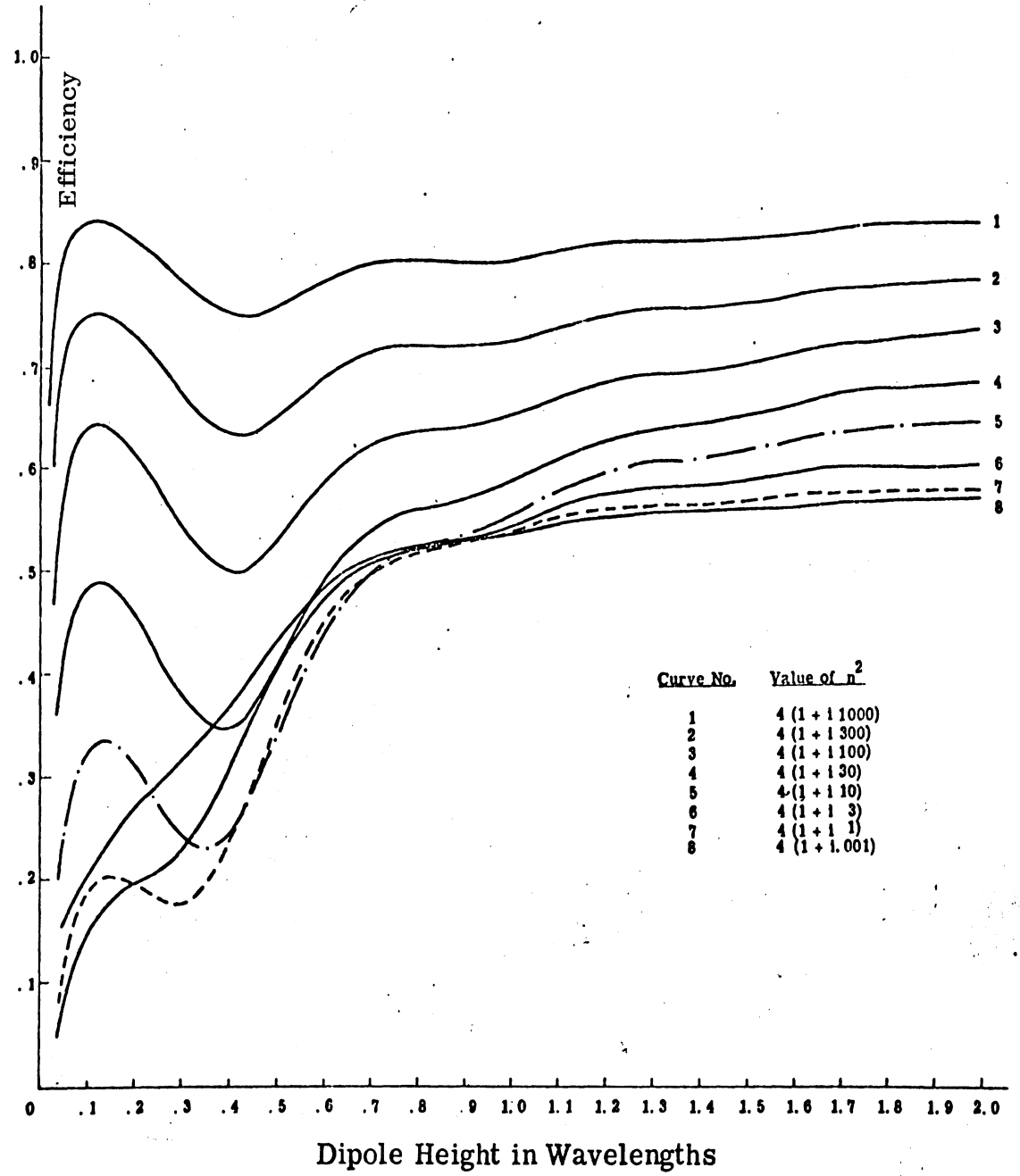

FIG. 5-3: Radiation Efficiency of the Vertical Hertzian Dipole.

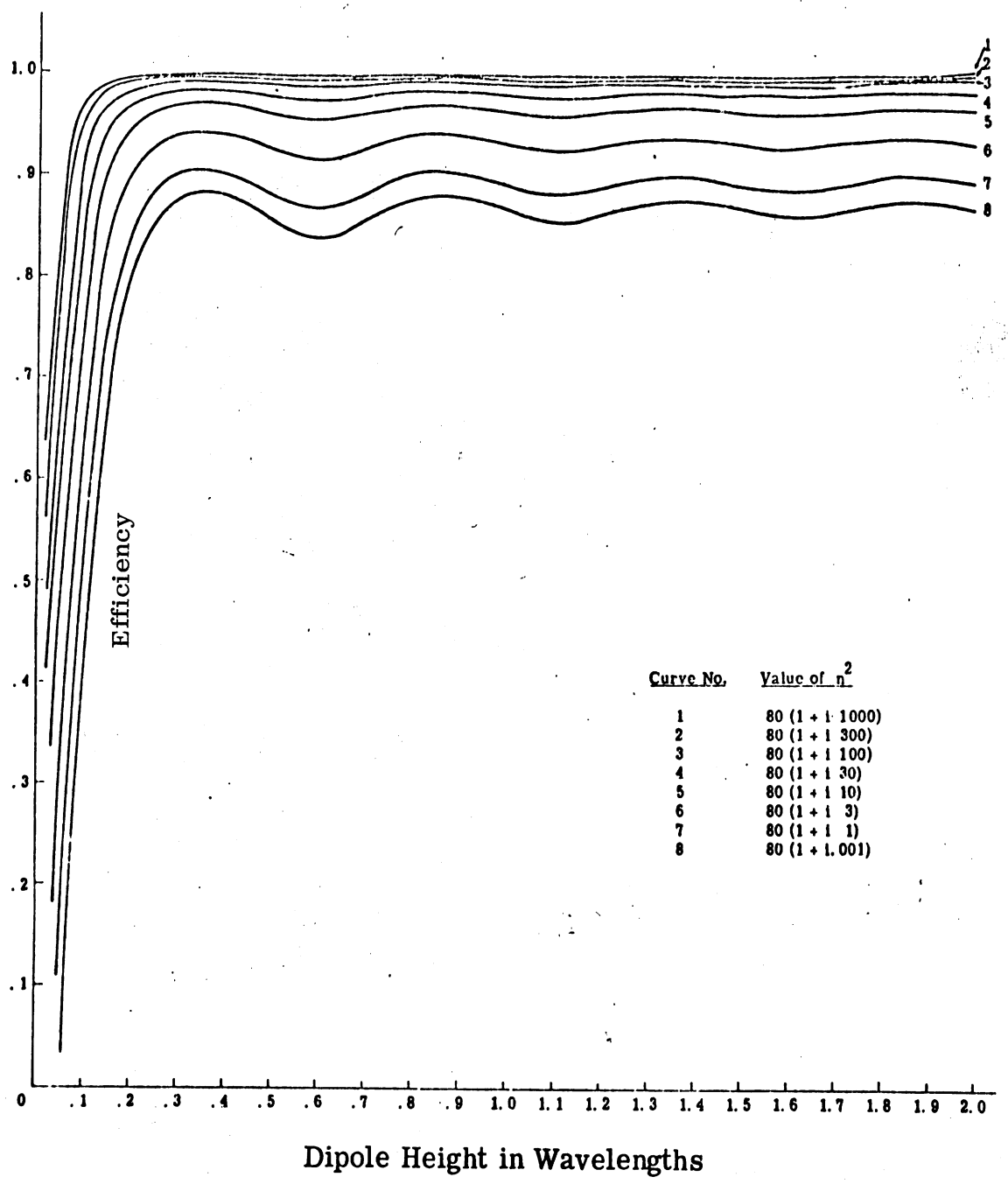

FIG. 5-4: Radiation Efficiency of the Horizontal Hertzian Dipole.

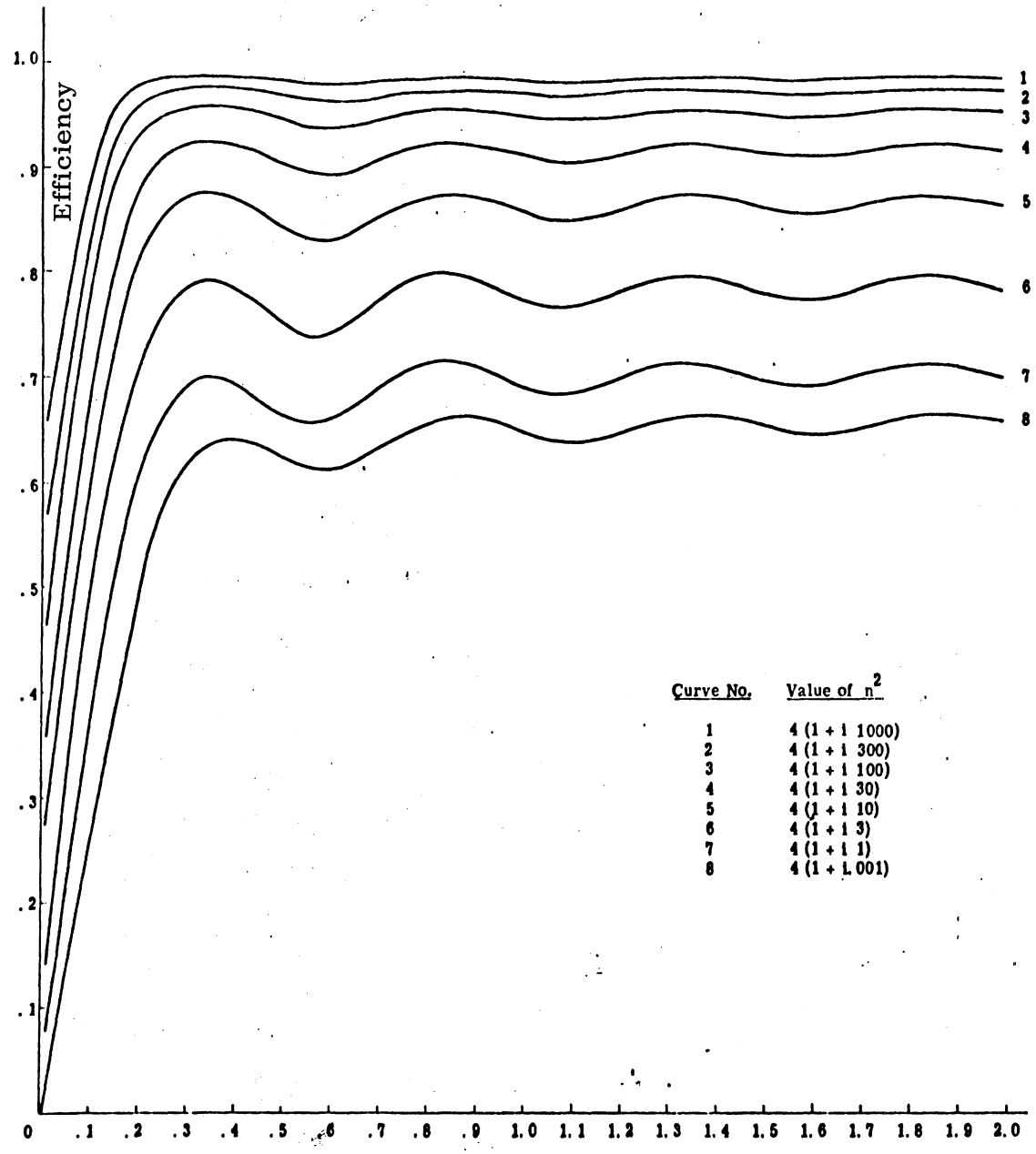

FIG. 5-6: Radiation Efficiency of the Horizontal Hertzian Dipole.

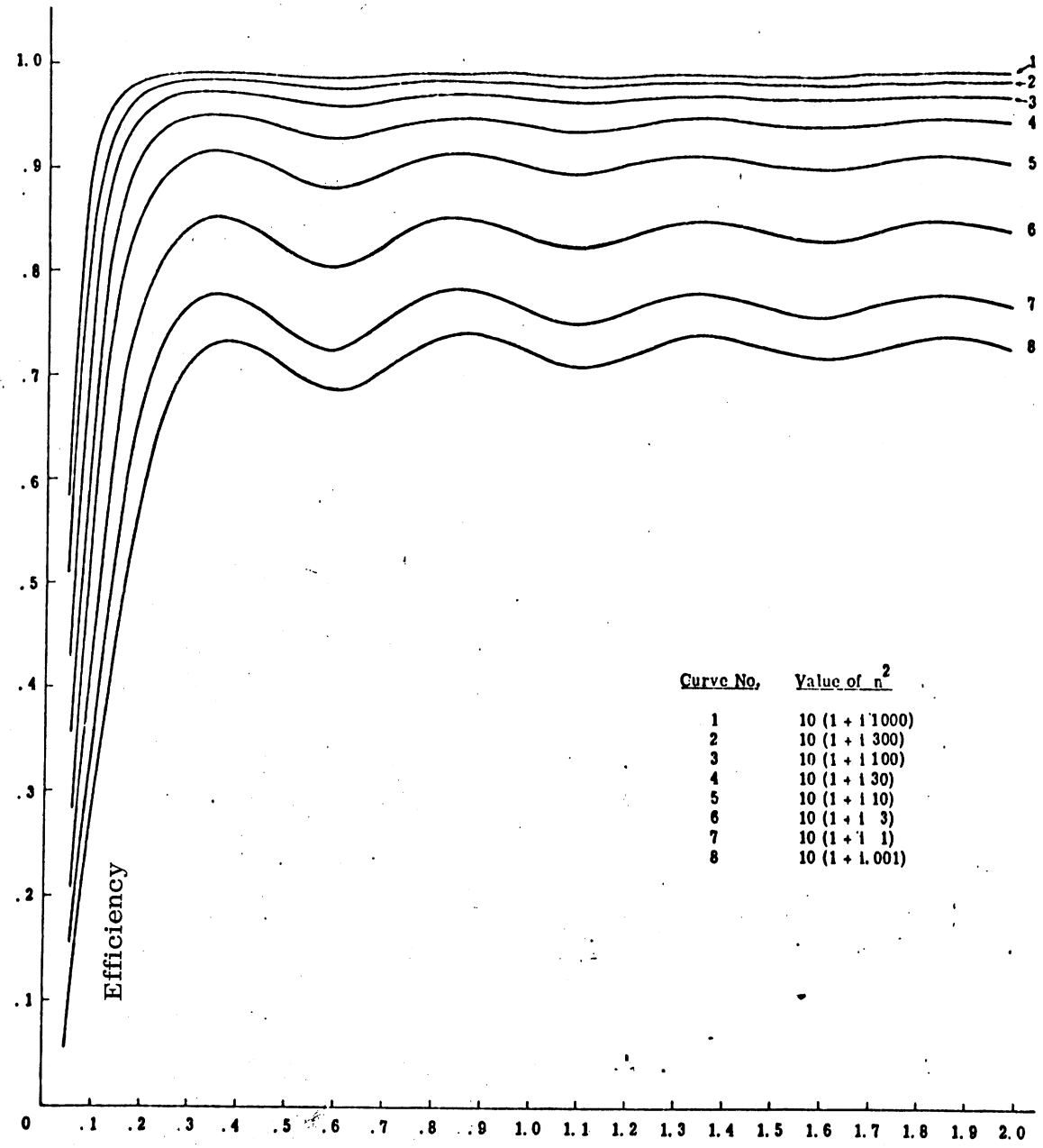

FIG. 5-5: Radiation Efficiency of the Horizontal Hertzian Dipole.

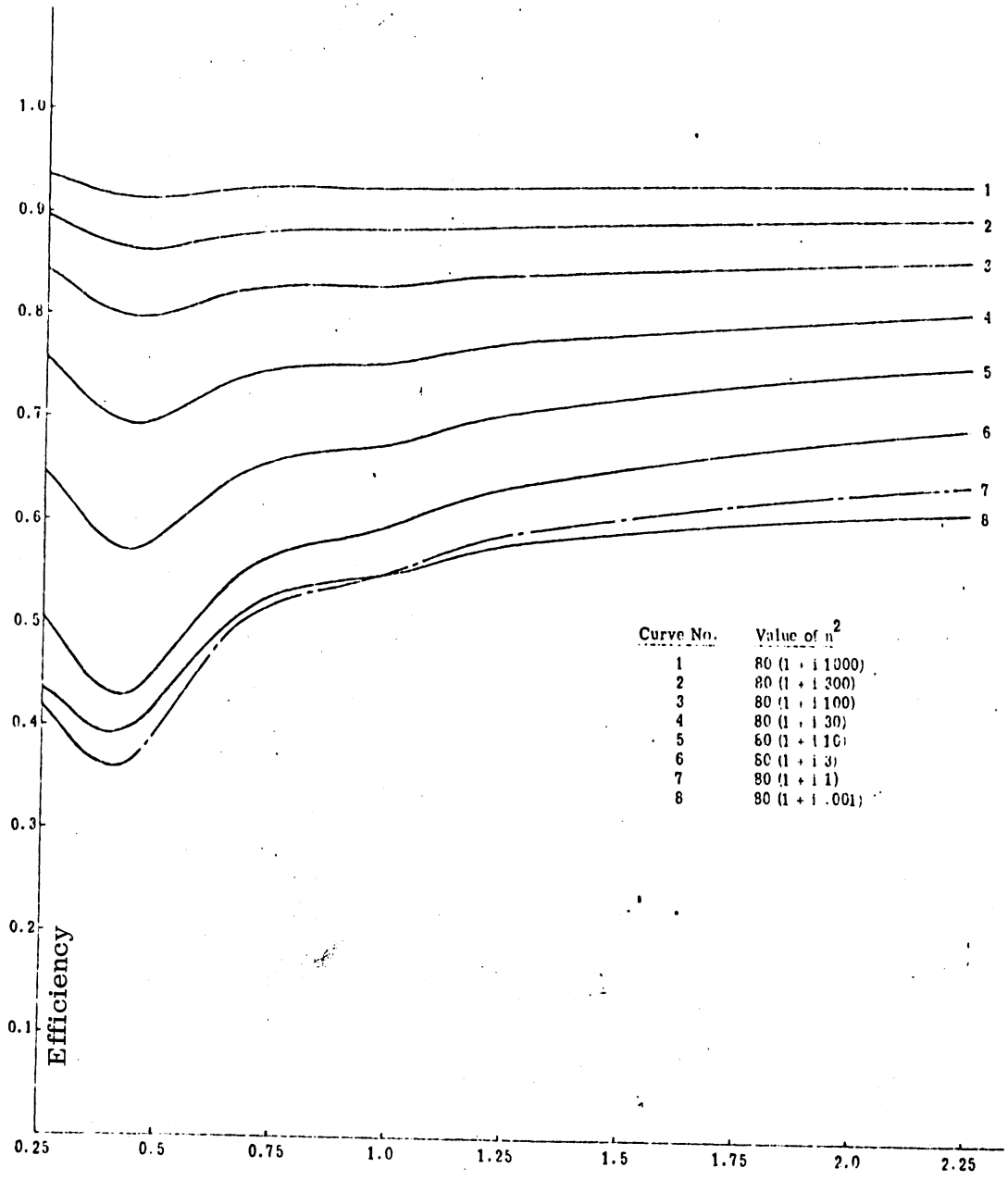

FIG. 5-7: Radiation Efficiency of the Vertical Half-wave Dipole.

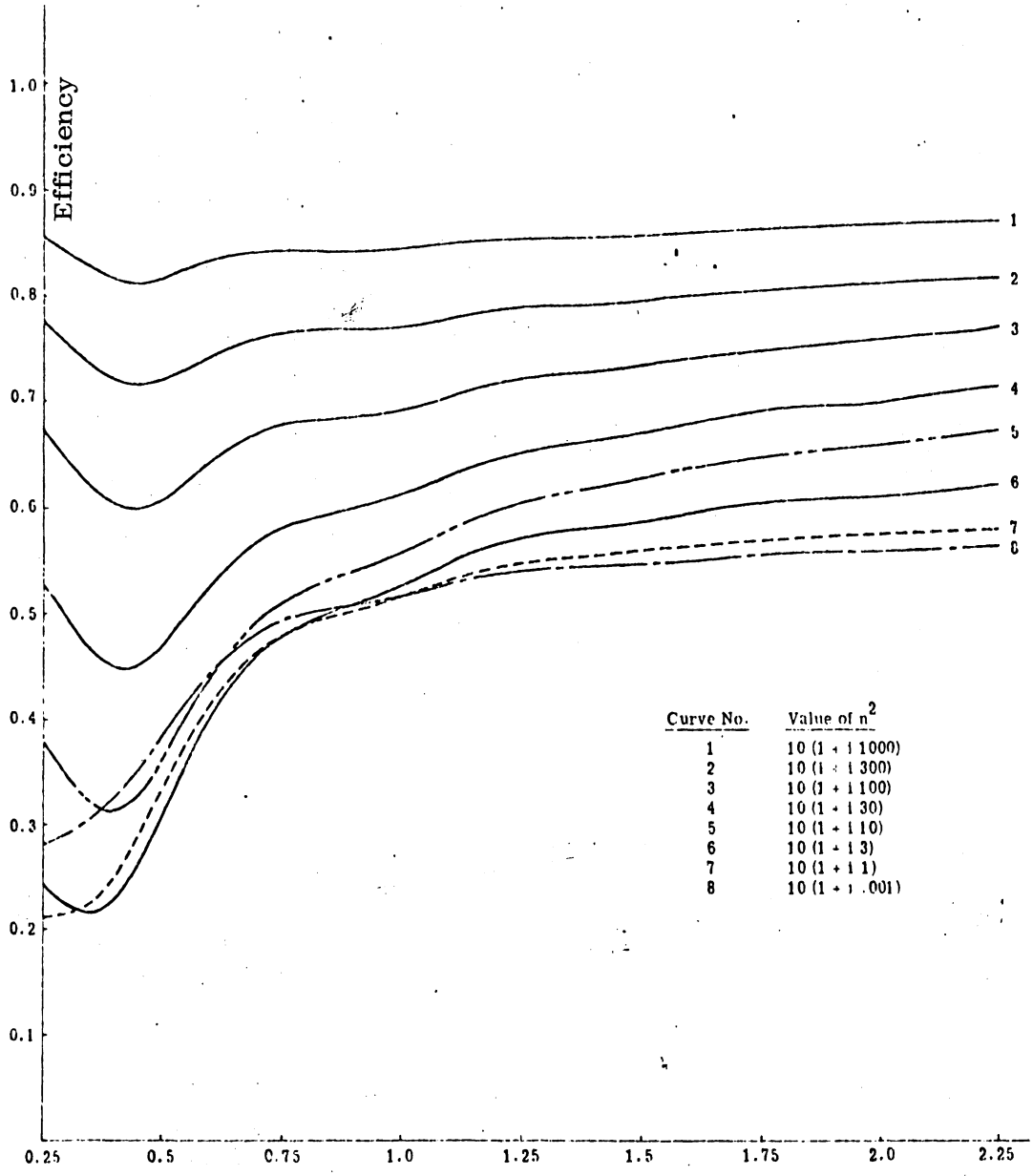

FIG. 5-8: Radiation Efficiency of the Vertical Half-wave Dipole.

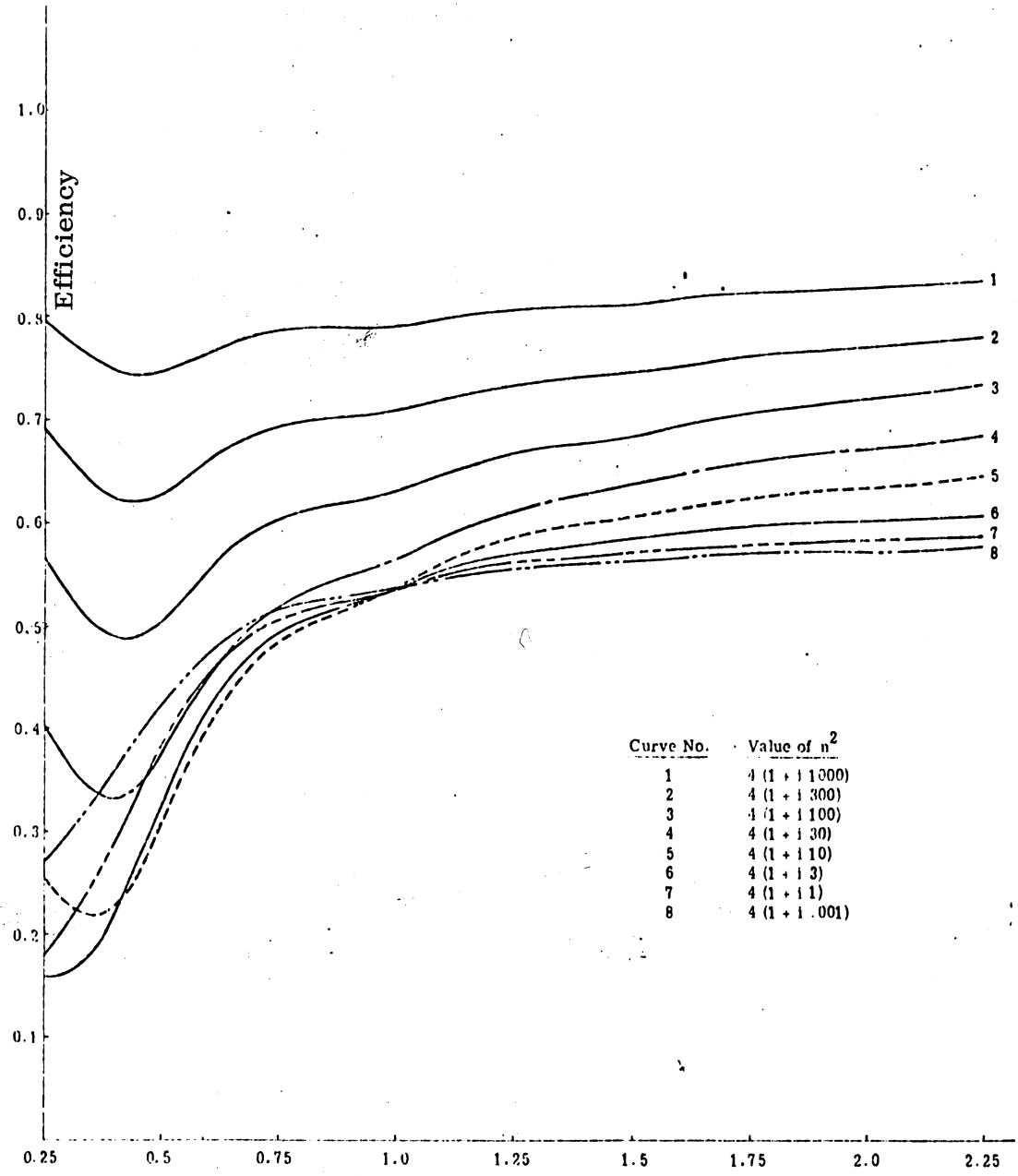

FIG. 5-9: Radiation Efficiency of the Vertical Half-wave Dipole.

5.4 Radiation Resistance Curves

All curves presented in this section (Figs. 5-10 through 5-18) have been normalized by the free space value of the radiation resistance for the particular antenna in question. This normalization constant has the value 73.2 ohms for the half wave dipole, and

$$(798) \cdot \left(\frac{\ell}{\lambda}\right)^2$$

for the Hertzian dipole.

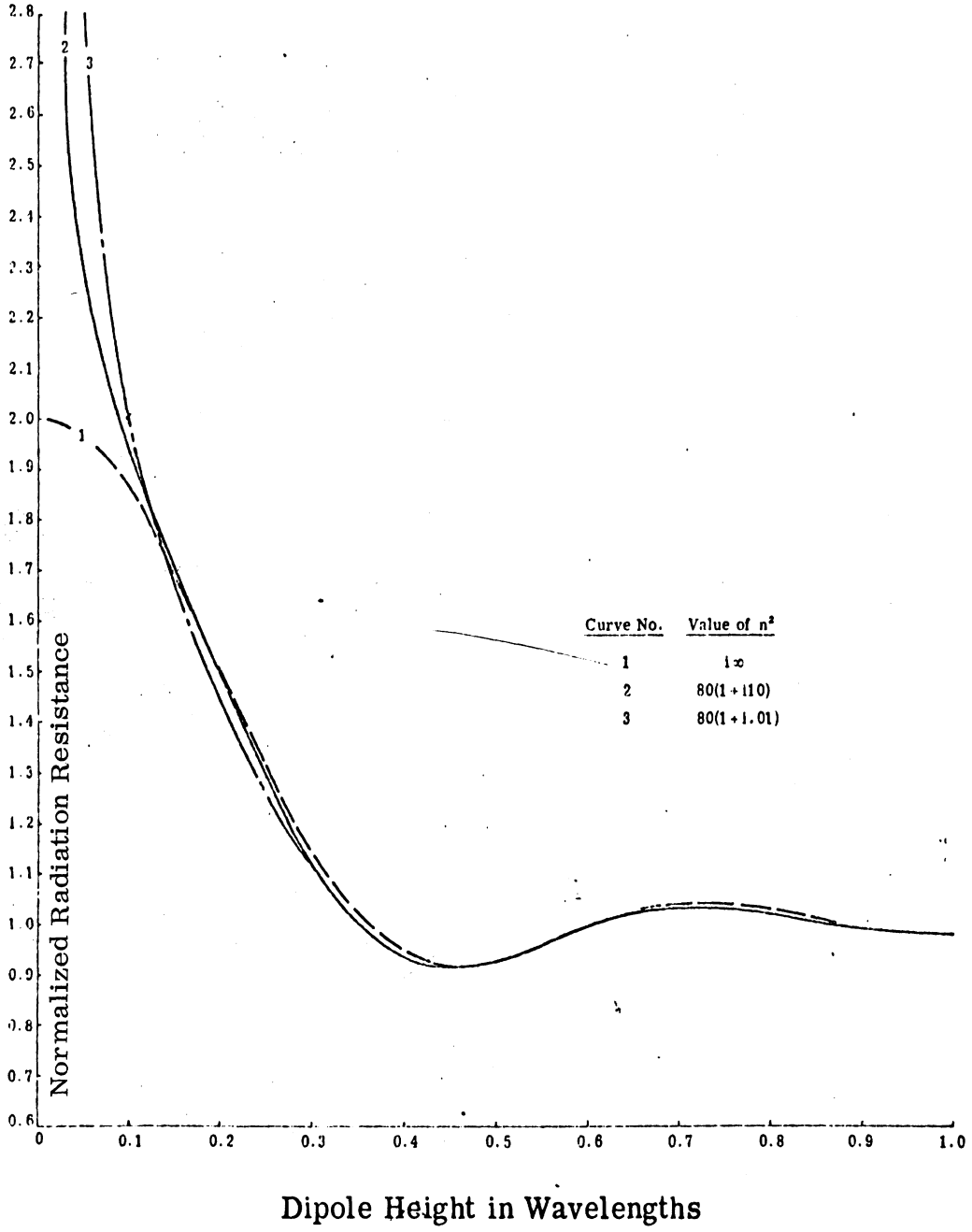

FIG. 5-10: Radiation Resistance of the Vertical Hertzian Dipole.

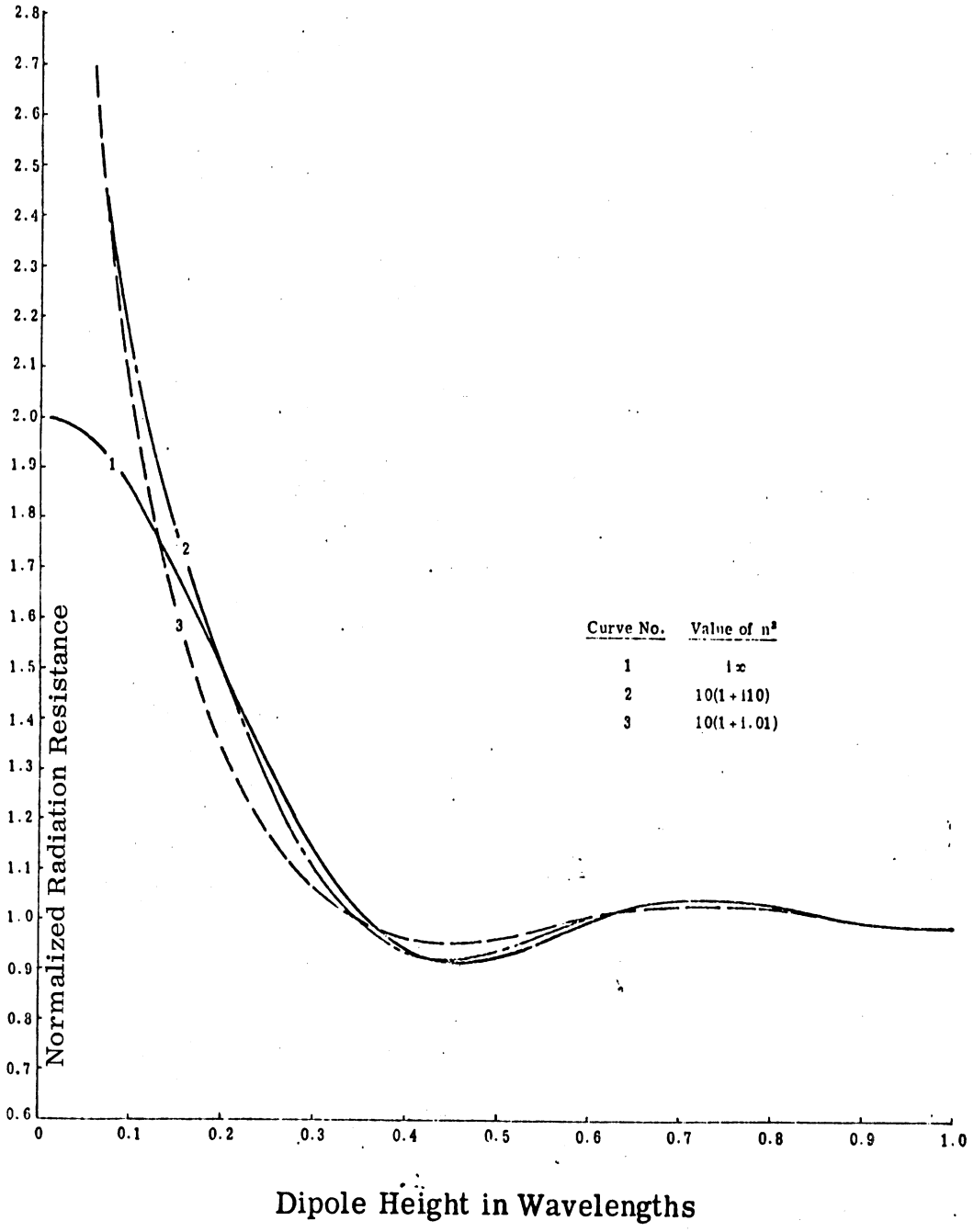

FIG. 5-11: Radiation Resistance of the Vertical Hertzian Dipole.

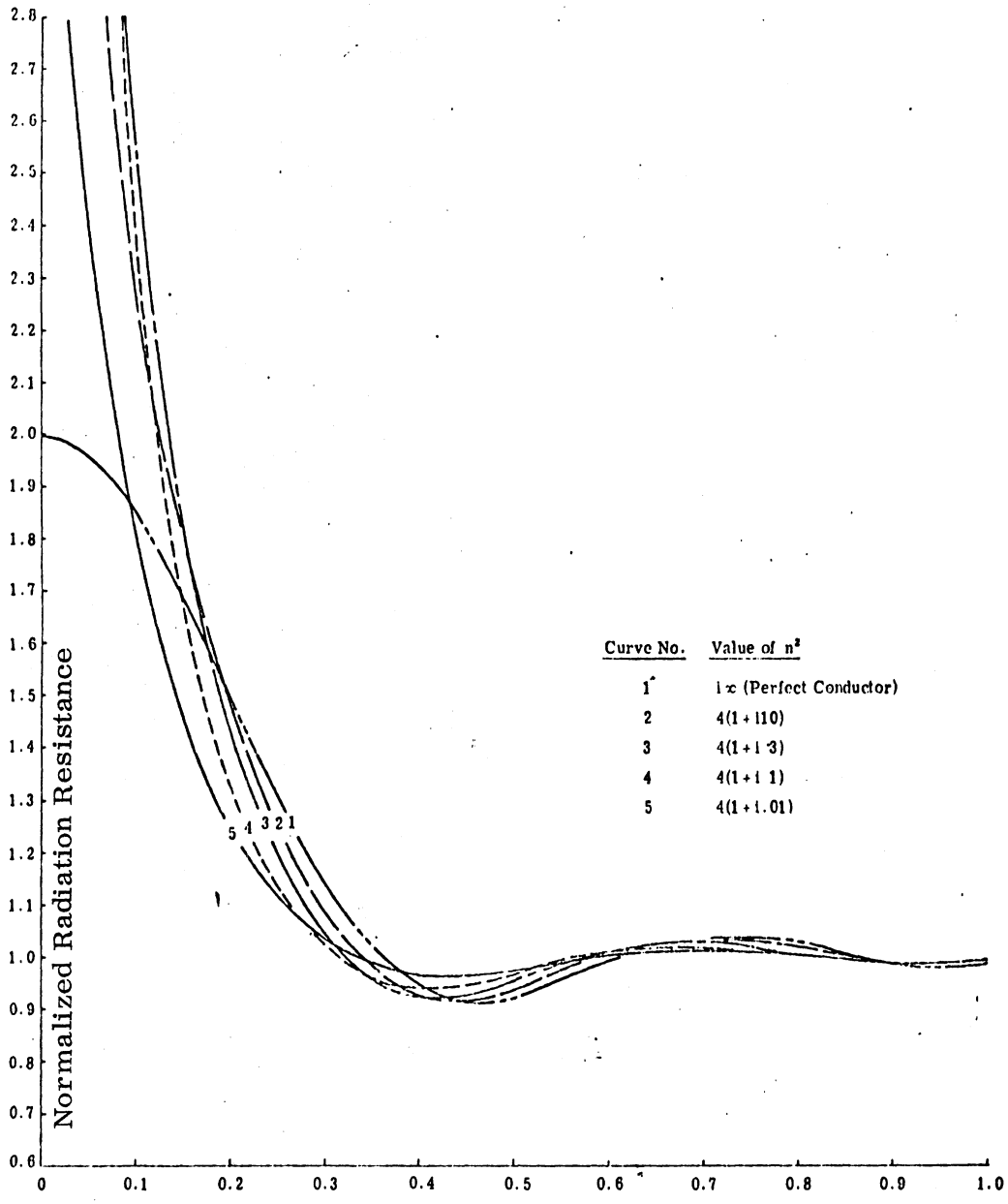

FIG. 5-12: Radiation Resistance of the Vertical Hertzian Dipole.

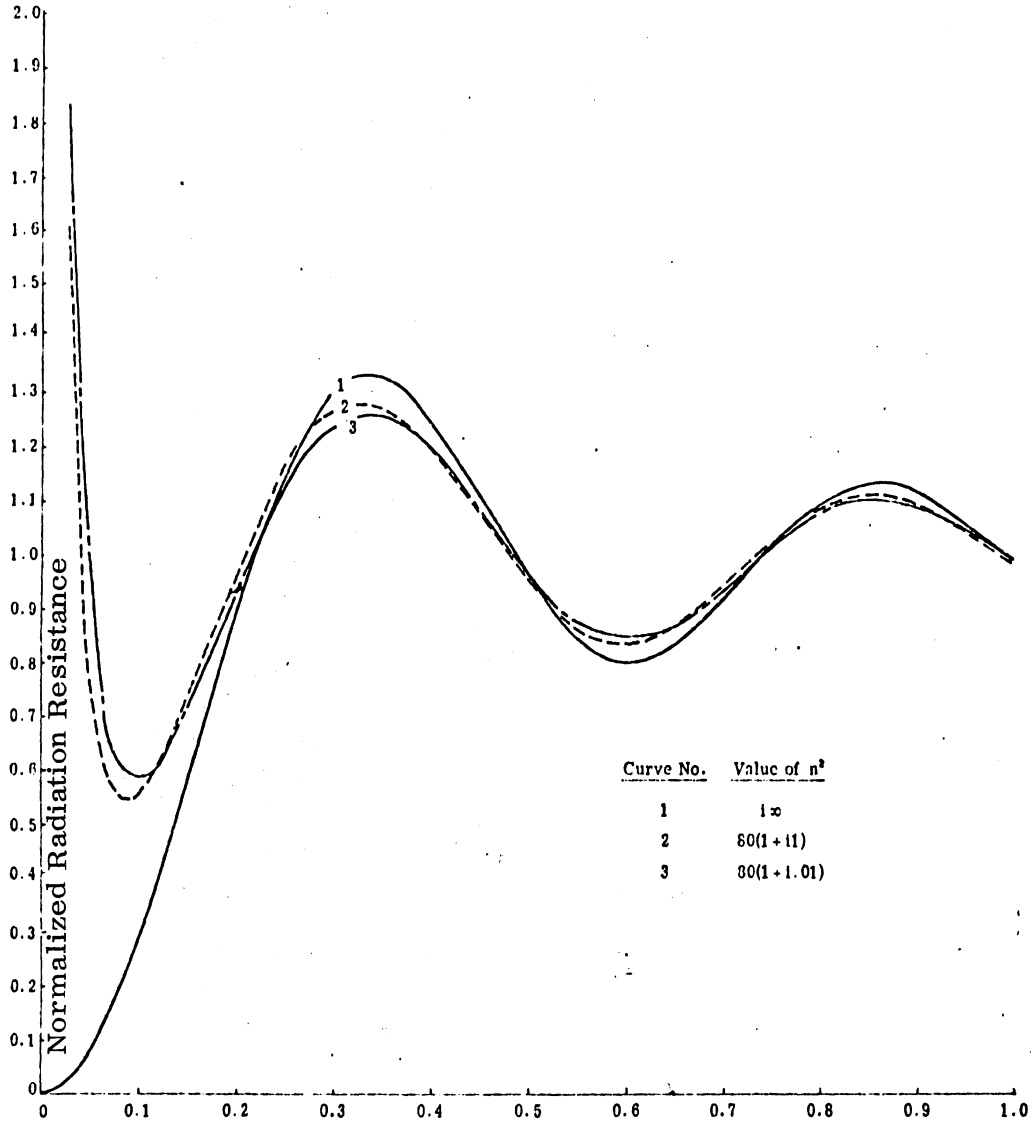

FIG. 5-13: Radiation Resistance of the Horizontal Hertzian Dipole.

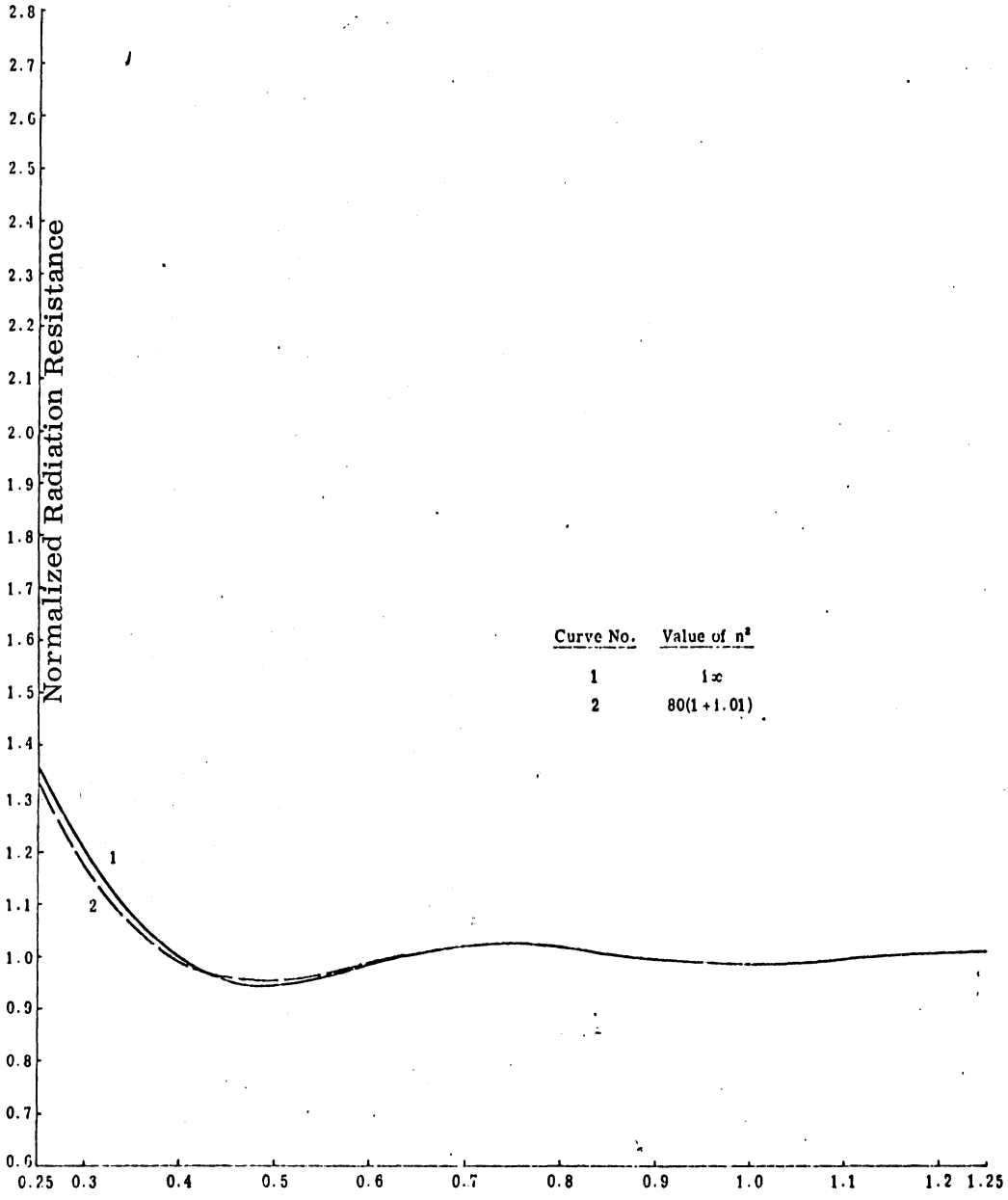

FIG. 5-16: Radiation Resistance of the Vertical Half-wave Dipole.

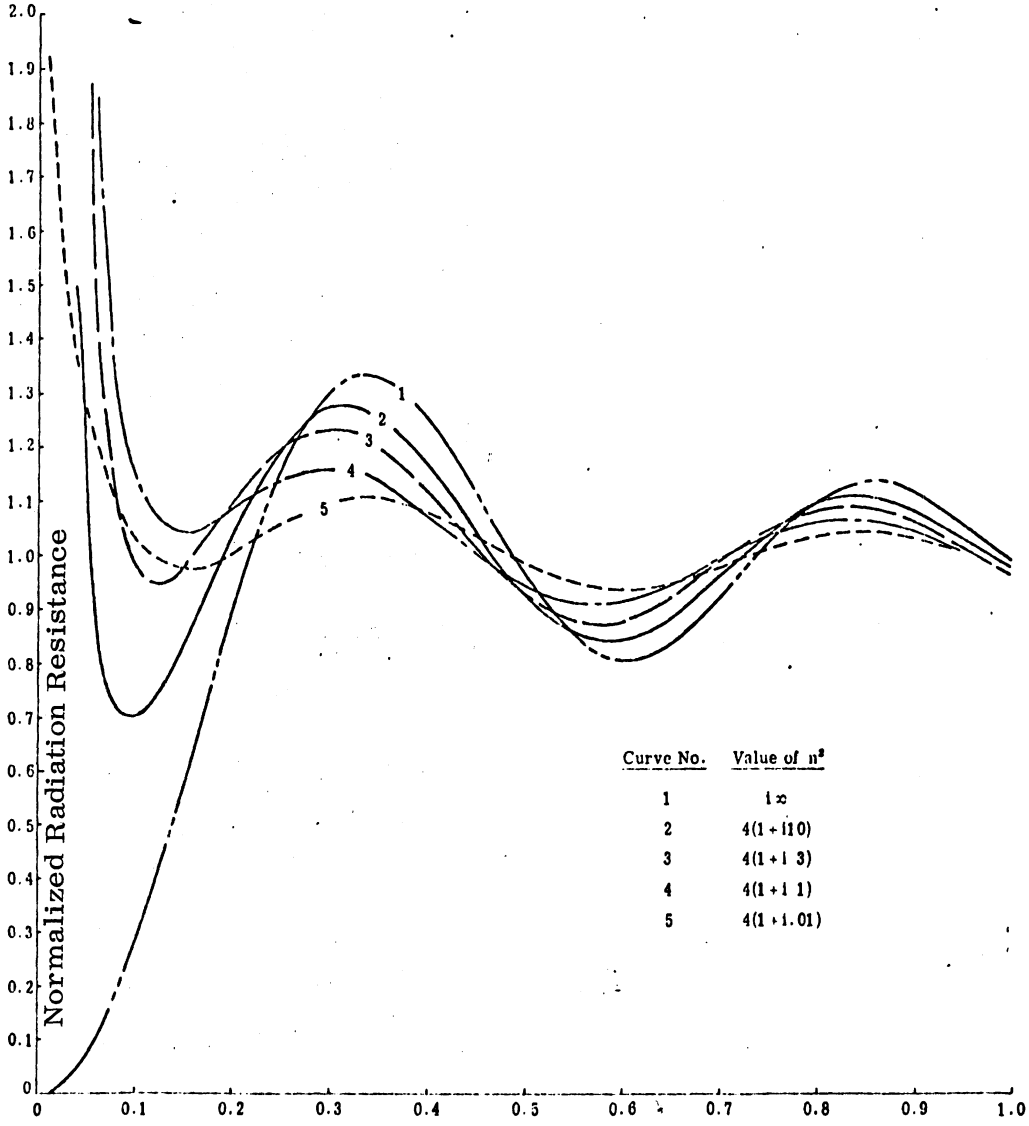

FIG. 5-15: Radiation Resistance of the Horizontal Hertzian Dipole.

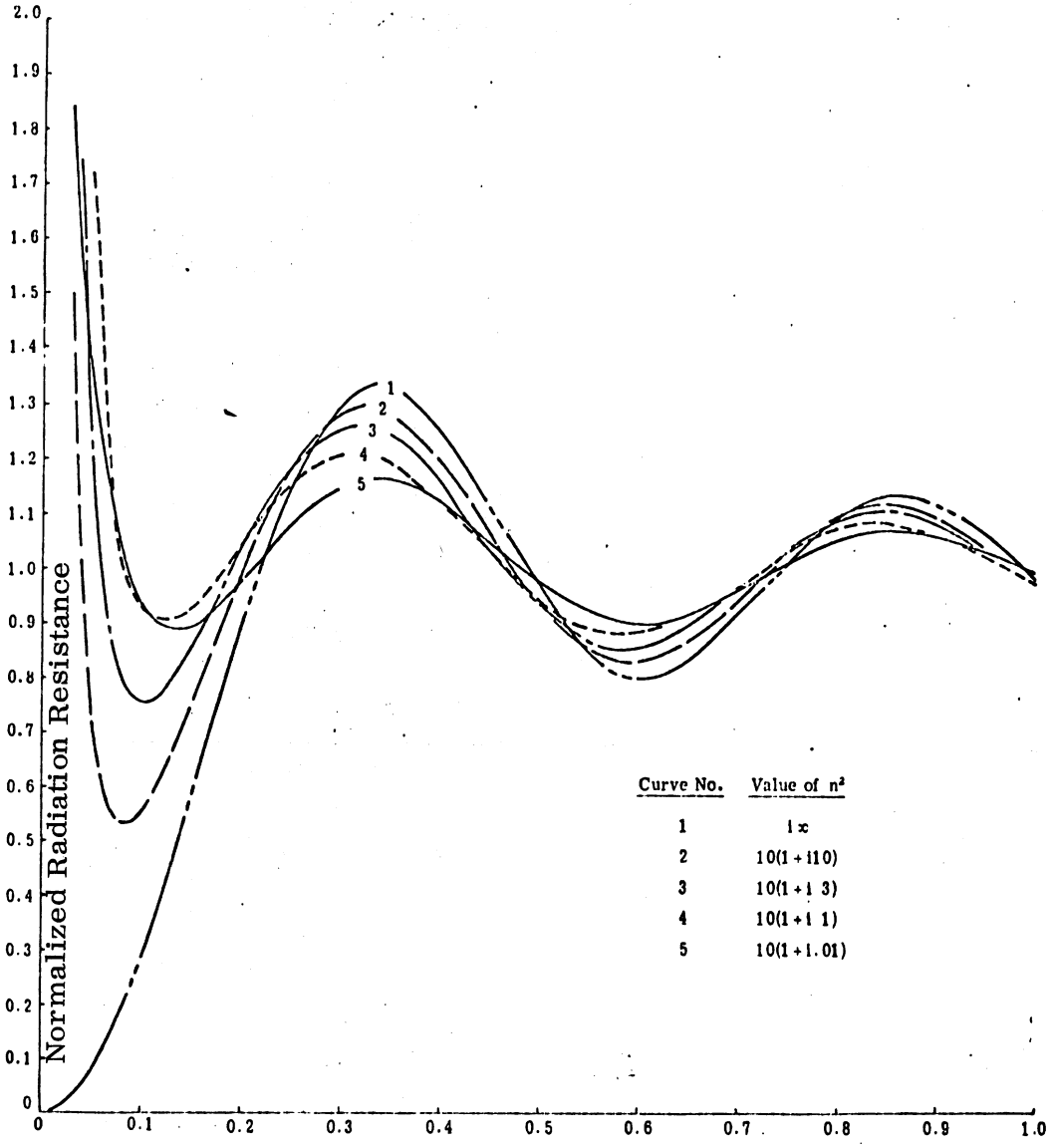

FIG. 5-14: Radiation Resistance of the Horizontal Hertzian Dipole.

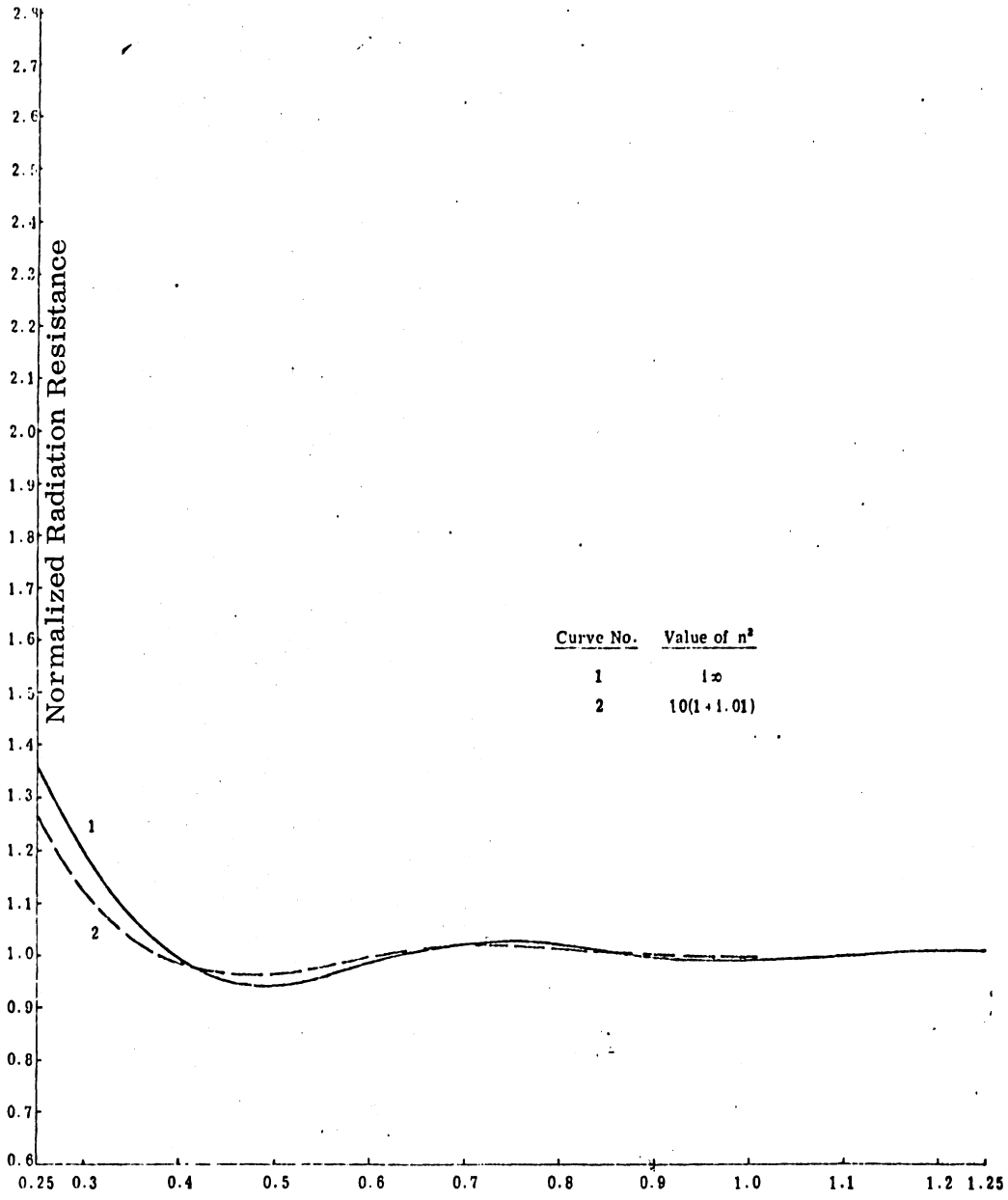

FIG. 5-17: Radiation Resistance of the Vertical Half-wave Dipole.

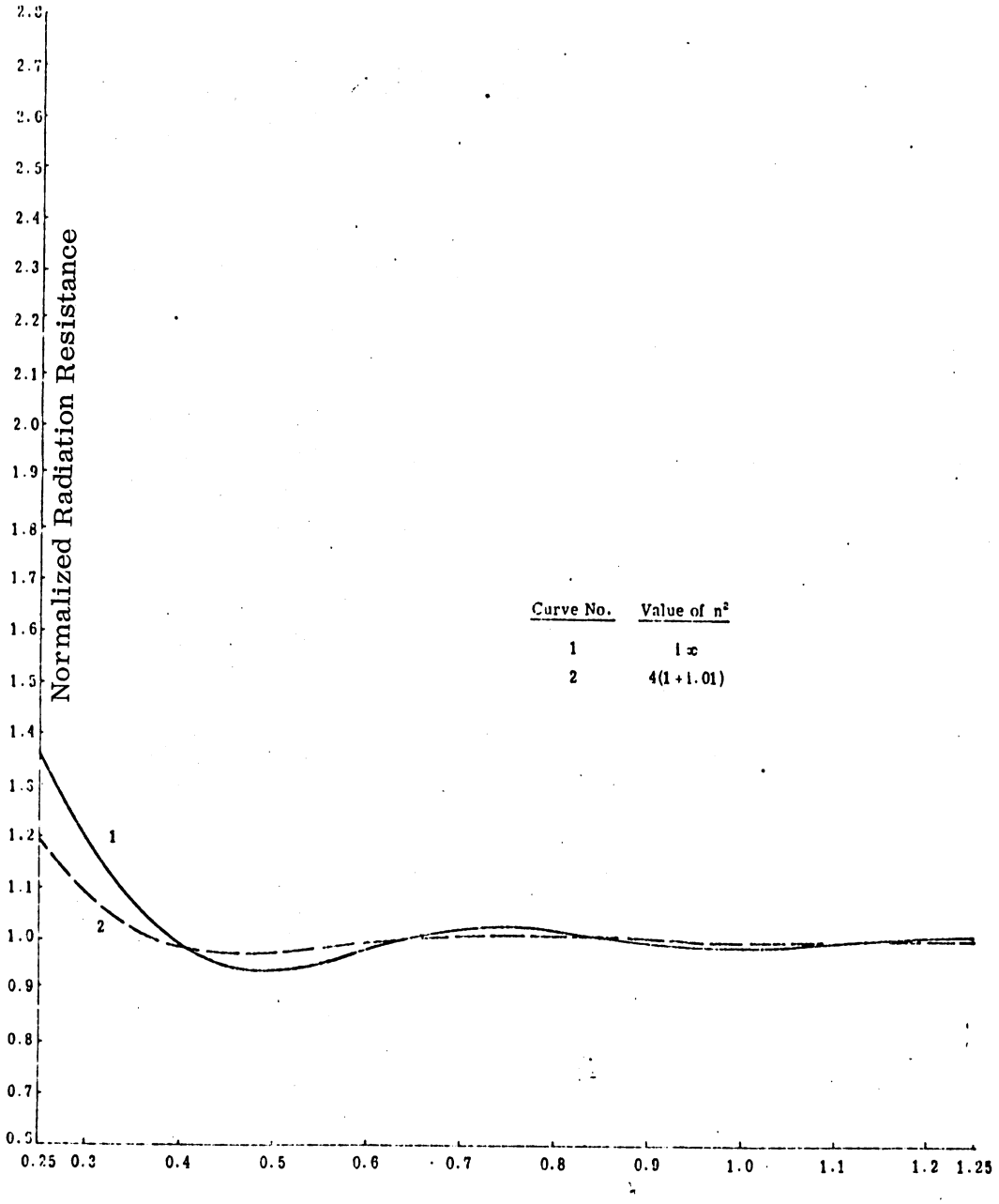

FIG. 5-18: Radiation Resistance of the Vertical Half-wave Dipole.

5.5 Reflection Coefficient Curves

The reflection coefficients, $A(\theta)$ and $B(\theta)$, for vertically and horizontally polarized plane waves at a plane surface are given by Eq. (3.13). The following graphs (Figs. 5-19 through 5-21) are computer generated plots of $|A(\theta)|$ and $|B(\theta)|$. Appendix C contains a listing of the program used to generate these plots.

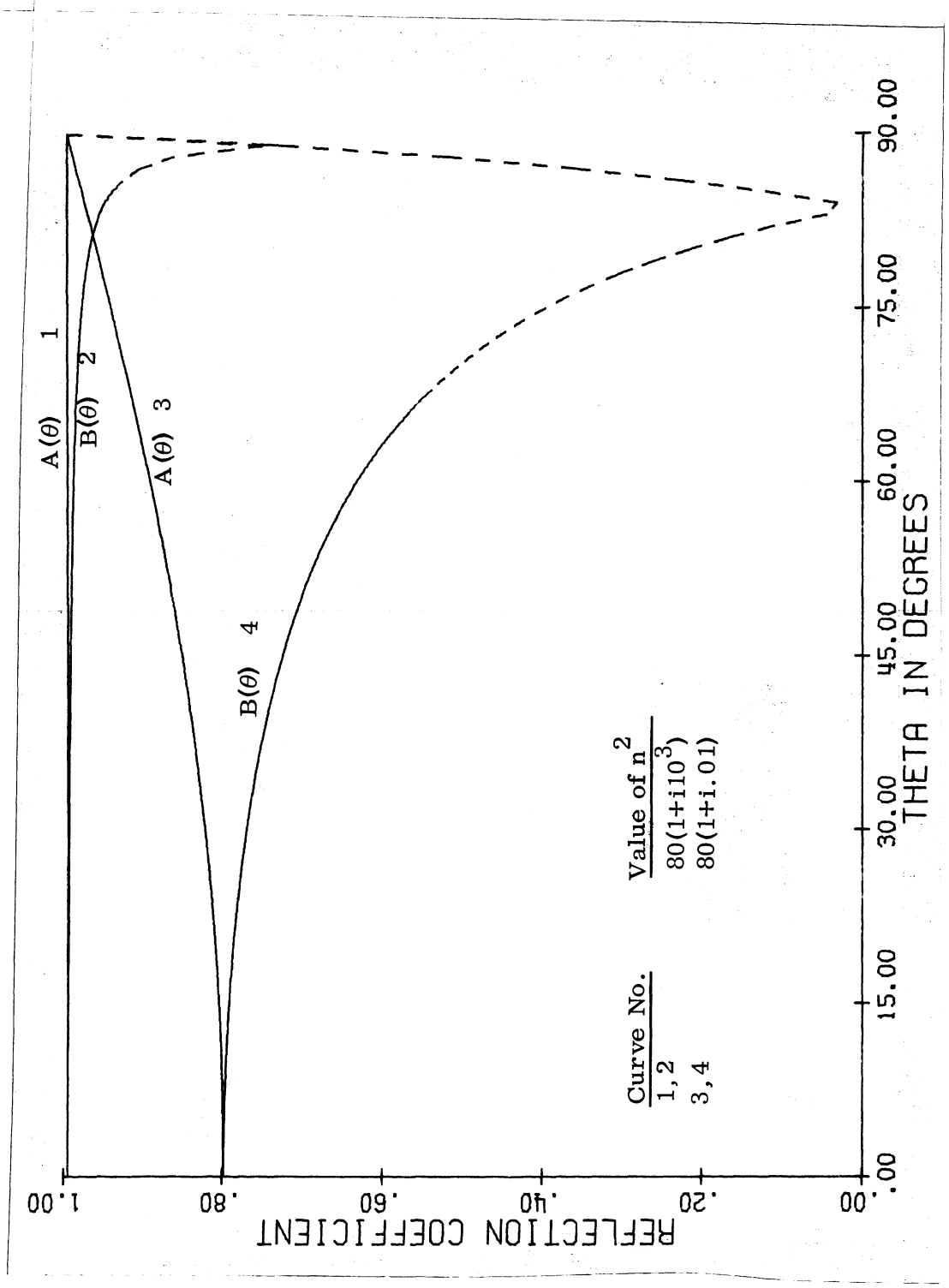

FIG. 5-19: Reflection Coefficient Modulus Versus Theta for Water.

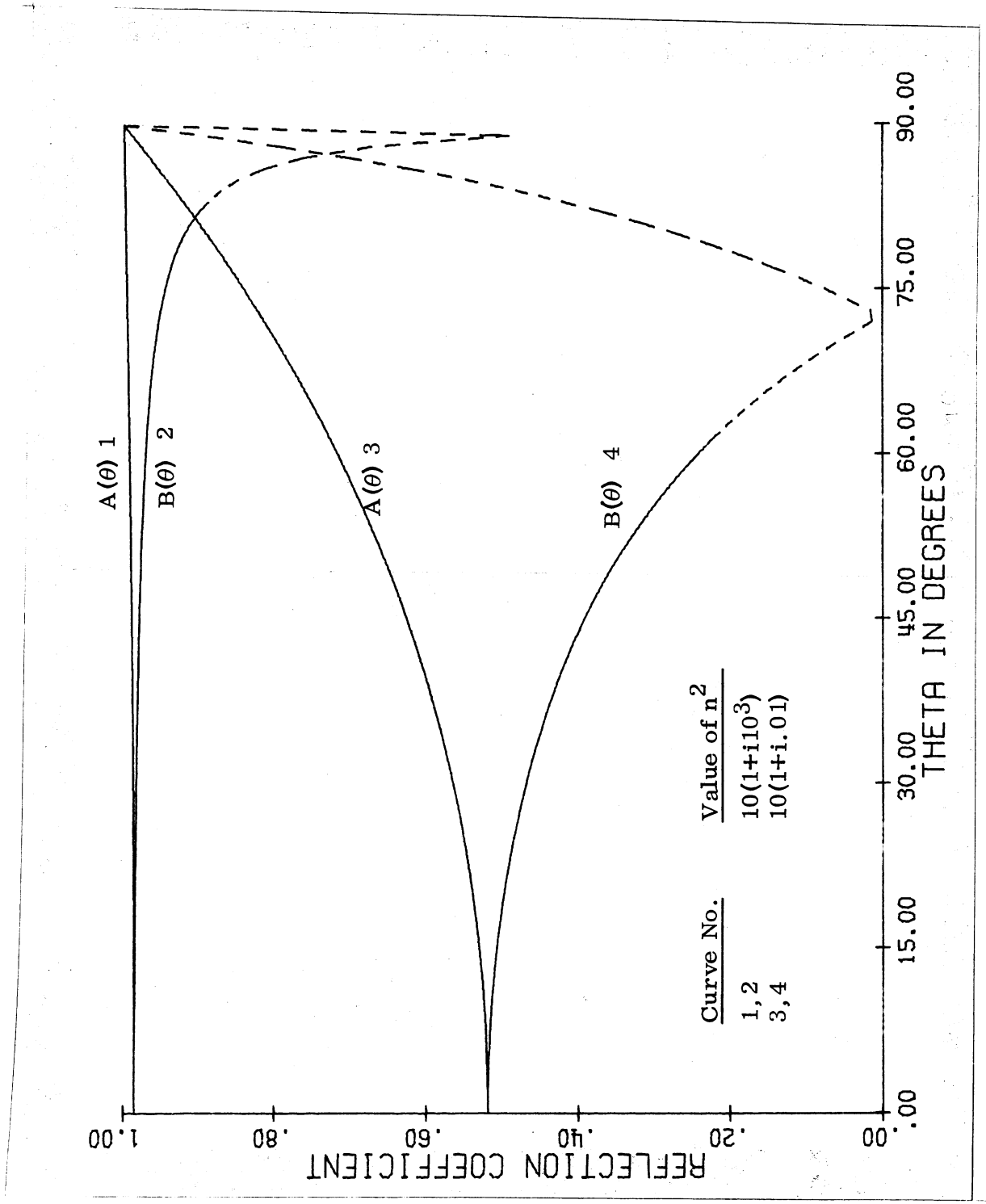

FIG. 5-20: Reflection Coefficient Modulus versus Theta for Good Earth.

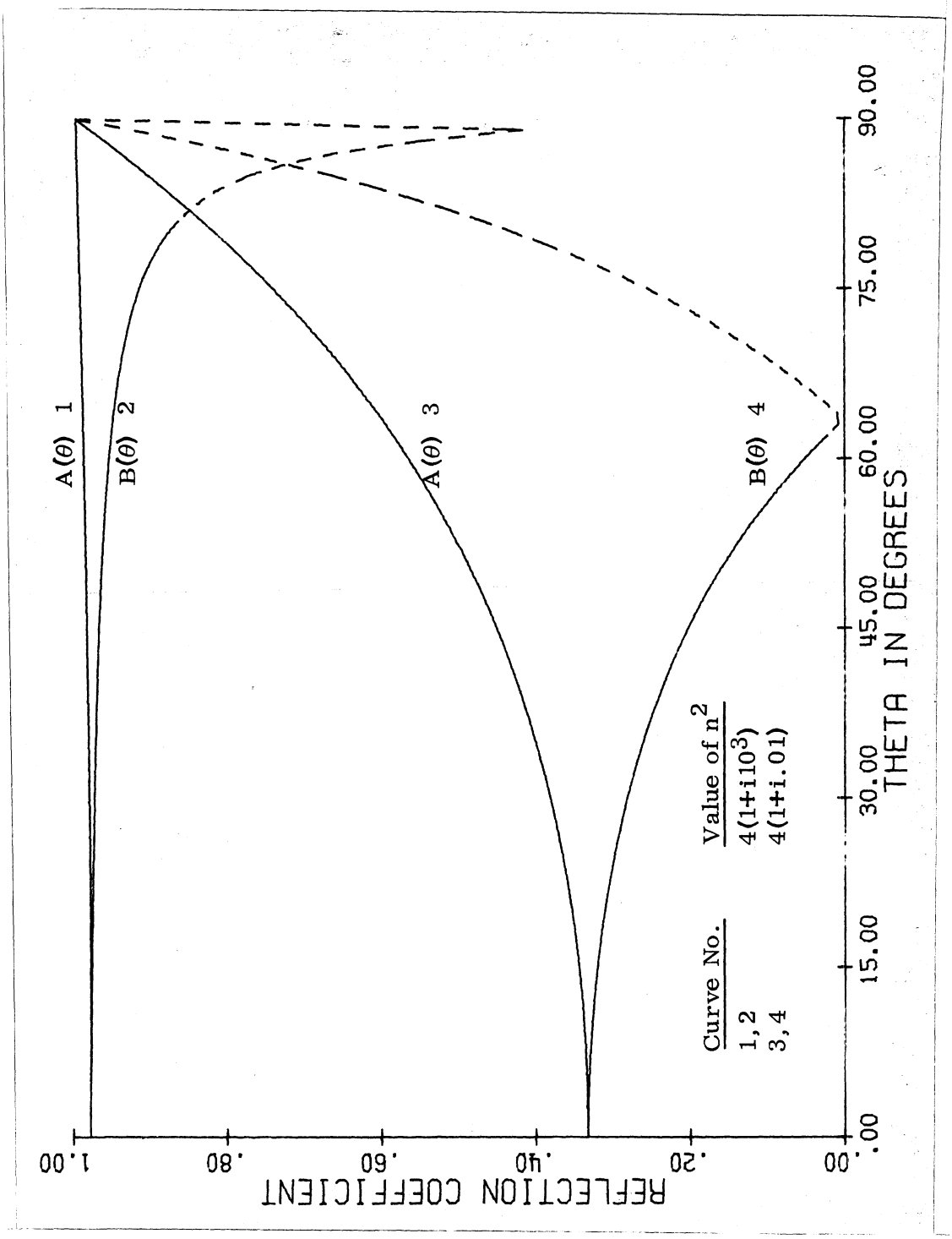

FIG. 5-21: Reflection Coefficient Modulus Versus Theta for Poor Earth.

5.6 Power Patterns

This section contains representative plots of the power patterns of the three antennas treated in Chapters III and IV. The actual formulae used to plot the curves were derived by normalizing $|\bar{E}|^2$ where $\bar{E}$ denotes the far-zone field. The functions used to generate the patterns are given below.

A. Vertical Hertzian Dipole

$$|\bar{E}|^2 \propto \left| e^{-ikz_o\cos\theta} + b(\theta) e^{ikz_o\cos\theta} \right|^2 \sin^2\theta \quad .$$

B. Horizontal Hertzian Dipole

$$|\bar{E}|^2 \propto \left| e^{-ikz_o\cos\theta} + a(\theta) e^{ikz_o\cos\theta} \right|^2 , \ \phi = \pi/2 \quad .$$

C. Vertical Half-wave Dipole

$$|\bar{E}|^2 \propto \left| e^{-ikz_o\cos\theta} + b(\theta) e^{ikz_o\cos\theta} \right|^2 \left\{ \frac{\cos\left(\frac{\pi}{2}\cos\theta\right)}{\sin\theta} \right\}^2$$

where the coefficients $a(\theta)$ and $b(\theta)$ are defined in Section 3.2.3.

In plotting these curves (Figs. 5-22 through 5-48), the maximum value of each pattern has been normalized to be the same for each curve.

It is observed that there is no ϕ-dependence for the vertical dipoles while for the horizontal dipole we have plotted the pattern corresponding to $\phi = \pi/2$.

A listing of the computer program that was used to generate these plots is included in Appendix C.

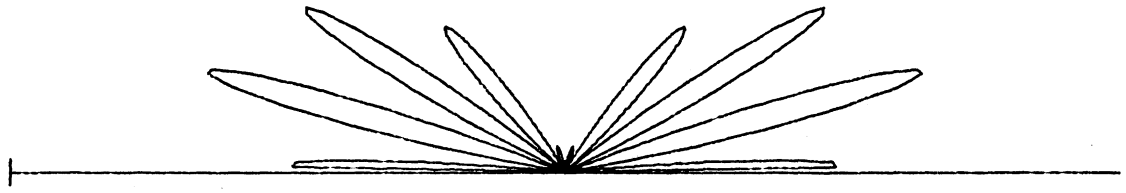

ANTENNA CENTER HEIGHT OF 2. WAVELENGTHS

ANTENNA CENTER HEIGHT OF .4 WAVELENGTHS

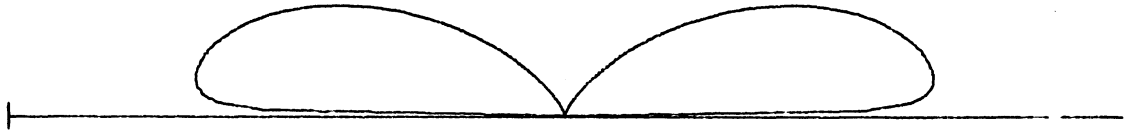

ANTENNA CENTER HEIGHT OF .2 WAVELENGTHS

FIG. 5-22: Power Patterns for the Vertical Hertzian Dipole; $n^2 = 80(1+i10^3)$.

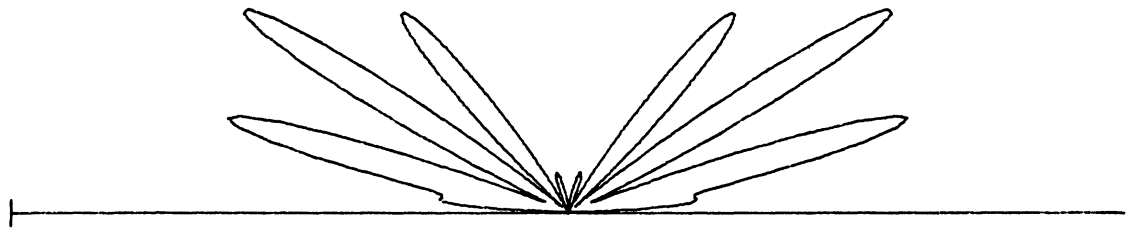

ANTENNA CENTER HEIGHT OF 2. WAVELENGTHS

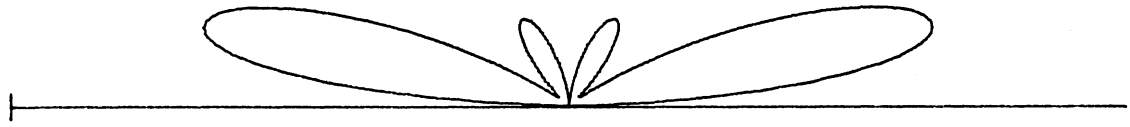

ANTENNA CENTER HEIGHT OF .4 WAVELENGTHS

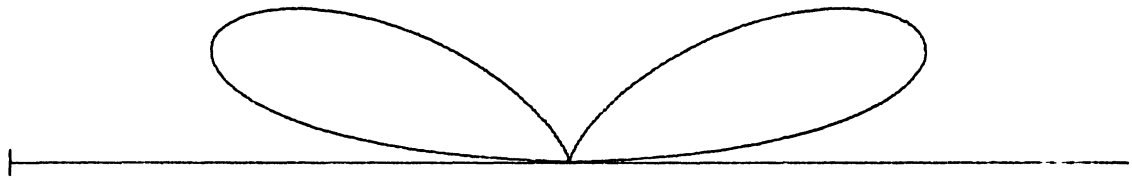

ANTENNA CENTER HEIGHT OF .2 WAVELENGTHS

FIG. 5-23: Power Patterns for the Vertical Hertzian Dipole; $n^2=80(1+i1)$.

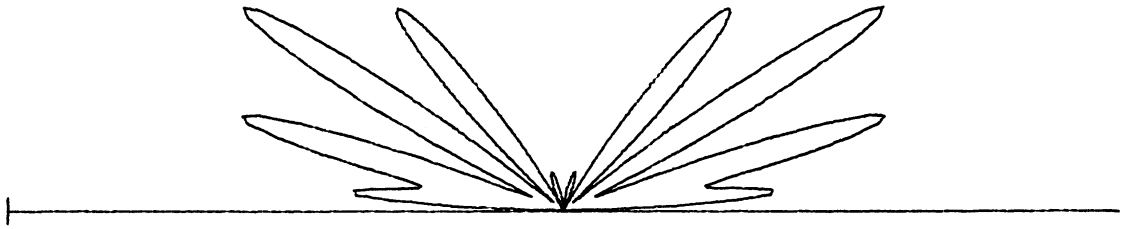

ANTENNA CENTER HEIGHT OF 2. WAVELENGTHS

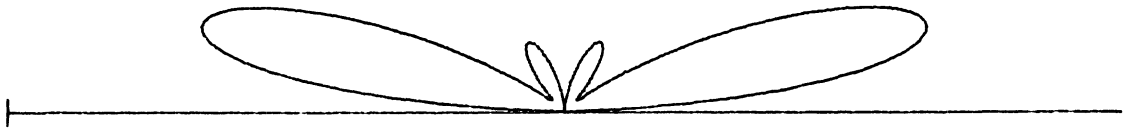

ANTENNA CENTER HEIGHT OF .4 WAVELENGTHS

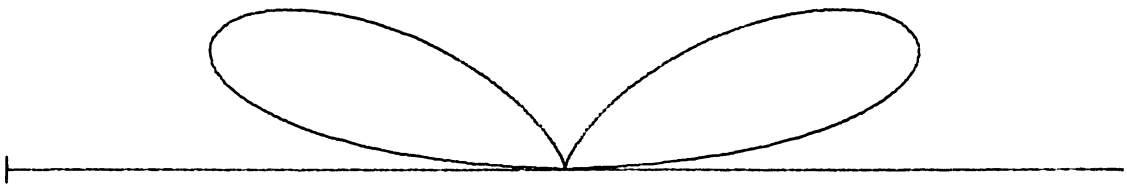

ANTENNA CENTER HEIGHT OF .2 WAVELENGTHS

FIG. 5-24: Power Patterns for the Vertical Hertzian Dipole; $n^2=80(1+i.01)$.

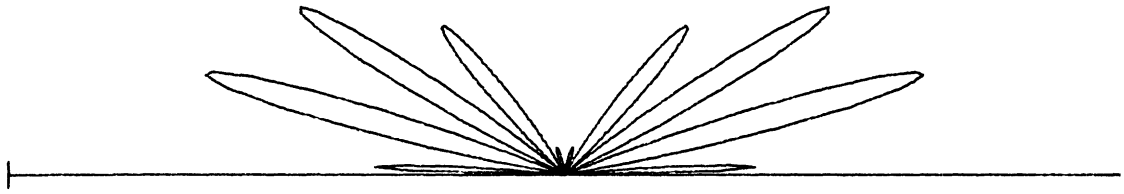

ANTENNA CENTER HEIGHT OF 2. WAVELENGTHS

ANTENNA CENTER HEIGHT OF .4 WAVELENGTHS

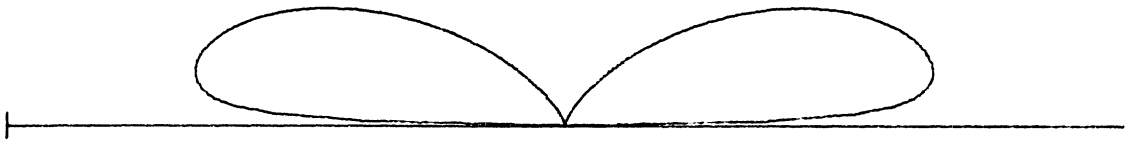

ANTENNA CENTER HEIGHT OF .2 WAVELENGTHS

FIG. 5-25: Power Patterns for the Vertical Hertzian Dipole; $n^2=10(1+i10^3)$.

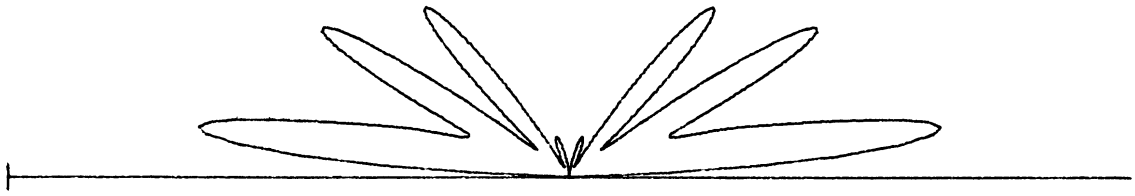

ANTENNA CENTER HEIGHT OF 2. WAVELENGTHS

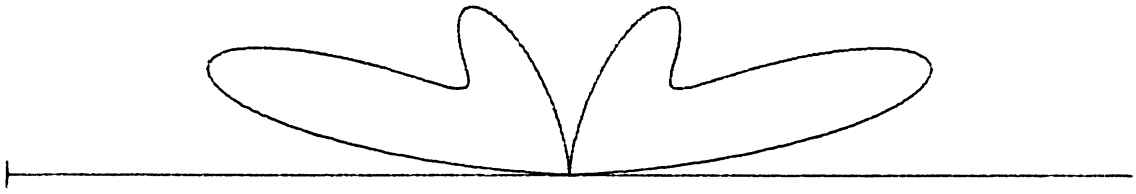

ANTENNA CENTER HEIGHT OF .4 WAVELENGTHS

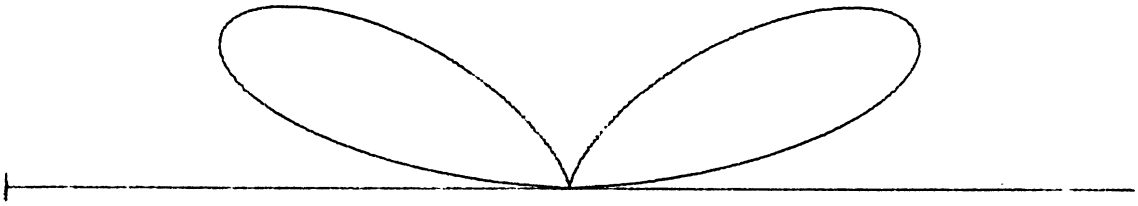

ANTENNA CENTER HEIGHT OF .2 WAVELENGTHS

FIG. 5-26: Power Patterns for the Vertical Hertzian Dipole; $n^2 = 10(1+i1)$.

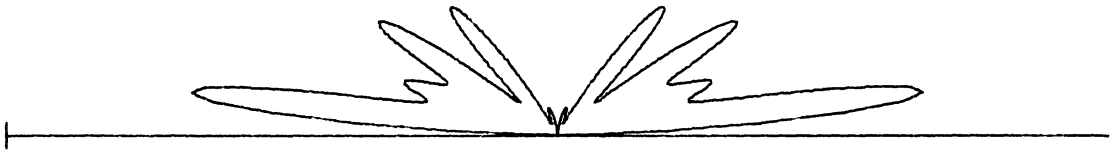

ANTENNA CENTER HEIGHT OF 2. WAVELENGTHS

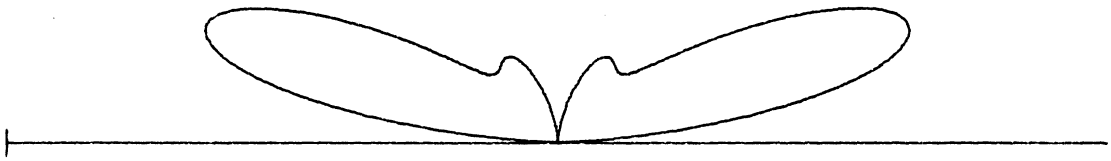

ANTENNA CENTER HEIGHT OF .4 WAVELENGTHS

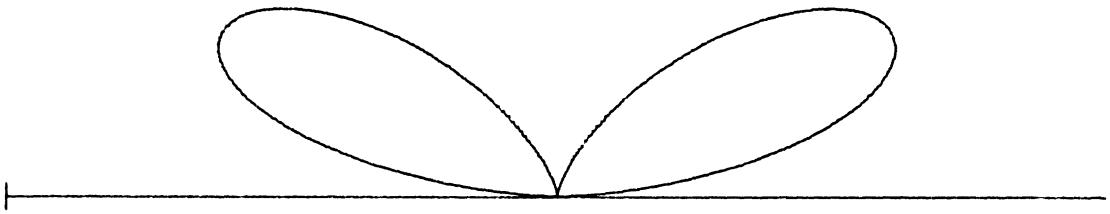

ANTENNA CENTER HEIGHT OF .2 WAVELENGTHS

FIG. 5-27: Power Patterns for the Vertical Hertzian Dipole; $n^2 = 10(1+i.01)$.

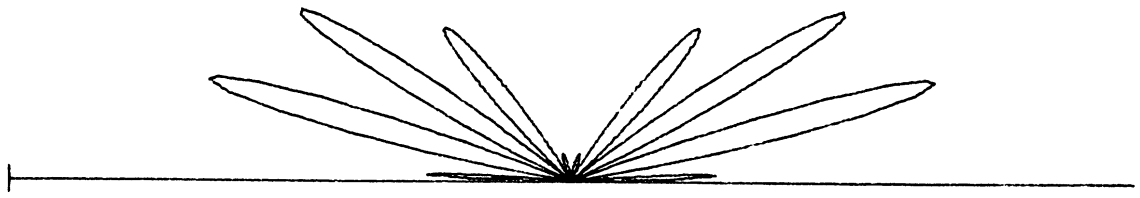

ANTENNA CENTER HEIGHT OF 2. WAVELENGTHS

ANTENNA CENTER HEIGHT OF .4 WAVELENGTHS

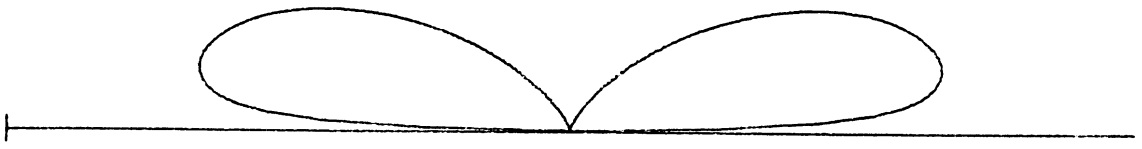

ANTENNA CENTER HEIGHT OF .2 WAVELENGTHS

FIG. 5-28: Power Patterns for the Vertical Hertzian Dipole; $n^2 = 4(1+i10^3)$.

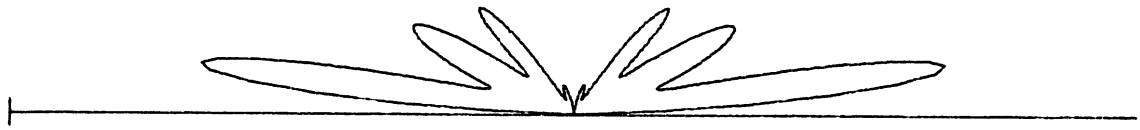

ANTENNA CENTER HEIGHT OF 2. WAVELENGTHS

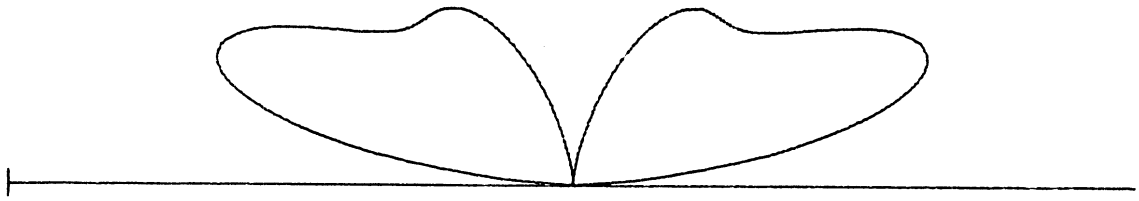

ANTENNA CENTER HEIGHT OF .4 WAVELENGTHS

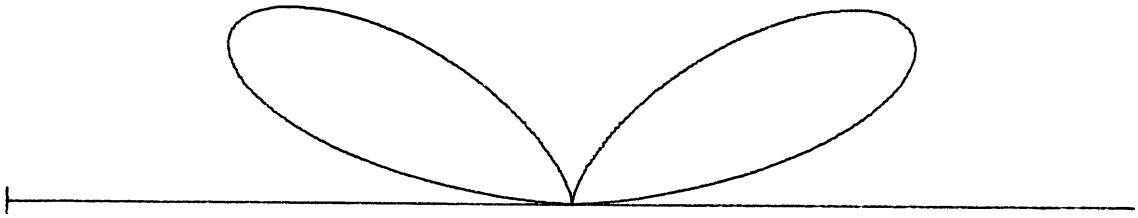

ANTENNA CENTER HEIGHT OF .2 WAVELENGTHS

FIG. 5-29: Power Patterns for the Vertical Hertzian Dipole; $n^2 = 4(1+i1)$.

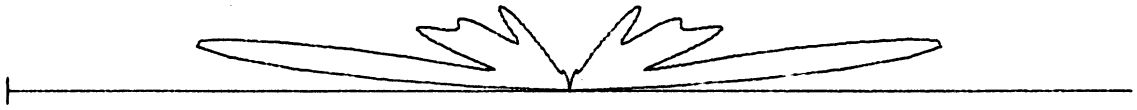

ANTENNA CENTER HEIGHT OF 2. WAVELENGTHS

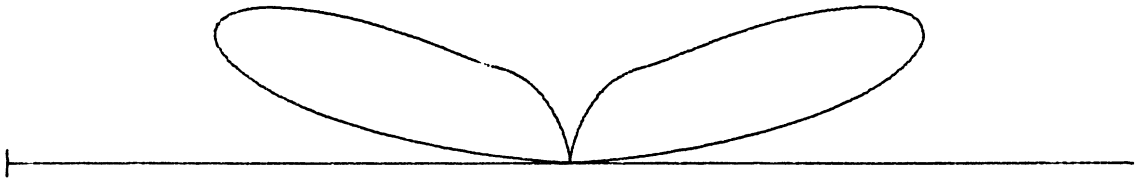

ANTENNA CENTER HEIGHT OF .4 WAVELENGTHS

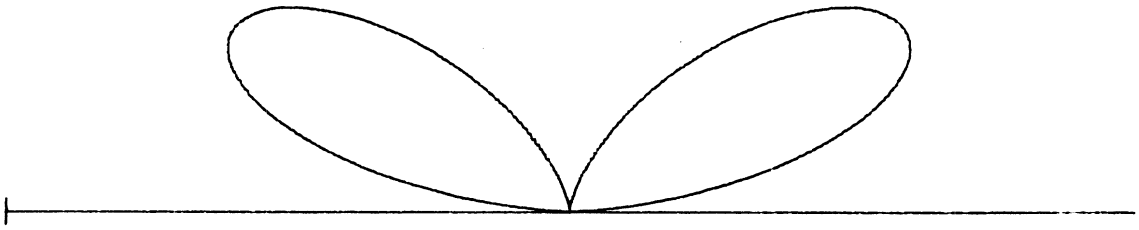

ANTENNA CENTER HEIGHT OF .2 WAVELENGTHS

FIG. 5-30: Power Patterns for the Vertical Hertzian Dipole; $n^2=4(1+i.01)$.

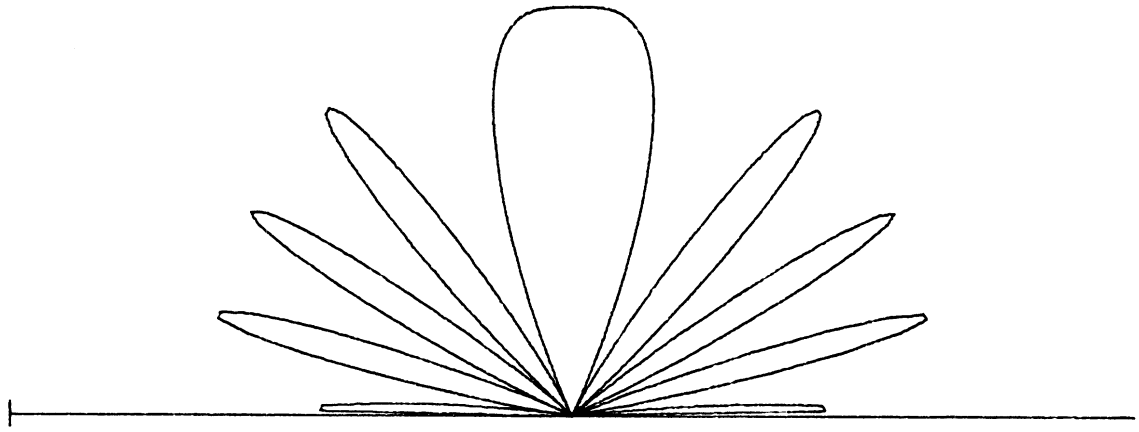

ANTENNA CENTER HEIGHT OF 2. WAVELENGTHS

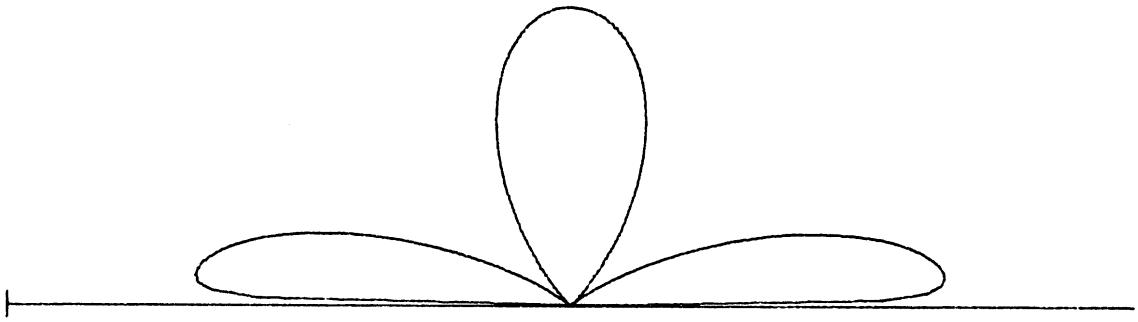

ANTENNA CENTER HEIGHT OF .4 WAVELENGTHS

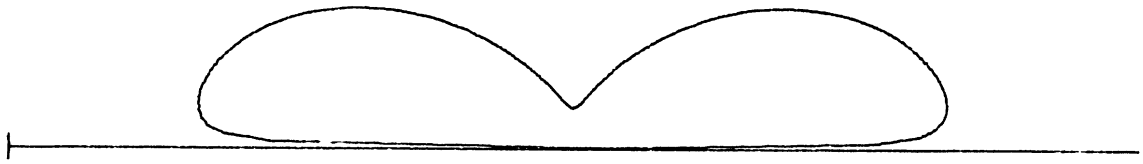

ANTENNA CENTER HEIGHT OF .2 WAVELENGTHS

FIG. 5-31: Power Patterns for the Horizontal Hertzian Dipole; $n^2 = 80(1+i10^3)$.

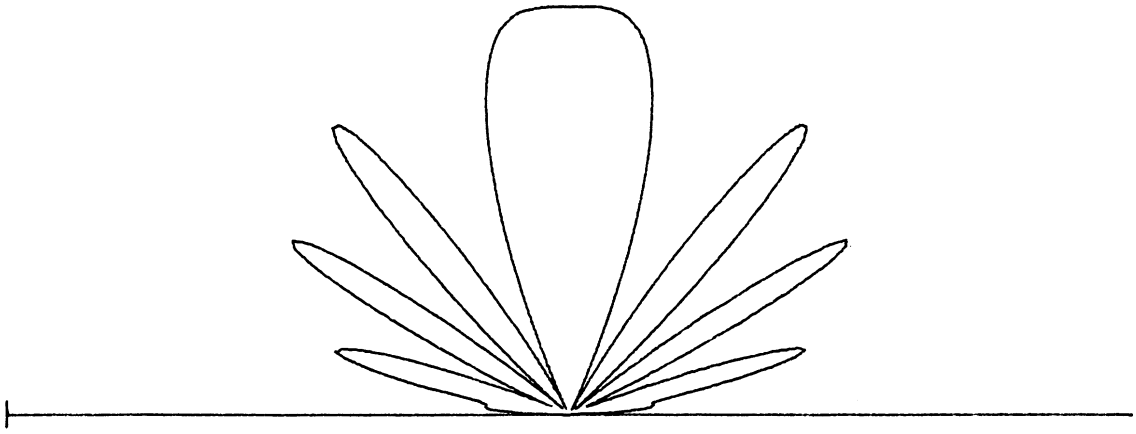

ANTENNA CENTER HEIGHT OF 2. WAVELENGTHS

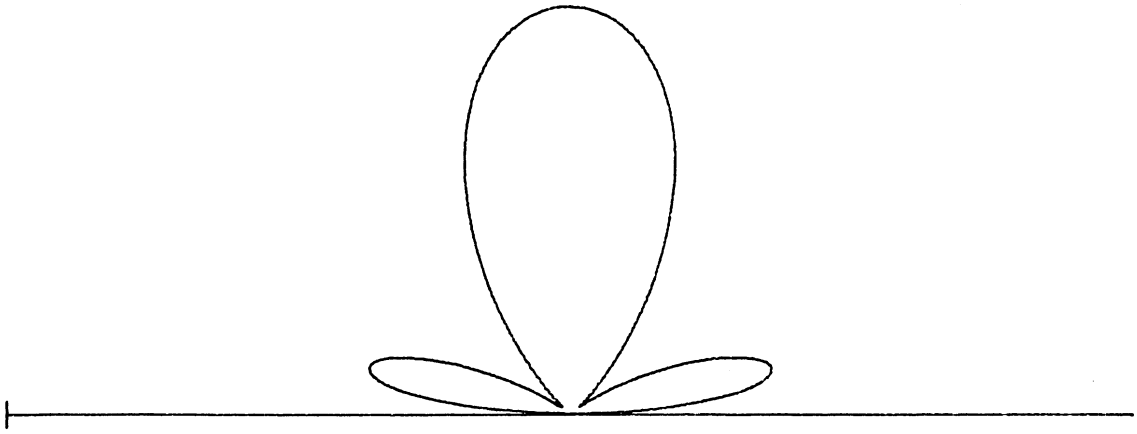

ANTENNA CENTER HEIGHT OF .4 WAVELENGTHS

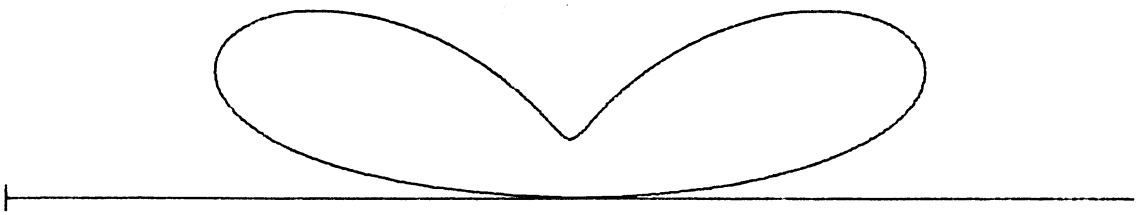

ANTENNA CENTER HEIGHT OF .2 WAVELENGTHS

FIG. 5-32: Power Patterns for the Horizontal Hertzian Dipole; $n^2 = 80(1+i1)$.

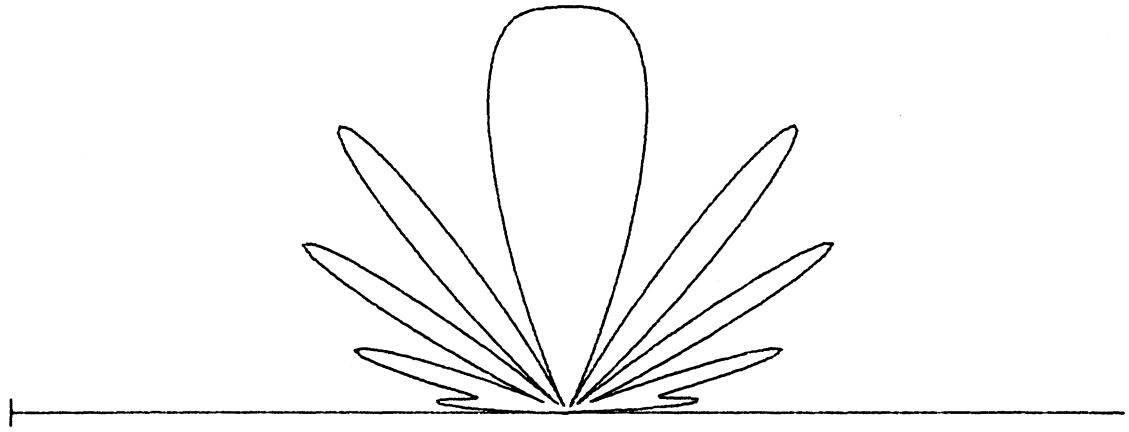

ANTENNA CENTER HEIGHT OF 2. WAVELENGTHS

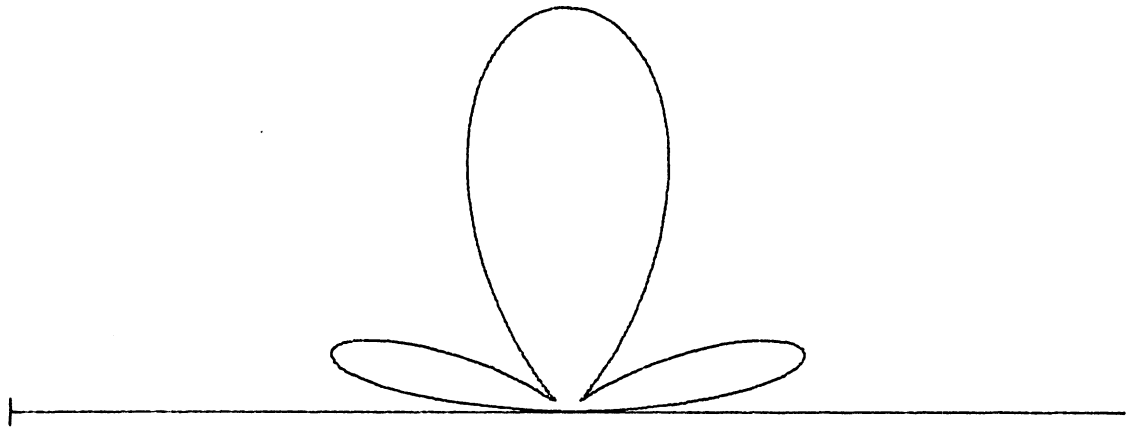

ANTENNA CENTER HEIGHT OF .4 WAVELENGTHS

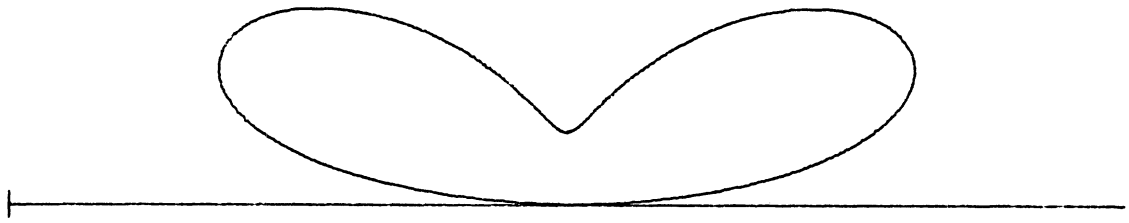

ANTENNA CENTER HEIGHT OF .2 WAVELENGTHS

FIG. 5-33: Power Patterns for the Horizontal Hertzian Dipole; $n^2 = 80(1+i.01)$.

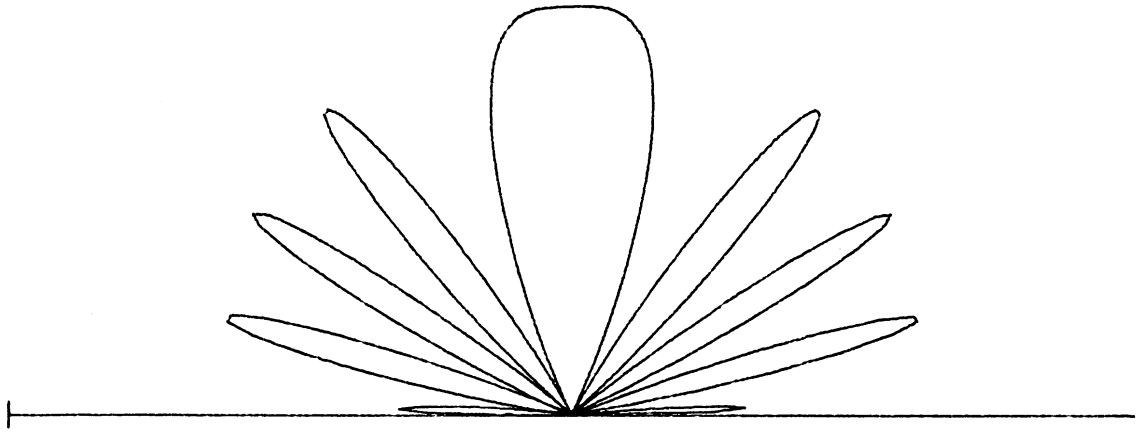

ANTENNA CENTER HEIGHT OF 2. WAVELENGTHS

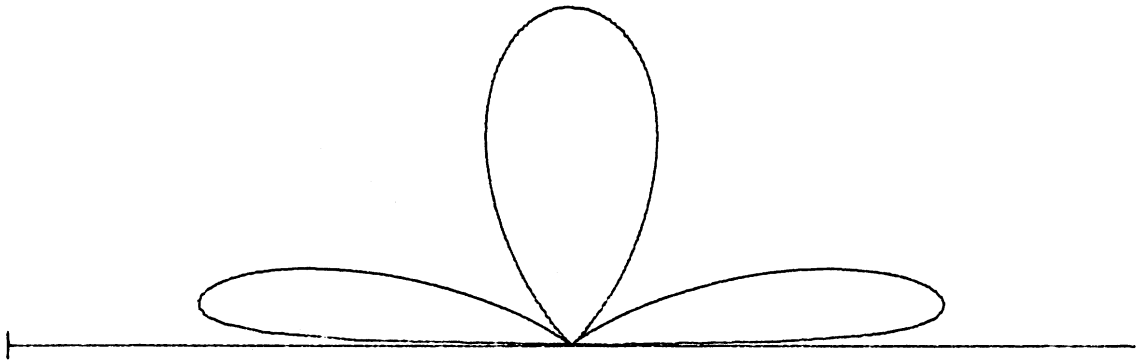

ANTENNA CENTER HEIGHT OF .4 WAVELENGTHS

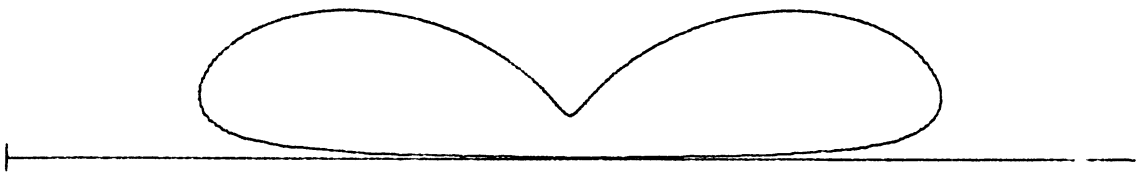

ANTENNA CENTER HEIGHT OF .2 WAVELENGTHS

FIG. 5-34: Power Patterns for the Horizontal Hertzian Dipole; $n^2=10(1+i10^3)$.

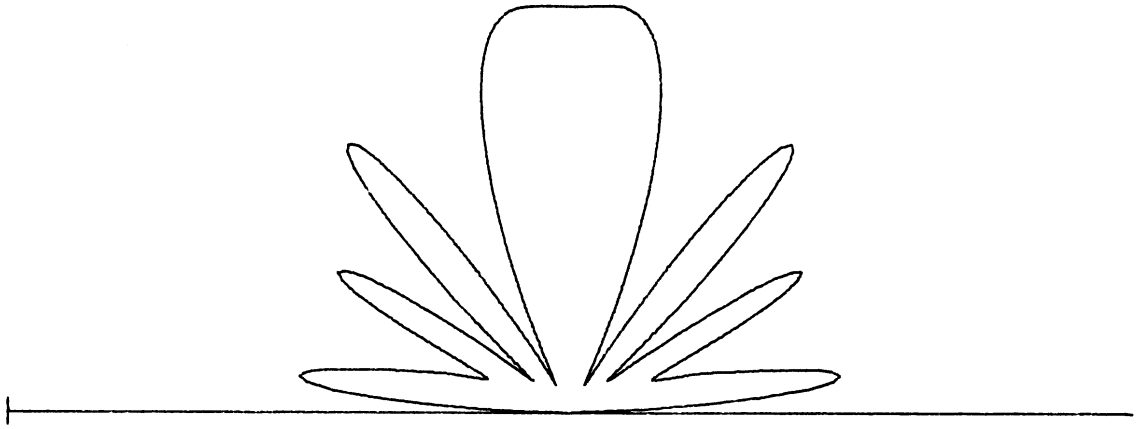

ANTENNA CENTER HEIGHT OF 2. WAVELENGTHS

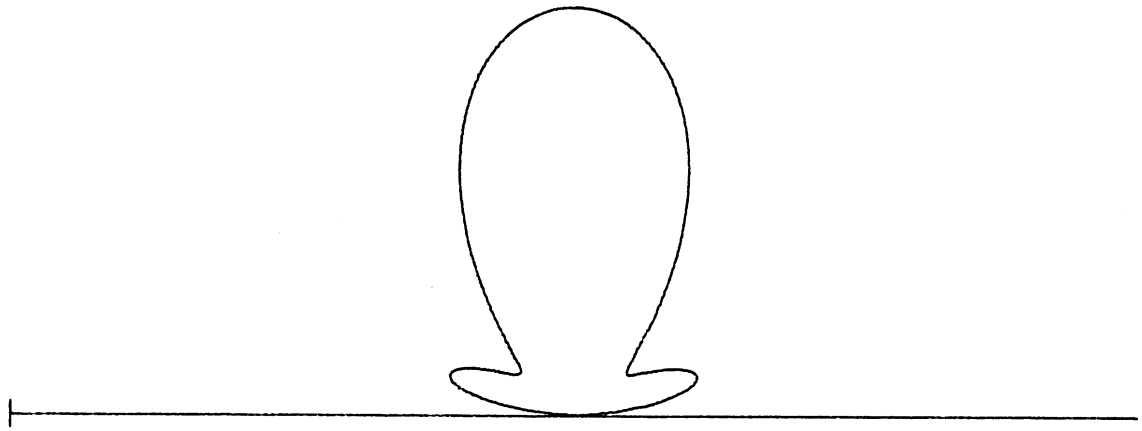

ANTENNA CENTER HEIGHT OF .4 WAVELENGTHS

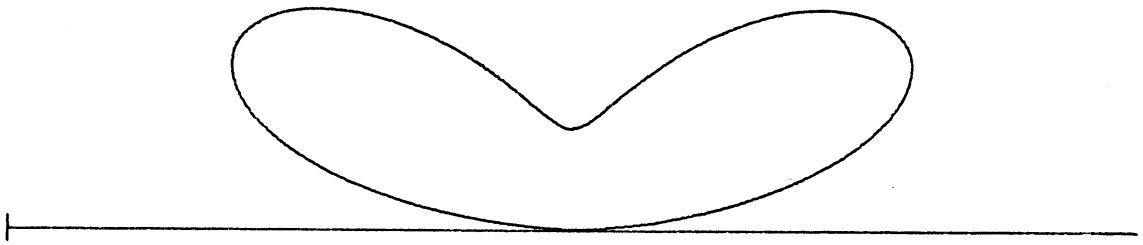

ANTENNA CENTER HEIGHT OF .2 WAVELENGTHS

FIG. 5-35: Power Patterns for the Horizontal Hertzian Dipole; $n^2 = 10(1+i1)$.

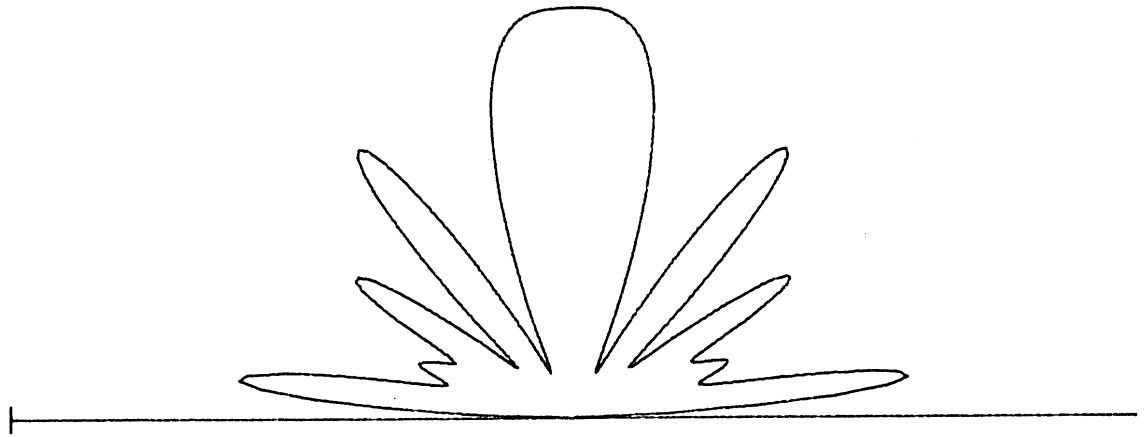

ANTENNA CENTER HEIGHT OF 2. WAVELENGTHS

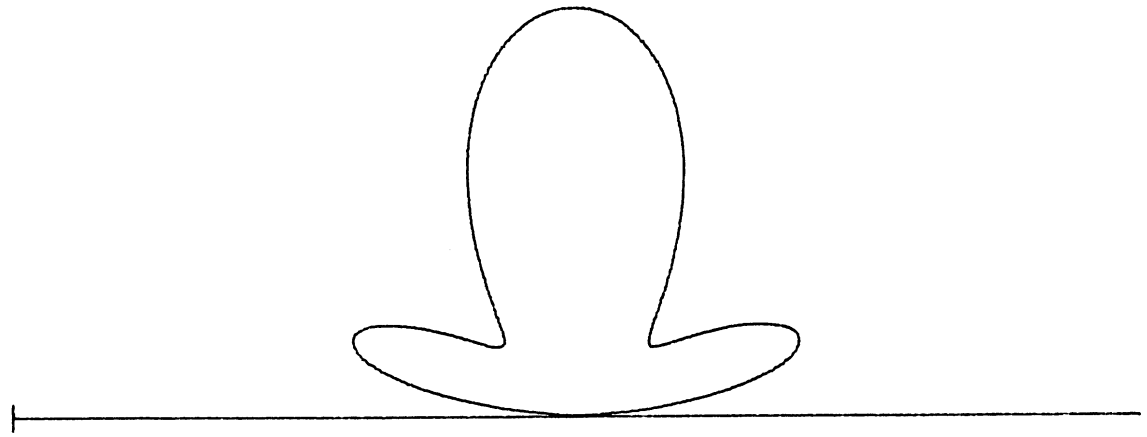

ANTENNA CENTER HEIGHT OF .4 WAVELENGTHS

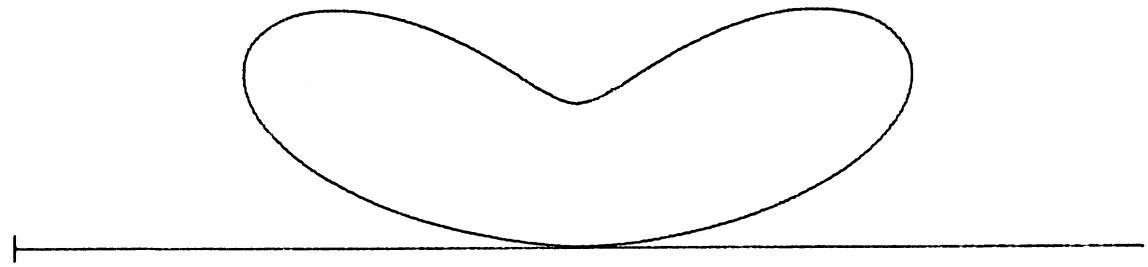

ANTENNA CENTER HEIGHT OF .2 WAVELENGTHS

FIG. 5-36: Power Patterns for the Horizontal Hertzian Dipole; $n^2=10(1+i.01)$.

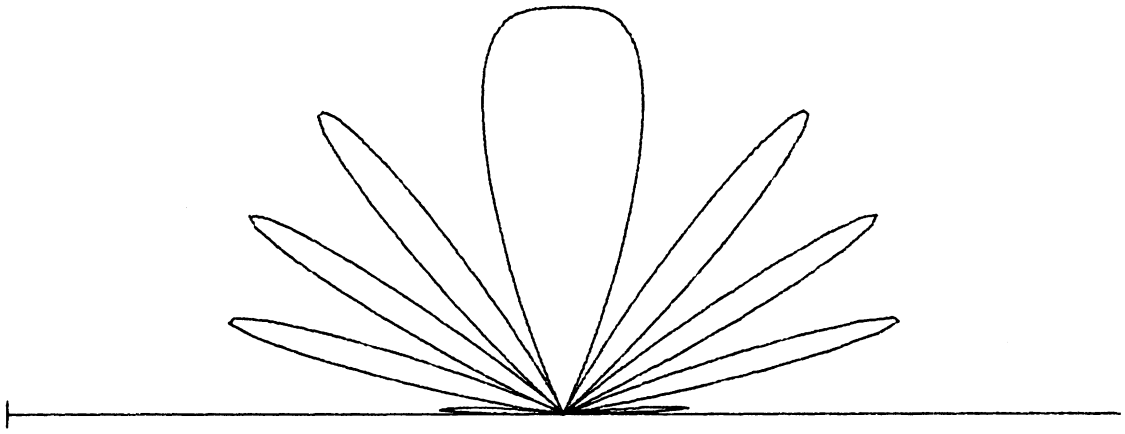

ANTENNA CENTER HEIGHT OF 2. WAVELENGTHS

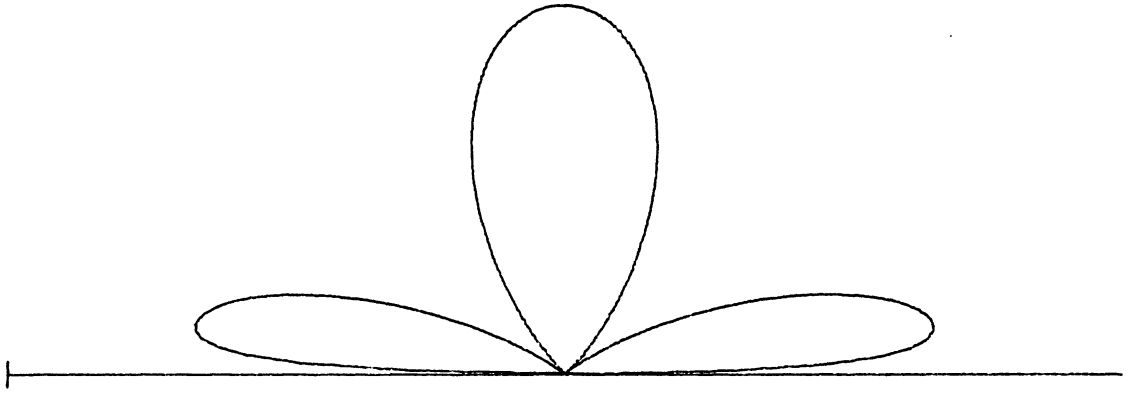

ANTENNA CENTER HEIGHT OF .4 WAVELENGTHS

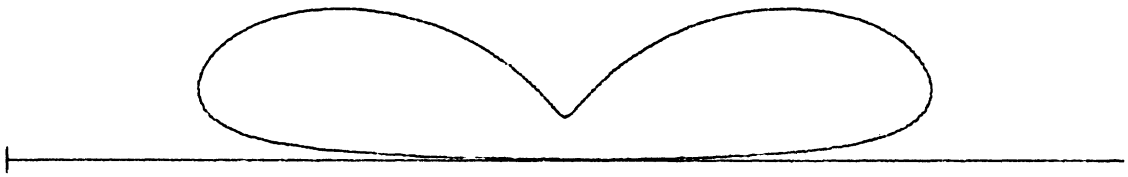

ANTENNA CENTER HEIGHT OF .2 WAVELENGTHS

FIG. 5-37: Power Patterns for the Horizontal Hertzian Dipole; $n^2 = 4(1+i10^3)$.

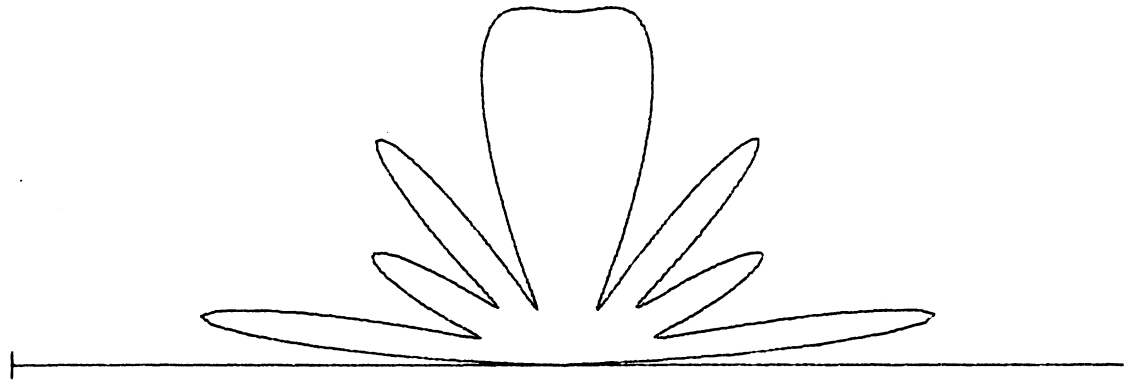

ANTENNA CENTER HEIGHT OF 2. WAVELENGTHS

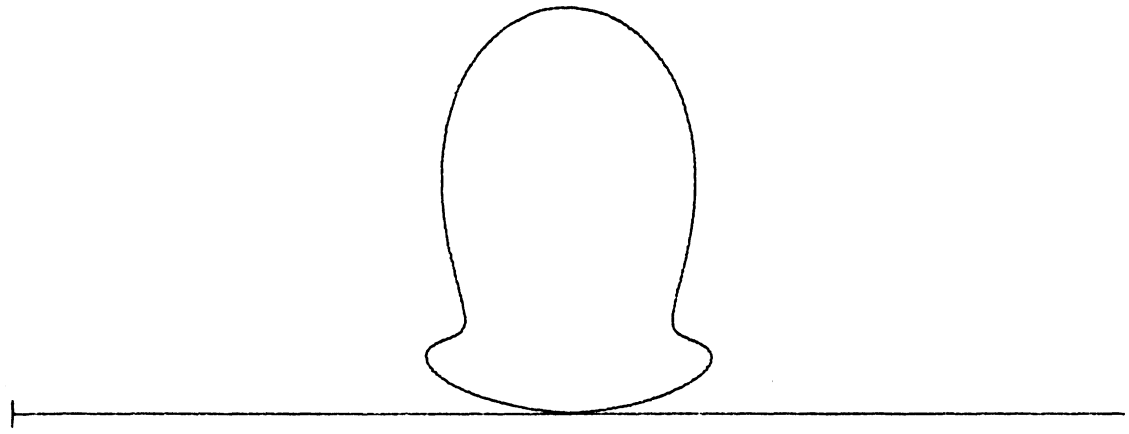

ANTENNA CENTER HEIGHT OF .4 WAVELENGTHS

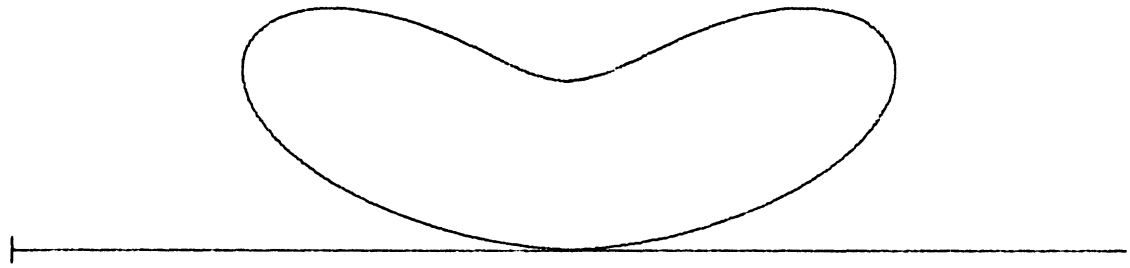

ANTENNA CENTER HEIGHT OF .2 WAVELENGTHS

FIG. 5-38: Power Patterns for the Horizontal Hertzian Dipole; $n^2=4(1+i1)$.

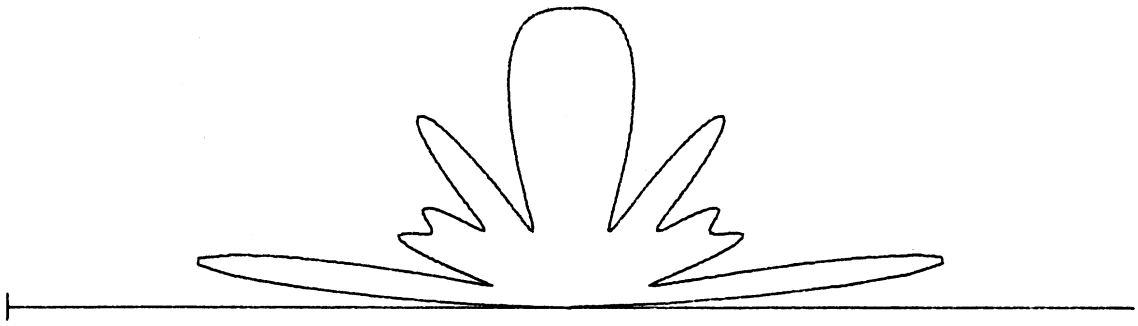

ANTENNA CENTER HEIGHT OF 2. WAVELENGTHS

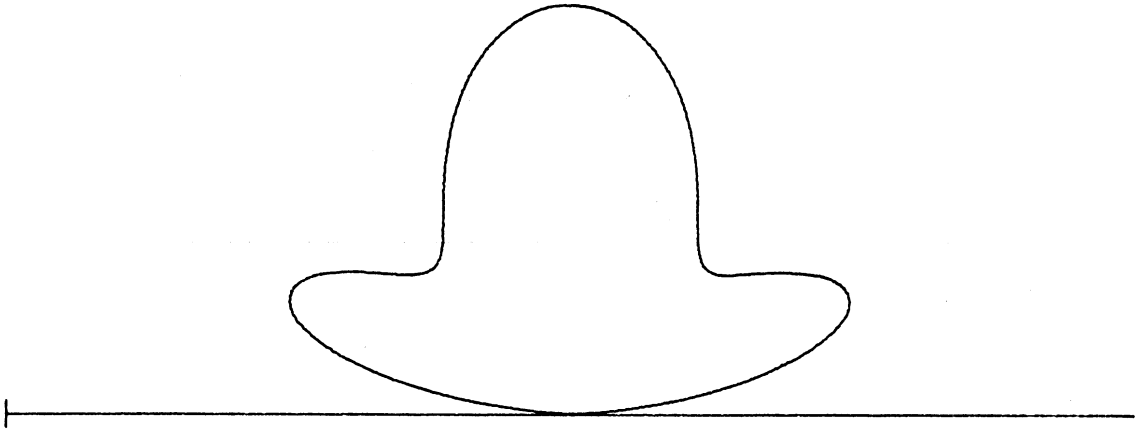

ANTENNA CENTER HEIGHT OF .4 WAVELENGTHS

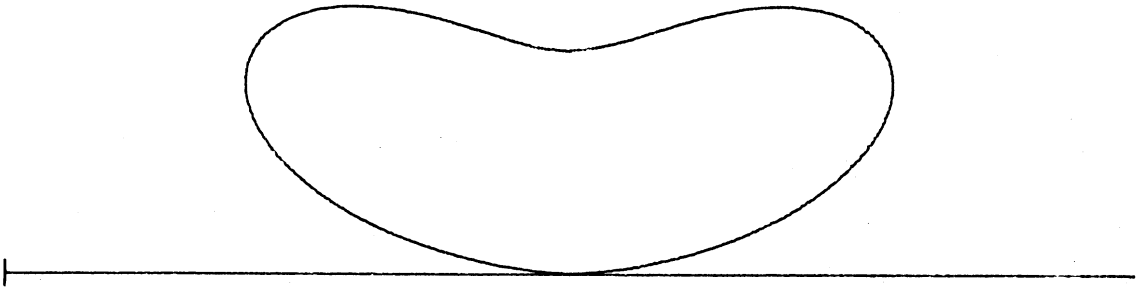

ANTENNA CENTER HEIGHT OF .2 WAVELENGTHS

FIG. 5-39: Power Patterns for the Horizontal Hertzian Dipole; $n^2 = 4(1+i.01)$.

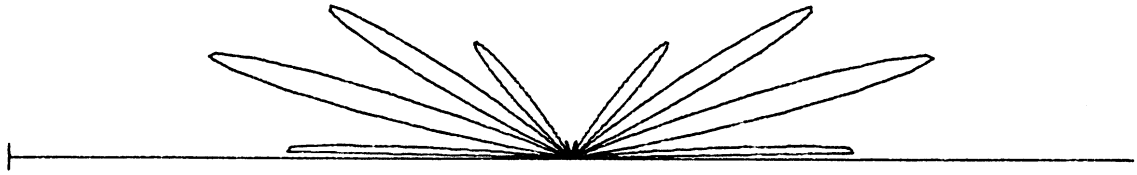

ANTENNA CENTER HEIGHT OF 2. WAVELENGTHS

ANTENNA CENTER HEIGHT OF .4 WAVELENGTHS

ANTENNA CENTER HEIGHT OF .25 WAVELENGTHS

FIG. 5-40: Power Patterns for the Vertical Half-wave Dipole; $n^2 = 80(1+i10^3)$.

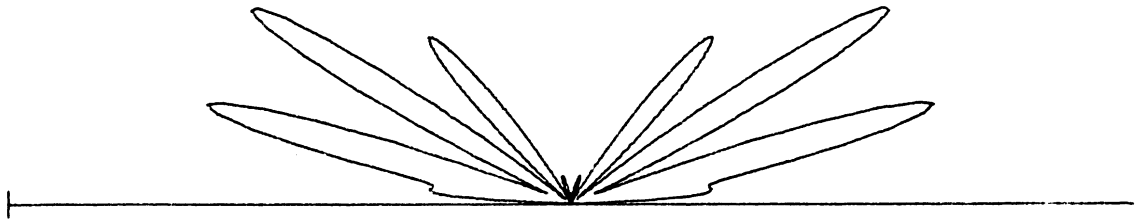

ANTENNA CENTER HEIGHT OF 2. WAVELENGTHS

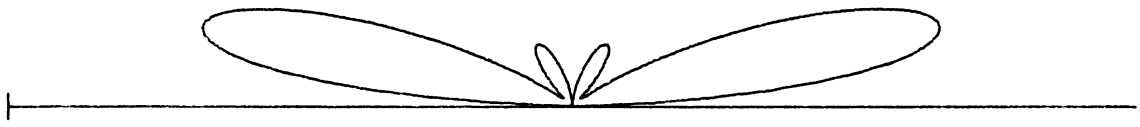

ANTENNA CENTER HEIGHT OF .4 WAVELENGTHS

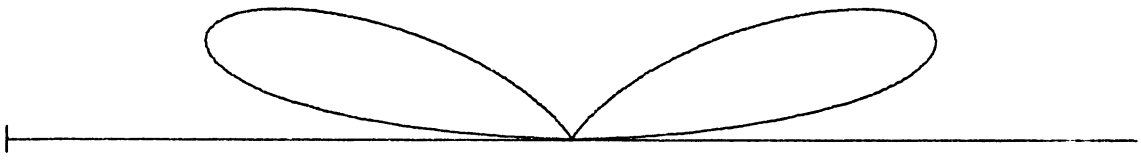

ANTENNA CENTER HEIGHT OF .25 WAVELENGTHS

FIG. 5-41: Power Patterns for the Vertical Half-wave Dipole; $n^2 = 80(1+i1)$.

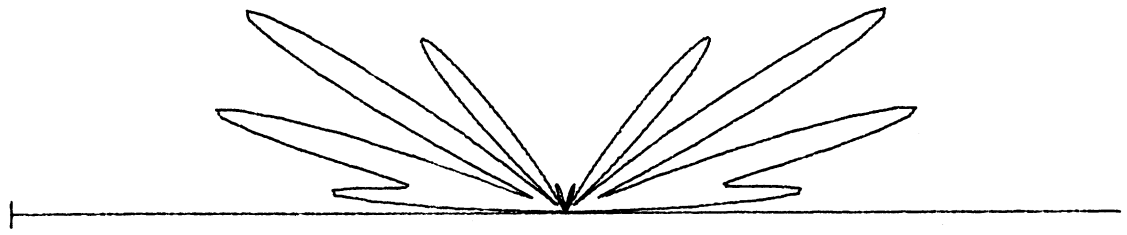

ANTENNA CENTER HEIGHT OF 2. WAVELENGTHS

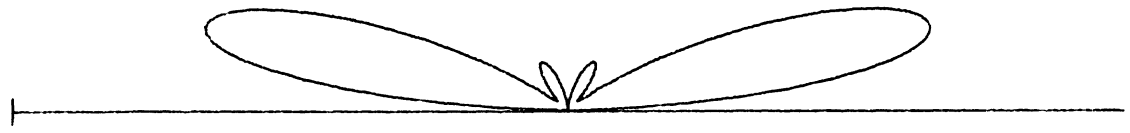

ANTENNA CENTER HEIGHT OF .4 WAVELENGTHS

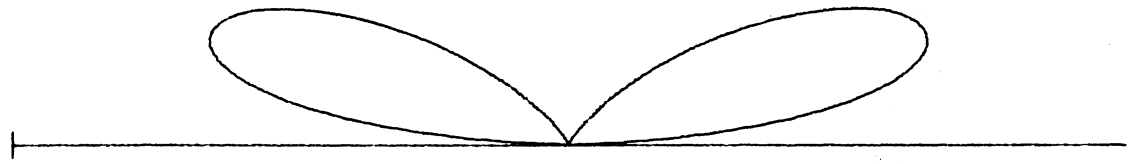

ANTENNA CENTER HEIGHT OF .25 WAVELENGTHS

FIG. 5-42: Power Patterns for the Vertical Half-wave Dipole; $n^2 = 80(1+i.01)$.

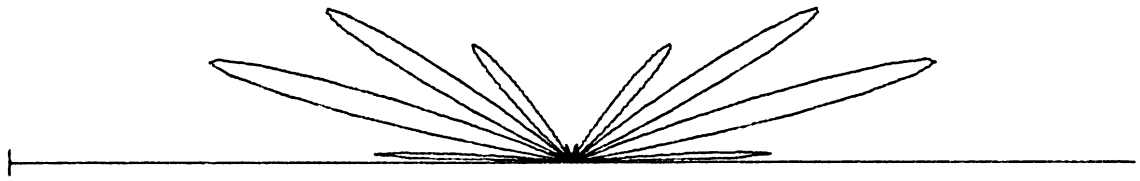

ANTENNA CENTER HEIGHT OF 2. WAVELENGTHS

ANTENNA CENTER HEIGHT OF .4 WAVELENGTHS

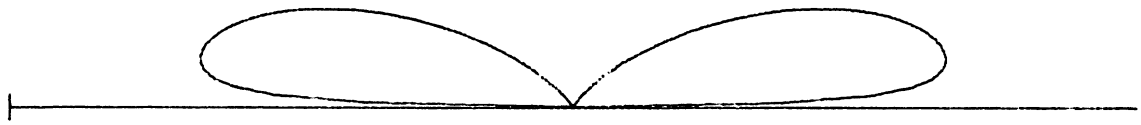

ANTENNA CENTER HEIGHT OF .25 WAVELENGTHS

FIG. 5-43: Power Patterns for the Vertical Half-wave Dipole; $n^2 = 10(1+i10^3)$.

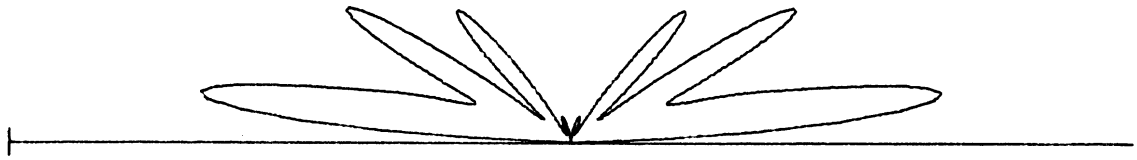

ANTENNA CENTER HEIGHT OF 2. WAVELENGTHS

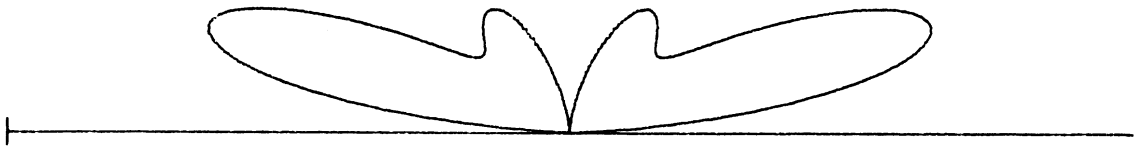

ANTENNA CENTER HEIGHT OF .4 WAVELENGTHS

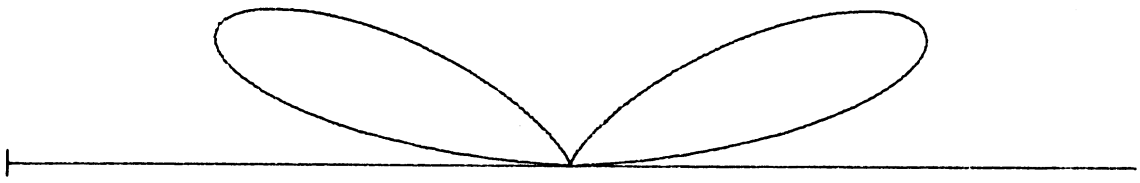

ANTENNA CENTER HEIGHT OF .25 WAVELENGTHS

FIG. 5-44: Power Patterns for the Vertical Half-wave Dipole; $n^2 = 10(1+i1)$.

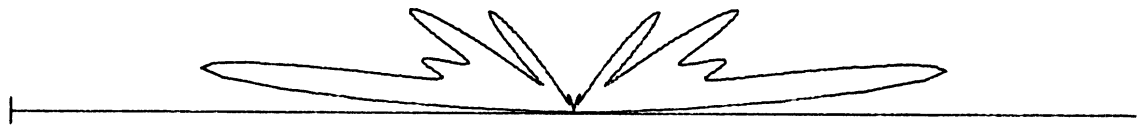

ANTENNA CENTER HEIGHT OF 2. WAVELENGTHS

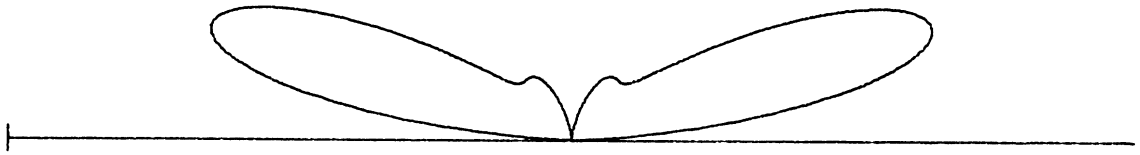

ANTENNA CENTER HEIGHT OF .4 WAVELENGTHS

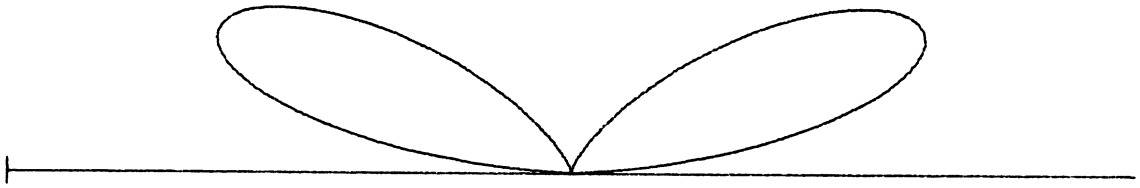

ANTENNA CENTER HEIGHT OF .25 WAVELENGTHS

FIG. 5-45: Power Patterns for the Vertical Half-wave Dipole; $n^2 = 10(1+i\,.01)$.

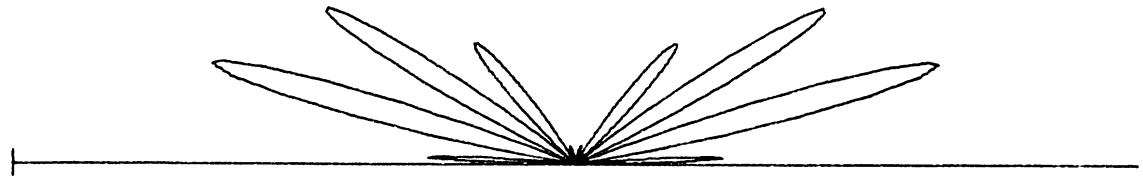

ANTENNA CENTER HEIGHT OF 2. WAVELENGTHS

ANTENNA CENTER HEIGHT OF .4 WAVELENGTHS

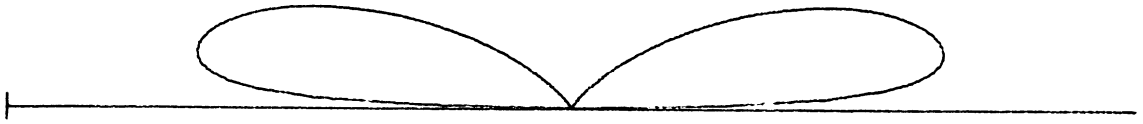

ANTENNA CENTER HEIGHT OF .25 WAVELENGTHS

FIG. 5-46: Power Patterns for the Vertical Half-wave Dipole; $n^2 = 4(1+i\,10^3)$.

ANTENNA CENTER HEIGHT OF 2. WAVELENGTHS

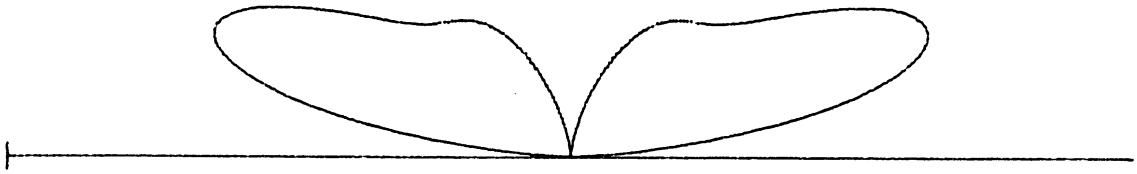

ANTENNA CENTER HEIGHT OF .4 WAVELENGTHS

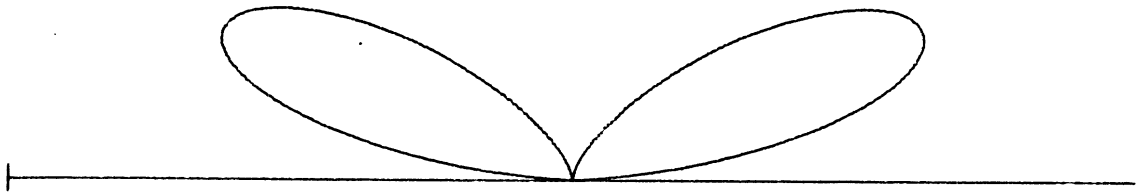

ANTENNA CENTER HEIGHT OF .25 WAVELENGTHS

FIG. 5-47: Power Patterns for the Vertical Half-wave Dipole; $n^2 = 4(1+i\,1)$.

ANTENNA CENTER HEIGHT OF 2. WAVELENGTHS

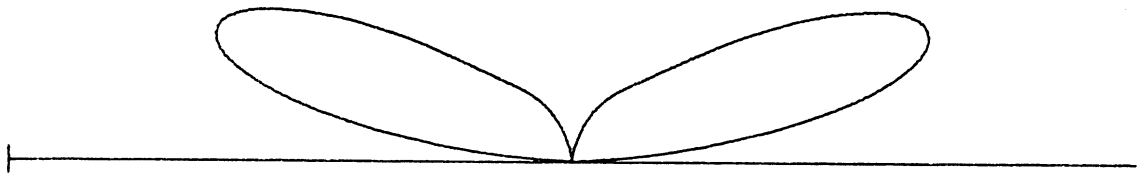

ANTENNA CENTER HEIGHT OF .4 WAVELENGTHS

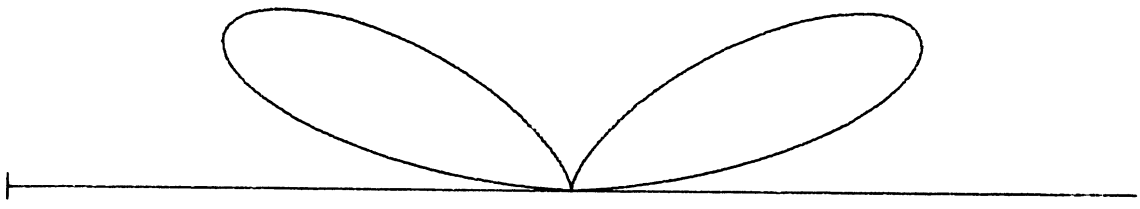

ANTENNA CENTER HEIGHT OF .25 WAVELENGTHS

FIG. 5-48: Power Patterns for the Vertical Half-wave Dipole; $n^2 = 4(1+i.01)$.

CHAPTER VI

CONCLUSIONS AND RECOMMENDATIONS

6.1 Discussion of Results

Some general conclusions about antenna efficiency may be drawn from the theoretical curves presented in Section 5.3.

For both vertical and horizontal Hertzian dipoles, the theory indicates that operation of the antenna very close to the earth results in very large losses. The vertical Hertzian dipole has a distinct peak in radiation efficiency at the point $z_o = .15 \lambda_o$. For the horizontal dipole this peak is not so pronounced. The relative change in the power loss between the first maximum and the first minimum is less than 2 dB for the vertical dipole and less than .5 dB for the horizontal antenna. These figures indicate that as long as the antenna is located at a moderate distance above the ground the radiation efficiency is fairly constant; hence, considerations of the effect of the antenna pattern are more important. Nevertheless, in order to maximize radiated power, the antenna should be located at a height whereby the radiation efficiency is maximum .

The curves presented in Section 5.3 indicate that the horizontal antenna is more efficient than the vertical antenna. This fact may be intuitively justified because the plane wave reflection coefficient for the vertically polarized wave has a deep minimum at the pseudo-Brewster angle while the horizontal reflection coefficient does not. This is indicated by the curves plotted in Section 5.5. However, as the antennas are lowered, the dominant effect is due to the more complicated near field coupling phenomenon . In this region the radiation efficiency curves indicate that the vertical antenna has an advantage over the horizontal antenna. This effect is somewhat more pronounced when the ground has a larger dielectric coefficient.

The radiation efficiency approaches zero for both antennas as they are brought very close to the earth. This is because $S_- \to \infty$ due to the second term of Eqs. (3.24) and (3.32). The physical implication being that it would require an infinite power input to maintain the assumed current near the earth.

The efficiency curves for the vertical half-wave dipole are very similar to those for the vertical Hertzian dipole except that they are valid only for $z_o \geq 0.25 \lambda_o$. Notice that the relative level of these curves is lowered somewhat due to the fact that the lower portion of the antenna is closer to the earth and tends to decrease the efficiency.

The curves of Section 5.3 indicate that the half-wave dipole is more efficient when $z_o = .25 \lambda_o$ than at moderate heights. This corresponds to the lower arm of the antenna just touching the earth.

6.2 Areas for Future Work

In the present investigation we have used an assumed current distribution in the calculation. For longer antennas the current distribution may be substantially different than the sinusoidal functions that have been assumed. For the half-wave dipole, as long as the antenna is thin, this approximation is very good. When the antenna is low the proximity of the earth may affect the current distribution (Ref. 37) and consequently, the efficiency, to some extent. However, a recent article by Chang and Wait (Ref. 38) indicates that the current distribution of a vertical dipole above a conducting ground is insensitive to changes in antenna height. A more refined investigation would probably find this a second-order effect.

A theoretical development of the efficiency expression for the long horizontal dipole can be obtained in the same manner as the expressions for the vertical dipole were. However, the resulting expressions for S_+ and S_- will contain two-dimensional integrals. The numerical results should not differ significantly from the curves of Section 5.1 for the horizontal Hertzian dipole. Analytically, however, it is an interesting problem and worth further consideration.

Throughout this dissertation the so-called ground wave is always included in S_-, the power absorbed by the earth. The problem of efficiently generating this type of wave has not been considered here. This problem has many practical applications and would merit further investigation.

Another area for future work would involve experimental verification of the radiation efficiency curves presented in Section 5.3. Such measurements would include the measurement of radiated power as well as the antenna input power for an antenna above a ground plane.

Investigation of the effect on the radiation efficiency of a finite size ground screen would also be quite interesting. It would seem that the efficiency would be most effected by the ground screen when the antenna is located near the earth.

Investigation of the radiation efficiency of an antenna located above a spherical earth could be approached in the same manner that is presented here; by using the appropriate dyadic Green's function (Ref. 11). This is a very interesting problem analytically and the results should differ significantly from the results of the flat earth case at large antenna heights. At small antenna heights the results should not differ drastically from the results given for the flat earth case. This is a significant problem and certainly merits further consideration.

6.3 Conclusions

In this thesis we have found the exact expression for the fields arising from three different current distributions located above a conducting earth. The approach used here is unique in that it is the first effective application of the dyadic Green's function technique to a problem of this type. The assumed current distributions that are used correspond to the thin vertical Hertzian dipole, the thin horizontal Hertzian dipole, and the thin vertical half-wave dipole.

The resulting field expressions are used to formulate expressions for the integral of the z-directed Poynting's vector over a surface above the antenna and a surface below the antenna. These integrals are designated S_+ and S_- and they are shown to be independent of the location of the plane of integration.

The expressions for S_+ and S_- are shown to be related to both radiation resistance and radiation efficiency. The results of extensive numerical evaluation of them are presented in the form of curves of radiation resistance and radiation efficiency plotted versus the antenna height. These curves show that the vertical Hertzian dipole has a definite peak when $z_o = .15\lambda_o$. There is a similar peak for the horizontal dipole but it is not so pronounced and its location depends on the ground parameters. For the vertical half-wave dipole the radiation efficiency reaches a minimum when the antenna center height is about .4 wavelengths above the ground. The radiation efficiency of the antenna increases as it is lowered below this point. Therefore, for an efficient operation, the antenna should be positioned as close to the ground as possible.

REFERENCES

1. IEEE (May 1969), "IEEE Standard Definitions of Terms for Antennas," IEEE Trans., AP-17, p. 265 .

2. Sommerfeld, A. (1909), "Uber die Ausbreitung der Wellen in der drahtlosen Telegraphie," Ann. Physik., 28, pp. 665-737 .

3. von Horschelman, H. (1911), "Uber die Wirkungsweise des geknickten Marconischen Senders in den drahtlosen Telegraphie," (Dissertation, Munich), Jahrb. d. drahtl. Telegra. und Teleph., 5, pp. 14-34, 5, pp. 188-211.

4. Elias, G.J. (1922), "Het Electromagnetische Veld van een Magnetischen Dipool," Physics, 2, pp. 207-217, and 361-375 .

5. Weyl, H. (1919), "Ausbreitung elektromagnetischer Wellen uber einem ebenen Leiter," Ann. Physik, 60, pp. 481-500 .

6. Kruger, M. (1943), "Die Theorie der in endlicher Entfernung von der Trennungsebene zweier Medien erregten Kugelwelle fur endliche Brechung Indizes," Z. Physik, 121, pp. 377-438 .

7. Sommerfeld, A. (1926), " Uber die Ausbreitung der Wellen in der Drahtlosen Telegraphie," Ann. Physik, 81, pp. 1135-1153 .

8. Baños, A. (1966), Dipole Radiation in the Presence of a Conducting Half Space, Pergamon Press.

9. Levine, H. and J. Schwinger, (December 1950), "On the Theory of Electromagnetic Wave Diffraction by an Aperture in an Infinite Plane Conducting Screen," Comm. Pure and Appl. Math., III, No.4, pp. 355-391 .

10. Kline, M. (1956), The Theory of Electromagnetic Waves, Dover. (Ref. 9 also appeared here.)

11. Tai, C-T (July 1954), "A Glossary of Dyadic Green's Functions," Stanford Research Institute Technical Report No. 46, Stanford, California. The original report is out of print. Copies are available from DDC.

12. Sommerfeld, A. and F. Renner (1941), "Strahlungsenergie und Erdabsorption bei Dipolantenneh," Ann. der Physik, 4, No.2 .

13. Sommerfeld, A. (1949), Partial Differential Equations, Academic Press.

14. Hansen, W.W. and J.G. Beckerley (June 1936), "Radiation from an Antenna over a Plane Earth of Arbitrary Characteristics," Physics, 7 , pp. 220-224 .

15. Wait, J.R. (May 1963), "Radiation Resistance of a Small Circular Loop in the Presence of a Conducting Ground," J.Appl.Phys., 24, pp. 646-649.

16. Bhattacharyya, B.K. (May 1963), "Input Resistances of Horizontal Electric and Vertical Magnetic Dipoles over a Homogeneous Ground," IEEE Trans., AP-11, pp. 261-266.

17. Tai, C-T (February 1969), "Dyadic Green's Functions," Lecture Notes for Antenna Course, The University of Michigan.

18. Stratton, J. (1941), Electromagnetic Theory, McGraw-Hill Book Co., Inc.

19. Senior, T.B.A. (1960), "A Note on Hansen's Vector Wave Functions," Canadian J.Phys., 38, pp. 1702-1705.

20. Spence, R.D. and C.P.Wells (1965), "Vector Wave Functions," The Theory of Electromagnetic Waves (Ed. M.Kline), Dover Publishing Company.

21. Stratton, J. (1941), Electromagnetic Theory, McGraw-Hill Book Co., Inc.

22. Morse, P.M. and H.Feshbach (1953), Methods of Theoretical Physics, McGraw-Hill Book Co., Inc.

23. Hansen, P.M. and C-T Tai (1970), "Radiation from Sources in the Presence of a Flat Earth," to be published in IEEE Trans. on Antennas and Propagation as a Communication.

24. Kraus, J.D. (1950), Antennas, McGraw-Hill Book Co., Inc.

25. Carter, P.S. (1932), "Circuit Relations in Radiating Systems and Applications to Antenna Problems," Proc.IRE, 20, pp.1004-1041.

26. Tai, C-T (1961), "Characteristics of Linear Antenna Elements," Ch.3, Antenna Engineering Handbook (Ed. Jasik), McGraw-Hill Book Co., Inc.

27. King, R.W.P. (1956), Theory of Linear Antennas, Harvard University Press.

28. Berry, L.A. and M.E.Chrisman (September 1966), "Linear High Frequency Antennas Over a Finitely Conducting Earth," ESSA Technical Report IER8ITSAS, Boulder Colorado.

29. Keller, J. (1967), Electrical Methods of Geophysical Prospecting, Pergamon Press.

30. Von Hippel, A.R. (1954), Dielectric Materials and Applications, John Wiley and Sons.

31. Vogler, L.E. and J.L.Nobel (1963), "Curves of Ground Proximity Loss for Dipole Antennas," National Bureau of Standards, Boulder Laboratories Technical Note 175.

32. Todd, J. (Ed.) (1962), Survey of Numerical Analysis, McGraw-Hill Book Co., Inc.

33. Tai, C-T (April 1951), "The Effect of a Grounded Slab on the Radiation From a Line Source," J. Appl. Phys., 22, No.4, pp.405-414.

34. Nomura, Y. (1953), "On the Theory of Propagation of Electric Waves Over a Plane Surface of the Homogeneous Earth," Reports of the Research Institute of Electrical Communication, Tôhoku University, Japan, 5, No.34, pp. 203-214 .

35. Feynburg, Ye. L. (1966), "The Propagation of Radio Waves Along the Surface of the Earth," Translation available from the Clearinghouse, AD 660 951 .

36. Collins, R. E. (1968), Mathematical Methods for Physicists and Engineers, Reinhold Publishing Company.

37. Rashid, A.F. (January 1970), "Quasi-Near-Zone Field of a Monopole Antenna and the Current Distribution of an Antenna on a Finite Conductive Earth," IEEE Trans., AP-18, pp. 22-28 .

38. Chang, D.C. and J.R.Wait (March 1970), "Theory of a Vertical Tubular Antenna Located Above a Conducting Half-Space," IEEE Trans., AP-18, pp. 182-197.

APPENDIX A

COMPUTER PROGRAM

A.1 Quadrature Methods

The numerical calculations necessary for this thesis involve numerically evaluating integrals of the type

$$\int_0^1 F(x)\,dx$$

$$\int_0^\infty G(x)\,e^{-x}\,dx$$

For integrations of the first type a subroutine called DINTG was written. This subroutine approximates the integral by evaluating the trapezoidal rule and mid-ordinate rule for increments successively halfed until the required accuracy is reached. The nth order mid-ordinate rule may be written as

$$M_n = \frac{1}{2^{n-1}} \sum_{i=1}^{2^{n-1}} F\left(\frac{2i-1}{2^n}\right)$$

where the number of increments from 0 to 1 will be 2^n.

The nth order trapezoidal rule has the same number of increments but since it includes the end points it uses one more function value than the nth order mid-ordinate rule. This rule may be written as

$$T_n = \begin{cases} \frac{1}{2}\left\{R(0) + F(1)\right\} & n = 1 \\ \frac{1}{2}\left\{R_{n-1} + M_{n-1}\right\} & n > 1 \end{cases}$$

where n is an integer greater than zero. The error for the mid-ordinate is

$$E_m = \frac{h^3}{3} f''(x_0)$$

where h is half the increment size equal to $1/2^{n+1}$ and x_0 is a value of x in the range from zero to one. The error for the trapezoidal rule is

$$E_T = -\frac{2}{3} h^3 F''(x_1) \quad .$$

As long as the step size is small enough it is possible to equate x_1 and x_0 and choose a value of x_0 such that $F''(x_0)$ is maximum. Thus we see that the maximum error term for the two rules is opposite in sign and of the same order. Therefore the true value of the integral must lie between M_n and T_n. The subroutine DINTG calculates M_n and T_n until

$$\frac{|M_n - T_n|}{|T_n|} \leq \frac{EPS}{100}$$

where EPS is an input variable representing the required percentage error. This subroutine was checked on various known functions and found to work well as long as the value of EPS was greater than .1. If the percentage error requirement was too stringent it was found that round-off error would prevent convergence.

Using DINTG it was found that the 32 point Gauss-Legendre method was accurate to three significant figures for the required functions of Chapter III and Chapter IV. Thus the subroutine DQG32 has been used to calculate integrals of the first type.

For integrations of the second type the normal method of integration used would be Gauss-Laguerre[1]. However, the highest order Gauss-Laguerre

[1] See Refs. 31 and 32 .

subroutine readily available is 32 and it was found that the fine structure of g(x) prevented this method from converging. The function g(x) behaved quite well for large values of x but in the region between zero and one it had a large spike. In order to ensure accuracy the function DINTG was used for the interval from zero to one, and then succeeding increments are found using DQG32. This method was found to have an accuracy of better than three significant figures.

A.2 Main Program for the Vertical Hertzian Dipole

This program calculates the values of S_+ and S_- given by Eqs. (3.23) and (3.24). The values of ξ used are such that

$$z_0/\lambda_0 = .01,\ .02,\ \ldots,\ .09,\ .1,\ .15,\ .2,\ \ldots,\ 1.9,\ 2.0\ .$$

More values were calculated in the region $z_0/\lambda_0 < .1$ because the slope of the efficiency and radiation resistance curves was found to be great in this region. For each value of z_0/λ_0 the program prints out the value of z_0/λ_0, efficiency, radiation resistance, and the perfectly conducting part of the radiation resistance.

```
C       MAIN PROGRAM FOR VERTICAL HERTZIAN DIPOLE
      IMPLICIT REAL*8 (A-H,O-Z)
      COMPLEX*16 NSQ
      COMMON NSQ,CHI
      NAMELIST/ONE/NSQ
      NAMELIST/TWO/ETASY
      DIMENSION H(200),SPC(200),SPC(200),ETA(200)
      EXTERNAL F,F1,F2
      READ(5,ONE)
      WRITE(6,ONE)
      CALL DQG32(0.D0,1.D0,F,SF)
      SFF=.75*SF
      WRITE(6,200)SFF
      ETASY=1.+SFF
      WRITE(6,TWO)
      DO 10 I=1,9
      H(I)=.01*I
      CHI=4.*3.14159*.01*I
      SPC=1.+3.*VPC(CHI)
      WRITE(6,200)SPC(I)
      CALL DQG32(0.D0,1.D0,F1,SF1)
      SF1=1.5*SF1
      WRITE(6,200)SF1
      SF2=CINTG(F2)
      SF2=.75*SF2
      WRITE(6,200)SF2
      SPL=SPC(I)+SFF-SF1
      SMIN=SFF-SF2
      S(I)=SPL-SMIN
      ETA(I)=SPL/S(I)
10    WRITE(6,200)H(I),S(I),ETA(I),SPC(I)
```

```
      DO 20 I=2,40
      H(I)=.05*I
      CHI=4.*3.14159*.05*I
      SPC=1.+3.*VPC(CHI)
      WRITE(6,200)SPC(I)
      CALL DQG32(0.D0,1.D0,F1,SF1)
      SF1=1.5*SF1
      WRITE(6,200)SF1
      SF2=CINTG(F2)
      SF2=.75*SF2
      WRITE(6,200)SF2
      SMIN=SFF-SF2
      SPL=SPC(I)+SFF-SF1
      S(I)=SPL-SMIN
      ETA(I)=SPL/S(I)
20    WRITE(6,100)H(I),S(I),ETA(I),SPC(I)
100   FORMAT(' ',8F10.5)
200   FORMAT(8F10.5)
      END
```

A.3 Main Program for the Horizontal Hertzian Dipole

This program calculates the values of S_+ and S_- given by Eqs. (3.31) and (3.32) using the subroutines of Section A.5. The values of ξ used are such that

$$z_0/\lambda_0 = .01,\ .02,\ \ldots,\ .09,\ .10,\ .15,\ .20,\ \ldots,\ 1.9,\ 2.0.$$

More values are needed in the region where $z_0/\lambda_0 < .1$ because the slope of the efficiency and radiation resistance curves is large in this region. For each value of z_0/λ_0 the program prints the value of z_0/λ, radiation resistance, efficiency, and the perfectly conducting part of the radiation resistance.

```
C      MAIN PROGRAM FOR HORIZONTAL HERTZIAN DIPOLE
       IMPLICIT REAL*8 (A-H,O-Z)
       COMPLEX*16 NSQ
       COMMON NSQ,CHI
       NAMELIST/ONE/NSQ
       NAMELIST/TWO/ETASY
       DIMENSION H(200),SPC(200),SPC(200),ETA(200)
       EXTERNAL G,G1,G2
       READ(5,ONE)
       WRITE(6,ONE)
       CALL DQG32(0.D0,1.D0,G,SG)
       SFF=.375*SG
       WRITE(6,200)SFF
       ETASY=1.+SFF
       WRITE(6,TWO)
       DO 10 I=1,9
       H(I)=.01*I
       CHI=4.*3.14159*.01*I
       SPC(I)=1.-1.5*HPC(CHI)
       WRITE(6,200)SPC(I)
       CALL DQG32(0.D0,1.D0,G1,SG1)
       SF1=.75*SG1
       WRITE(6,200)SF1
       SG2=CINTG(G2)
       SF2=.75*SG2
       WRITE(6,200)SF2
       SPL=SPC(I)+SFF+SF1
       SMIN=SFF-SF2
       S(I)=SPL-SMIN
       ETA(I)=SPL/S(I)
10     WRITE(6,200)H(I),S(I),ETA(I),SPC(I)
```

```
      DO 20 I=2,40
      H(I)=.05*I
      CHI=4.*3.14159*.05*I
      SPC(I)=1.-1.5*HPC(CHI)
      WRITE(6,200)SPC(I)
      CALL DQG32(0.D0,1.D0,G1,SG1)
      SF1=.75*SG1
      WRITE(6,200)SF1
      SG2=CINTG(G2)
      SF2=.75*SG2
      WRITE(6,200)SF2
      SMIN=SFF-SF2
      SPL=SPC(I)+SFF+SF1
      S(I)=SPL-SMIN
      ETA(I)=SPL/S(I)
20    WRITE(6,100)H(I),S(I),ETA(I),SPC(I)
100   FORMAT(' ',8F10.5)
200   FORMAT(8F10.5)
      END
```

A.4 Main Program for the Vertical Half Wave Dipole

This program calculates the values of S_+ and S_- as given in Eqs. (4.22) and (4.23). The subroutines used are given in Section A.5. The values of ξ used are such that

$$z_0/\lambda_0 = .25,\ .26,\ \ldots,\ .35,\ .40,\ \ldots,\ 2.25.$$

For each value of z_0/λ_0 the program prints out the value of z_0/λ_0, efficiency, radiation resistance, and the perfectly conducting part of the radiation resistance.

```
100             C      MAIN PROGRAM FOR VERTICAL HALF WAVE CIRCLE
100.1            IMPLICIT REAL*8 (A-H,O-Z)
101              COMPLEX*16 NSG
102              COMMON NSG,CHI
103              NAMELIST/ONE/NSG
104              NAMELIST/TWO/ETASY
105              DIMENSION HH(200),S(200),SPC(200),ETA(200)
106              EXTERNAL H,H1,H2,DPC,C
107              SK=1.DO/1.218625887600
108              PI=3.14159265358979200
109              READ(5,ONE)
109.1            WRITE(6,ONE)
110              CALL DGQ32(0.DO,1.DO,H,SH)
111              SFF=SK*SH
112              WRITE(6,200)SFF
113              ETASY=1.DO+SFF
114              WRITE(6,TWO)
115              DO 10 I=1,10
116              HH(I)=.01D0*I+.24DO
117              CHI=4.DO*PI*HH(I)
118              CALL DGQ32(0.DO,1.DO,DPC,PC)
119              SPC(I)=1.DO+2.DO*SK*PC
120              WRITE(6,200)SPC(I)
121              CALL DGQ32(0.DO,1.DO,H1,SH1)
122              SF1=2.DO*SK*SH1
123              WRITE(6,200)SF1
124              SF2=CINTC(H2)
125              SF2=SK*SF2
126              WRITE(6,200)SF2
127              SPL=SPC(I)+SFF-SF1
128              SMIN=SFF-SF2
129              S(I)=SPL-SMIN
129.1            ETA(I)=SPL/S(I)
130        10    WRITE(6,200)HH(I),S(I),ETA(I),SPC(I)
```

```
      DO 20 I=2,40
      HH(I)=.050*I+.250
      PHI=4.00*PI*HH(I)
      CALL DGQ32(0.00,1.00,DPC,PC)
      SPC(I)=1.00+2.00*SK*PC
      WRITE(6,200)SPC(I)
      CALL DGQ32(0.00,1.00,F1,SH1)
      SF1=2.00*SK*SH1
      WRITE(6,200)SF1
      SF2=CINTG(F2)
      SF2=SK*SF2
      WRITE(6,200)SF2
      SPL=SPC(I)+SFF-SF1
      SMIN=SFF-SF2
      S(I)=SPL-SMIN
      ETA(I)=SPL/S(I)
   20 WRITE(6,200)HH(I),S(I),ETA(I),SPC(I)
  200 FORMAT(8F10.5)
      END
```

A.5 Subroutines

A.5.1 General Remarks

All subroutines are written in FORTRAN IV G level compiler language for the IBM 360/67. They all make use of the double precision mode. A listing of each of the subroutines with the exception of DQG32 is included at the end of this section. A more detailed description of DQG32 plus a listing may be found in IBM manual number 360A-CM-03X, "Systems/360 Scientific Subroutine Package".

A.5.2 Subroutines for All Three Cases

Subroutine: AB1

Usage: Call AB1(A, B, U)

Where:

$$A = \frac{2u}{u + \sqrt{n^2 - 1 + u^2}}$$

$$B = \frac{2\sqrt{n^2 - 1 + u^2}}{\sqrt{n^2 - 1 + u^2} + n^2 u}$$

n^2 = complex index of refraction

$u = kh$ = variable of integration

Comment: The values returned are A(u) and B(u). The complex functions of Eqs. (3.22) and (3.29).

Subroutine: AB2

Usage: Call AB2(A, B, V)

Where:

$$A = \frac{2\,iv}{iv + \sqrt{n^2 - 1 - v^2}}$$

$$B = \frac{2\sqrt{n^2 - 1 - v^2}}{in^2 v + \sqrt{n^2 - 1 - v^2}}$$

$V = ikh$ = variable of integration.

Comments: The values returned to A and B are the complex functions A(v) and B(v). See Eqs. (3.22) and (3.29).

Subroutine: DINTG

Usage: A = DINTG(F, ER, EA)

Where: $A = \int_0^1 F(x)\,dx$

F = double precision function to be integrated

ER = required error in percent

EA = actual error in percent.

Comments: The difference between mid-ordinate rule and the trapezoidal rule using smaller and smaller increments is checked until the required accuracy is reached.

Subroutine: CINTG

Usage: A = CINTG(F)

Where: $A = \int_0^\infty F(x)\,dx$

F = double precision function to be integrated.

Comments: The integral is divided up into the following infinite series

$$\int_0^\infty F(x)\,dx = \int_0^1 F(x)\,dx + \int_1^{1.5} F(x)\,dx + \int_{1.5}^2 F(x)\,dx + \cdots$$

The first term of the series is calculated by using DINTG. The remaining terms are calculated by DQG32. The terms are individually calculated in order from left to right and summed until the next term is less than 10^{-5} times the sum. This scheme works well for integrals containing e^{-x} or of the form $1/x^2$.

Subroutine: DQG32

Usage: Call CQG32(XL, XU, F, S)

Where: $S = \int_{XL}^{XU} F(x)\,dx$

XL = lower limit of integration

XU = upper limit of integration

F = double precision function to be integrated.

Comment: This subroutine uses the Gauss-Legendre quadrature scheme. For details and a listing, see IBM manual No. 360A-CM-03X, "System/360 Scientific Subroutine Package".

A.5.2 Subroutines for the Vertical Hertzian Dipole Case

Subroutine: VPC

Usage: = VPC(CHI)

Where: $VPC = \dfrac{\sin \xi - \xi \cos \xi}{\xi^3}$

$CHI = \xi = 2kz_0$

Comments: This subroutine calculates the perfectly conducting term of Eq. (3.23).

Subroutine: F

Usage: = F(u)

Where: $F(u) = \left\{|B|^2 - B - B^*\right\}(1 + u^2)$

$u = kh$ = variable of integration

Comments: See Eqs. (3.23) and (3.24).

Subroutine: F1

Usage: = F1(u)

Where: $F1 = \text{Re}\left\{B\, e^{i\xi u}(1 - u)^2\right\}$

$u = kh$ = variable of integration

Comment: See Eq. (3.23).

Subroutine: F2

Usage: = F2(v)

Where: $F2(v) = \text{Re}\, i\left\{(b - B^*)\right\}\ (1 + v^2)\, e^{-\xi v}$

$v = ikh$ = variable of integration

Comment: See Eq. (3.24).

A.5.3 Subroutines for the Horizontal Hertzian Dipole Case

Subroutine: HPC

Usage: = HPC(CHI)

Where: $HPC = \dfrac{(\xi^2-1)\sin\xi + \xi\cos\xi}{\xi^3}$

$CHI = \xi = 2kz_0$

Comment: This subroutine calculates the perfectly conducting term of Eq. (3.31).

Subroutine: G

Usage: = G(u)

Where: $G = |A|^2 - A - A^* + u^2(|B|^2 - B - B^*)$

Comment: See Eqs. (3.31) and (3.32).

Subroutine: G1

Usage: = G1 (u)

Where: $G1(u) = \mathrm{Re}\left\{(A + u^2B)\, e^{i\xi u}\right\}$

$u = kh$ = variable of integration

Comment: See Eq. (3.31).

Subroutine: G2

Usage: = G2(v)

Where: $G2(v) = \mathrm{Im}\left\{A - v^2B\right\} e^{-\xi v}$

$v = ikh$ = variable of integration

Comment: See Eq. (3.32).

A.5.4 Subroutines for the Vertical Half Wave Dipole Case

Subroutine: C

Usage: = C(u)

Where: $C = \dfrac{\cos^2(\pi/2\, u)}{1 - u^2}$

$u = kh$ = variable of integration

Comment: This function has an apparent singularity at the point $u = 1$. In the vicinity of $u = 1$ the function was calculated as a series expansion which does not contain the apparent singularity. See Eqs. (4.22) and (4.23).

Subroutine: DPC

Usage: = DPC(chi)

Where: $DPC(chi) = C(u) \cdot \cos \xi u$

$chi = \xi = 2kz_0$

$u = kh$ = variable of integration

C(u) = is defined above

Comment: This integral of this subroutine calculates the perfectly conducting term of Eq. (4.22).

Subroutine: H

Usage: = H(u)

Where: $H(u) = (|B|^2 - B - B^*) \cdot C(u)$

$u = kh$ = variable of integration

C(u) is defined above

Comment: See Eqs. (4.22) and (4.23).

Subroutine: H1

Usage: = H1 (u)

Where: $H1(u) = \mathrm{Re}\{B\, e^{i\xi u}\} \cdot C(u)$

$u = kh$ = variable of integration

C(u) is defined above

Comment: See Eq. (4.22).

Subroutine: H2

Usage: = H2(v)

Where: $H2(v) = \text{Re } i\ (B - B^*)\ \dfrac{\cosh^2\left(\frac{\pi}{2} v\right)}{1 + v^2}\ e^{i\xi v}$

v = ikh = variable of integration

Comment: See Eq. (4.23).

A.5.5 Subroutine Listings

```
200         SUBROUTINE AB1(A1,B1,U)
201         COMPLEX*16 NSQ,A1,B1,Z,CDSQRT
202         REAL*8 CHI,U,USQ
203         COMMON NSQ,CHI
204         USQ=U*U
205         Z=NSQ-1.+USQ
206         Z=CDSQRT(Z)
207         A1=U+Z
208         A1=2./A1
209         A1=U*A1
210         B1=Z+NSQ*U
211         B1=Z/B1
212         B1=B1+B1
213         RETURN
214         END
300         SUBROUTINE AB2(A2,B2,V)
301         COMPLEX*16 NSQ,A2,B2,Z,IV,CDSQRT,I
302         REAL*8 CHI,V,VSQ
303         COMMON NSQ,CHI
304         I=(0.,1.)
305         VSQ=V*V
306         Z=NSQ-1.*VSQ
307         Z=CDSQRT(Z)
308         IV=I*V
309         A2=IV+IV
310         A2=A2/(IV+Z)
311         IV=IV*NSQ
312         B2=Z+Z
313         B2=B2/(IV+Z)
314         RETURN
315         END
```

```
400             FUNCTION CINTG(F,P,EI)
401             REAL*8 M,MID,CINTG,F,P,TRAP,A,C,AC,EI,B,CABS
402             REAL*8 ZERO,ONE,HALF
403             ZERO=0.
404             HALF=.5
405             ONE=1.
406              TRAP=.5*(F(ZERO)+F(ONE))
407              MID=F(HALF)
408              A=100.
409             K=1
410             C=2.
411              N=1
412       5      IF(P-A) 10,40,40
413      10      N=N+1
414             IF(N.GE.15)GO TO 30
415              TRAP=.5*(TRAP+MID)
416              M=0.
417             K=K+K
418             C=C+C
419             AC=1./C
420             A=AC
421              DO 15 I=1,K
422              M=M+F(A)
423      15     A=A+AC+AC
424             MID=(M+M)/C
425             EI=DABS(MID-TRAP)
426             B=CABS(TRAP)
427             A=100.*EI/B
428      20      IF(N.LE.5) GO TO 10
429              GO TO 5
430      40     CINTG=TRAP
431              RETURN
432      30      WRITE(6,100)A
433             GO TO 40
434     100      FORMAT(1HC,11HINTG ERROR=,E6.4,7HPERCENT)
435      200    FORMAT(3D12.5)
```

```
500             FUNCTION CINTG(F)
501             REAL*8 CINTG,CINTG,F,SUM,EI,X,Y,S,EPS,DABS,ONE
502             EXTERNAL F
503             ONE=1.
504             SUM=CINTG(F,ONE,EI)
505             X=1.
506             Y=1.5
507       1     CALL DQG32(X,Y,F,S)
508             SUM=SUM+S
509             EPS=S/SUM
510             EPS=DABS(EPS)
511             X=X+.5
512             Y=Y+.5
513             IF(EPS.GT..00001)GO TO 1
514             CINTG=SUM
515             RETURN
516       100   FORMAT(3D12.5)
517             END
550             FUNCTION C(U)
551             *IMPLICIT REAL*8 (A-H,O-Z)
552             ONE=1.0D 00
553             PI2=.15707963267948960 01
554             PI2SQ=PI2*PI2
555             IF((ONE-U).LT.1.0D-05)GO TO 10
556             X=PI2*U
557             A=DCOS(X)
558             A=A*A
559             B=ONE-U*U
560             C=A/B
561             RETURN
562       10    A=ONE+U
563             B=ONE-U
564             C=PI2SQ*B/A
565             RETURN
566             END
```

```
      FUNCTION DPC(U)
      IMPLICIT REAL*8 (A-H,O-Z)
      COMPLEX*16 NSG
      COMMON NSG,CHI
      DPC=DCOS(CHI*U)*C(U)
      RETURN
      END
      FUNCTION VPC(CHI)
      REAL*8 CHI,CHI3,VPC
      CHI3=CHI*CHI*CHI
      VPC=(DSIN(CHI)-CHI*DCOS(CHI))/CHI3
      RETURN
      END
      FUNCTION F(U)
      COMPLEX*16 NSG,A,B,BB,TB
      REAL*8 CHI,F,USG,U
      COMMON NSG,CHI
      CALL AB1(A,B,U)
      USG=U*U
      USG=1.D0-USG
      BB=DCONJG(B)
      TB=B*BB-B-BB
      F=USG*TB
      RETURN
      END
```

```
700             FUNCTION F1(U)
701             COMPLEX*16 NSQ,A,B,BB,I
702             COMPLEX*16 ARG
703             REAL*8 CHI,F1,U,USQ
704             COMMON NSQ,CHI
705             I=(0.D0,1.D0)
706             CALL AB1(A,B,U)
707             ARG=I*CHI*U
708             A=CDEXP(ARG)
709             USQ=1.D0-U*U
710             B=B*A*USQ
711             F1=B
712             RETURN
713             END
800             FUNCTION F2(V)
801             COMPLEX*16 NSQ,A,B,BB,I
802             REAL*8 CHI,F2,V,VSQ
803             COMMON NSQ,CHI
804             I=(0.D0,1.D0)
805             CALL AB2(A,B,V)
806             A=DCONJG(B)
807             B=B-A
808             VSQ=1.D0+V*V
809             CHI=CDEXP(-CHI*V)
810             F2=I*VSQ*B*CHI
811             RETURN
812             END
1600            FUNCTION HPC(CHI)
1601            REAL*8 CHI,CHI2,CHI3,HPC
1602            CHI2=CHI*CHI
1603            CHI3=CHI2*CHI
1604            HPC=((CHI2-1.D0)*DSIN(CHI)+CHI*DCOS(CHI))/CHI3
1605            RETURN
1606            END
```

```
      FUNCTION G(L)
      REAL*8 G,L,CHI,USQ
      COMPLEX*16 NSQ,A,B,AA,BB,DCONJG,TA,TB
      COMMON NSQ,CHI
      CALL AB1(A,B,L)
      USQ=U*U
      AA=DCONJG(A)
      BB=DCONJG(B)
      TA=A*AA-A-AA
      TB=B*BB-B-BB
      TB=USQ*TB
      TA=TA+TB
      G=TA
      RETURN
      END
      FUNCTION G1(U)
      COMPLEX*16 NSQ,A,B,AA,BB,I,ARG,CDEXP
      REAL*8 G1,U,CHI,USQ
      COMMON NSQ,CHI
      USQ=U*U
      I=(0.,1.)
      CALL AB1(A,B,L)
      A=A+USQ*B
      ARG=I*CHI*U
      B=CDEXP(ARG)
      A=A*B
      G1=A
      RETURN
      END
```

```
      FUNCTION G2(V)
      COMPLEX*16 A,B,NSQ,I,DCONJG
      REAL*8 V,CHI,DEXP,G2
      COMMON NSQ,CHI
      VSQ=V*V
      I=(0.,1.)
      CALL AB2(A,B,V)
      B=VSQ*B
      A=A-B
      B=DCONJG(A)
      A=A-B
      A=-I*A/2.
      G2=A
      G2=G2*DEXP(-CHI*V)
      RETURN
      END
      FUNCTION C(U)
      IMPLICIT REAL*8 (A-H,O-Z)
      ONE=1.0D 00
      PI2=.15707963267948966D 01
      PI2SQ=PI2*PI2
      IF((ONE-U).LT.1.0D-05)GO TO 10
      X=PI2*U
      A=DCOS(X)
      A=A*A
      B=ONE-U*U
      C=A/B
      RETURN
   10 A=ONE+U
      B=ONE-U
      C=PI2SQ*B/A
      RETURN
      END
```

```
      570           FUNCTION DPC(U)
      571           IMPLICIT REAL*8 (A-H,O-Z)
      572           COMPLEX*16 NSQ
      573           COMMON NSQ,CHI
      574           DPC=DCOS(CHI*U)*C(U)
      575           RETURN
      576           END
     1300           FUNCTION H(U)
     1301           COMPLEX*16 NSQ,A,B,BB,TB
     1302           REAL*8 CHI,H,USQ,U
     1303           COMMON NSQ,CHI
     1304           CALL AB1(A,B,U)
     1305           USQ=C(U)
     1306           BB=DCONJG(B)
     1307           TB=B*BB-B-BB
     1308           H=USQ*TB
     1309           RETURN
     1310           END
     1400           FUNCTION H1(U)
     1401           COMPLEX*16 NSQ,A,B,BB,I
     1402           COMPLEX*16 ARG
     1403           REAL*8 CHI,H1,U,USQ
     1404           COMMON NSQ,CHI
     1405           I=(0.D0,1.D0)
     1406           CALL AB1(A,B,U)
     1407           ARG=I*CHI*U
     1408           A=CDEXP(ARG)
     1409           USQ=C(U)
     1410           B=B*A*USQ
     1411           H1=B
     1412           RETURN
     1413           END
```

```
      FUNCTION F2(V)
      REAL*8 DEXP,DCOSH
      REAL*8 ABS,PI
      COMPLEX*16 DCONJG
      REAL*8 F2,V,VSQ,CHI
      COMPLEX*16 ASQ,A,B,BB,I
      COMMON ASQ,CHI
      I=(0.D0,1.D0)
      PI=3.14159265358979320
      VSQ=DEXP(-CHI*V)
      VSQ=VSQ+.5D0*DEXP(-(CHI+PI)*V)
      VSQ=VSQ+.5D0*DEXP(-(CHI-PI)*V)
      VSQ=.5D0*VSQ/(1.D0+V*V)
      CALL AE2(A,B,V)
      BB=DCONJG(B)
      B=B-BB
      F2=B*VSQ*I
      RETURN
      END
```

APPENDIX B

FAR ZONE FIELD EXPANSION

In this appendix, as an example of the technique, we will asymptotically evaluate equation (3.4) for kR very large. The same method may be applied to equations (3.8) and (4.8) to obtain the asymptotic expressions given in section 3.2.3.

We will only consider the fields in the region above the antenna. The field for a vertical Hertzian dipole is given by (3.4) and is repeated here, neglecting the constant multiplier.

$$\bar{E} = \int_0^\infty d\lambda \, \frac{\lambda}{h} \left\{ \bar{N}_{e0\lambda}(h) \left[e^{-ihz_o} + b\, e^{ihz_o} \right] \right\} z > z_o \quad . \tag{B.1}$$

It can be shown by use of the "half circuit" relations given by Sommerfeld[1] that (B.1) may be re-written as

$$\bar{E} = \int_{-\infty}^\infty d\lambda \, \frac{\lambda}{h} \left\{ \bar{N}^{(1)}_{e0\lambda}(h) \left[e^{-ihz_o} + b\, e^{ihz_o} \right] \right\} \tag{B.2}$$

where $\bar{M}^{(1)}$ and $\bar{N}^{(1)}$ are defined in section 2.3.

The asymptotic forms of $\bar{M}^{(1)}$ and $\bar{N}^{(1)}$ may be obtained by substituting the well known expansions of $H_n^{(1)}$ and neglecting higher order terms.

$$M^{(1)}_{\substack{e \\ o}\, n\lambda}(h) \doteq (-i)^{n+3/2} \sqrt{\frac{2}{\pi \lambda r}}\, e^{i(\lambda r + hz)} \begin{matrix} \cos \\ \sin \end{matrix} n\phi \; \hat{\phi}$$

[1] See reference 13,

$$\bar{N}^{(1)}_{\substack{e\\o}\, n\lambda}(h) \doteq (-i)^{n+1/3} \sqrt{\frac{2}{\pi \lambda r}}\, e^{i(\lambda r + hz)} \begin{matrix}\cos \\ \sin\end{matrix} n\phi\, \frac{(\lambda \hat{z} - h \hat{r})}{k}$$

Accordingly (B.2) has the following asymptotic form

$$\bar{E} \doteq -\frac{2i}{\pi r} \int_{-\infty}^{\infty} d\lambda\, \frac{\lambda^{3/2}}{h}\, e^{i(\lambda r + h z)} \left[e^{-ihz_o} + b\, e^{ihz_o} \right] \frac{(\lambda \hat{z} - h \hat{r})}{k} \tag{B.3}$$

The λ integration may be treated as a path integral over the real axis. This particular integral, sometimes referred to in the literature as Sommerfeld's problem, has been extensively studied by other authors[1]. The common method of evaluating the integral is to apply the following two transformations:

$$r = R \sin \theta \qquad \lambda = k \sin \beta$$

$$z = R \cos \theta \qquad h = k \cos \beta$$

Equation (B.3) becomes

$$\bar{E} \doteq \sqrt{-\frac{2i}{\pi r}}\, k^{3/2} \int_{\pi/2 - i\infty}^{-\pi/2 + i\infty} d\beta \sin^{3/2} \beta\, e^{ikr(\cos(\beta - \theta))} \cdot$$

$$\left[e^{-ikz_o \cos \beta} + b(\beta)\, e^{ikz_o \cos \beta} \right] (\hat{z} \sin \beta - \hat{r} \cos \beta) \cdot$$

The new path in the β plane may be deformed through the saddle point at $\beta = 0$ and evaluated by the saddle point formula[2]. The result is

$$\bar{E} = -2ik \sin \theta\, \frac{e^{ikr}}{R} \left[e^{-ikz_o \cos \theta} + b(\theta)\, e^{ikz_o \cos \theta} \right] \hat{\theta} \tag{B.4}$$

---

[1] See references 8, 33, 34, 35. Nomura (Ref. 34) and Banos (8) are particularly complete on this subject.

[2] For example, see reference 36.

where $b(\theta)$ is given by

$$b(\theta) = \frac{n^2 \cos\theta - \sqrt{n^2 - \sin^2\theta}}{n^2 \cos\theta - \sqrt{n^2 - \sin^2\theta}} \quad .$$

Note that $b(\theta)$ is equivalent to the plane wave reflection coefficient for vertically polarized waves.

When $\theta \longrightarrow \frac{\pi}{2}$ and $|n|^2 >> 1$ then the path of integration must pass very near a pole. The pole contribution appears as a so-called ground wave. Feynburg (ref. 35) has a very good discussion on the limits of validity of equations such as (B.4) which ignore the pole contribution. In rough terms he has shown that (B.4) is accurate near the ground as long as the so-called numerical distance is larger than 5.

$$\text{numerical distance} = \left|\frac{n-1}{n^2}\right| \frac{kR}{2} \quad .$$

When the numerical distance is small the field behaves as if the ground were a perfect conductor. For (B.1) this would mean a maximum in the $\theta = \frac{\pi}{2}$ direction. The asymptotic expression(B.4) has a zero in the $\theta = \frac{\pi}{2}$ direction. This effect is caused by a ground wave that attenuates slowly close to the antenna but dies out rapidly with increasing distance.

APPENDIX C

CURVE PLOTTING PROGRAMS

C.1 Reflection Coefficient Curves

A digital plotting system for producing computer generated drawings on the University of Michigan's IBM 360/67 exists. This plotting system runs under the Michigan Terminal System and is described in "The University of Michigan Digital Plotting System". A program making use of the available plotting system subroutines was written in FORTRAN IV/G to plot the absolute value of the reflection coefficients given in equation (3.13). The program listing follows.

```
      DIMENSION A(91),B(91),TH(91)
      COMPLEX*8 NSQ,CSQRT,F,G
      NAMELIST/ONE/AA
      READ(5,ONE)
      WRITE(5,ONE)
      NSQ=CMPLX(AA,.01*AA)
      CALL PAXIS(5.,5.,'THETA IN DEGREES',-16,
     16.,0.,0.,15.,1.)
      CALL PAXIS(5.,5.,'REFLECTION COEFFICIENT',22,
     15.,90.,0.,.2,1.)
      CALL PLOTPS(0.,15.,0.,.2,5.,5.)
      DO 20 J=1,2
      DO 10 I=1,91
      TH(I)=I-1
      G=TH(I)*.01745329251994
      C=COS(G)
      S=SIN(G)
      F=S*S
      F=NSQ-F
      F=CSQRT(F)
      G=(C-F)/(C+F)
      A(I)=CABS(G)
      G=(NSQ*C-F)/(NSQ*C+F)
      B(I)=CABS(G)
10    CONTINUE
      CALL PLINE(TH,A,91,1,0,0,1)
      CALL PDSHLN(TH,B,91,1,0,1)
20    NSQ=CMPLX(AA,1000.*AA)
100   FORMAT(3F10.5)
      END
```

C.2 Power Patterns

The Michigan Terminal System Plotting system was used to generate the actual plots. The curves are plots of $R^2 \cdot |\bar{E}|^2$ where $\bar{E}$ is defined by equation (3.11), (3.12) or (4.10) depending upon the type of antenna. Each curve was normalized in order to have a maximum radius of two inches. The program listing that follows was used to plot power patterns for the vertical Hertzian dipole. Program listings for the other two cases have not been included because they are very similar.

```
      DIMENSION TH(91),THN(91),R(91)
      COMPLEX*8 A,B,NSQ,J,P,Q
      COMMON NSQ
      NAMELIST/ONE/NSQ
      J=(0.,1.)
      READ(5,ONE)
      WRITE(6,ONE)
      ZC=2.
      ZOK=ZC*2.*3.1415926536
      RMAX=0.
      DO 10 I=1,91
      TH(I)=I-1
      THN(I)=-TH(I)
      Q=TH(I)*.01745329251994
      S=SIN(Q)
      C=COS(Q)
      CALL AB(A,B,Q)
      P=CEXP(-J*ZOK*C)
      Q=CEXP(J*ZOK*C)
      C=B*Q
      P=P+Q
      F=CABS(P)
      R(I)=S*S*F*F
      IF(R(I)-RMAX)10,10,5
    5 RMAX=R(I)
   10 CONTINUE
      WRITE(6,200)RMAX
      CALL PAXIS(-5.,10.5,
     1'ANTENNA CENTER HEIGHT OF 2. WAVELENGTHS',
     2-39,-6.,0.,0.,1.,1.)
      CALL PAXIS(-5.,7.75,
     1'ANTENNA CENTER HEIGHT OF .4 WAVELENGTHS',
     2-39,-6.,0.,0.,1.,1.)
      CALL PAXIS(-5.,5.,
     1'ANTENNA CENTER HEIGHT OF .2 WAVELENGTHS',
     2-39,-6.,0.,0.,1.,1.)
      RFACT=RMAX/2.
      CALL PLTPOL(1)
      CALL PLTOFS(0.,RFACT,90.,1.,8.,10.5)
      CALL PLINE(R,TH,91,1,0,0,1)
      CALL PLINE(R,THN,91,1,0,0,1)
      CONTINUE
      ZC=.4
      ZOK=ZC*2.*3.1415926536
      RMAX=0.
      DO 20 I=1,91
      TH(I)=I-1
      THN(I)=-TH(I)
      Q=TH(I)*.01745329251994
      S=SIN(Q)
```

```
      C=CCS(Q)
      CALL AB(A,B,Q)
      P=CEXP(-J*ZCK*C)
      Q=CEXP(J*ZCK*C)
      P=B*C
      P=P+C
      F=CABS(P)
      R(I)=S*S*F*F
      IF(R(I)-RMAX)20,20,15
   15  RMAX=R(I)
   20 CONTINUE
      WRITE(6,200)RMAX
      CALL PLTOFS(0.,RFACT,90.,1.,8.,7.75)
      CALL PLINE(R,TH,91,1,0,0,1)
      CALL PLINE(R,THN,91,1,0,0,1)
      ZC=.2
      ZCK=ZC*2.*3.1415926536
      RMAX=0.
      DO 30 I=1,91
      TH(I)=I-1
      THN(I)=-TH(I)
      Q=TH(I)*.017453292519943
      S=SIN(Q)
      C=CCS(Q)
      CALL AB(A,B,Q)
      P=CEXP(-J*ZCK*C)
      Q=CEXP(J*ZCK*C)
      Q=B*Q
      P=P+C
      F=CABS(P)
      R(I)=S*S*F*F
      IF(R(I)-RMAX)30,30,25
   25  RMAX=R(I)
   30 CONTINUE
      WRITE(6,200)RMAX
      CALL PLTOFS(0.,RFACT,90.,1.,8.,5.)
      CALL PLINE(R,TH,91,1,0,0,1)
      CALL PLINE(R,TH,91,1,0,0,1)
  200 FORMAT(4F10.5)
      END
      SUBROUTINE AB(A,B,Q)
      COMPLEX*8 A,B,NSQ,F
      COMMON NSQ
      C=CCS(Q)
      S=SIN(Q)
      F=S*S
      F=NSQ-F
      F=CSQRT(F)
      A=(C-F)/(C+F)
      B=(NSQ*C-F)/(NSQ*C+F)
      RETURN
      END
```